The Dissertation Committee for Brian C. Trinque Certifies that this is the approved version of the following dissertation:

SYNTHESIS, COPOLYMERIZATION STUDIES AND 157 nm PHOTOLITHOGRAPHY APPLICATIONS OF 2-TRIFLUOROMETHYLACRYLATES

Committee:

C. Grant Willson, Supervisor

Brent L. Iverson

Hiroshi Ito

Michael J. Krische

Stephen E. Webber

SYNTHESIS, COPOLYMERIZATION STUDIES AND 157 nm PHOTOLITHOGRAPHY APPLICATIONS OF 2-TRIFLUOROMETHYLACRYLATES

by

Brian C. Trinque, B.A.

Dissertation

Presented to the Faculty of the Graduate School of

The University of Texas at Austin

in Partial Fulfillment

of the Requirements

for the Degree of

Doctor of Philosophy

The University of Texas at Austin

May, 2003

For AKT

Acknowledgements

First and foremost, I am most indebted to my research advisor, Professor Grant Willson. I thank him for giving me the opportunity and support to study chemistry in his research group. I am also grateful for the encouragement and guidance of Dr. Peter Tattersall, who first taught me the majority of the chemistry laboratory skills required to perform the experiments in this dissertation. I also acknowledge Dr. Hiroshi Ito, whom, through the help of Professor Willson, I worked with at the IBM Almaden Research Center in the summer of 2003. I learned a great deal during this collaboration.

I must also thank my fellow colleagues in the Willson Group for their assistance with the contents of this dissertation. I remember times when I thought that, due to periods of no success, my graduate career would come to a screeching halt. However, it was during these times that both Matthew Pinnow and Takashi Chiba successfully synthesized molecules that breathed new life into my research. I also thank two undergraduate researchers who were a pleasure to work with: Jennifer Wunderlich and Schuyler Corry. I thank Dr. Colin Brodsky and Brian Osborn for help with acquiring all of the gas phase data shown on these pages. I am also fortunate to have had a chance to do research with Sean Burns, Michael Stewart, Gerard Schmid, Heather Johnson, and EK Kim. I am grateful for many helpful discussions with Charles Chambers, Will Conley, Dr. Ryan Callahan, Dr. Thomas Mrozek, Shiro Kusumoto, Dr. Dave Johnson, Dr. Raymond Hung, Dr. H.V. Tran, Bill Heath, Stefan Caporale, and Dr. Scott Grayson. I must also not

forget the assistance that Kathleen Sparks has given me over the years. I am certain that I would not have graduated when I did without the help of all of those mentioned above.

Finally, I must thank Anne for her love, patience, and endless support.

SYNTHESIS, COPOLYMERIZATION STUDIES AND 157 nm PHOTOLITHOGRAPHY APPLICATIONS OF 2-TRIFLUOROMETHYLACRYLATES

Publication No._____

Brian C. Trinque, Ph. D.

The University of Texas at Austin, 2003

Supervisor: C. Grant Willson

Advances in microelectronic devices have relied heavily on improved photolithographic imaging capabilities. The resolution limit of optical lithography can be improved by lowering the wavelength of exposure light. The latest reduction in exposure wavelength is from 193 nm to 157 nm. The focus of this work is the synthesis, copolymerization studies and lithographic imaging capabilities of 2-trifluoromethylacrylates. Model calculations and gas phase absorbance measurements of model compounds first suggested that these materials would provide suitable transparency at the 157 nm wavelength. Methyl 2-trifluoromethylacrylate was synthesized and aniocically polymerized and variable angle spectroscopic ellipsometry showed that this material had an

absorbance that was 1,000 times more transparent than its non-fluorinated analogue. A variety of relatively transparent resist materials based on a 2-trifluoromethylacrylate backbone were synthesized by anionic polymerization, and these materials were successfully imaged at 157 nm. While 2-trifluoromethylacrylates do not undergo homopolymerization with radical initiators, they do radically copolymerize with various norbornenes. Interestingly, these materials exhibit a 2:1 (2-trifluromethacrylate:norbornene) monomer incorporation. This phenomenon was exploited to produce a number of relatively transparent materials that produced positive-tone structures when imaged at the 157 nm wavelength. Kinetic studies were performed to show that the copolymerizations of 2-trifluormethacrylates and norbornene derivatives deviate from the terminal model and follow the penultimate model. Competitive reaction studies using the "mercury method" were performed to demonstrate that substitution of a trifluoromethyl group can indeed effect the reactivity of a propagating radical, lending support to the proposed penultimate model. The structure of the 2-trifluoromethylacrylate propagating radical will also be investigated by electron spin resonance spectroscopy.

Table of Contents

List of Tables

List of Figures

CHAPTER 1: INTRODUCTION

Moore's Law

There is little doubt that since the invention of the integrated circuit in 1959, the semiconductor has had an impact on our society that overshadows advancements in almost any other area of technology. It is difficult to find a business, university, or any other organization that does not rely heavily on sophisticated machinery that functions as a result of major advancements in the semiconductor field. While the consumer enjoys watching the prices of such machinery decrease, chemists, physicists, and engineers continue to work relentlessly to create smaller, more complex devices that function at new levels of sophistication. In 1964 semiconductor engineer Gordon Moore (who co-founded Intel four years later) noticed an interesting trend in the unprecedented rate of advancements in this field: the amount of information storable on a given amount of silicon has roughly doubled every year since the technology was invented.[1] This relation, which has come to be known as Moore's Law, held until the late 1970s, at which point the doubling period slowed to 18 months (figure 1.1).[2] Chip manufacturers use this trend in order to set long-term goals for new technology. Predictions can be made as to what speeds a processor must operate at in future years, and this forces researchers to develop new technologies in order to keep up with societal demands.

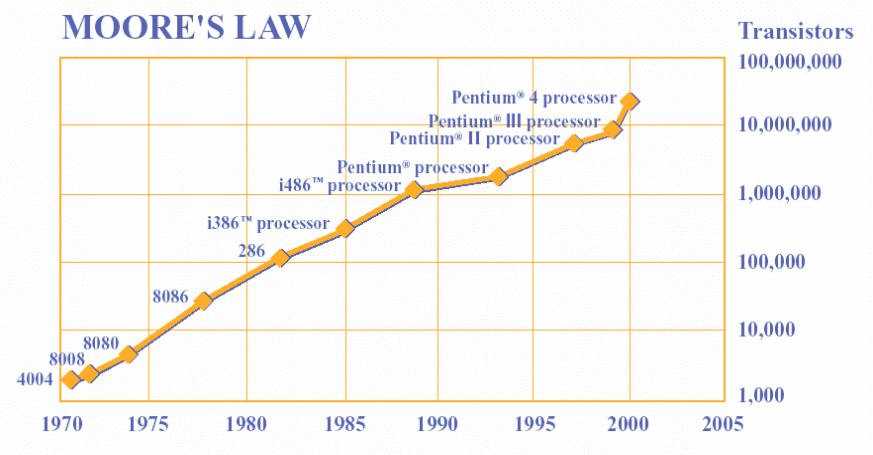

Figure 1.1: The transistor count per inch^2 doubles every 18 months.

Microlithography

Underlying this incredible progress is microlithography: the core technology for the volume production of integrated circuits. A key component in the microlithographic process is a polymeric material called a photoresist (the subject of this dissertation). This material serves two functions: to convert an optical image of a circuit pattern into a 3D relief pattern through a photochemical reaction which alters its solubility in a developer solution ("photo-") and to resist subsequent processes used to transfer the relief image into the underlying substrate ("-resist"). A description of the microlithographic process (Figure 1.2) will explain how this material is used in production.

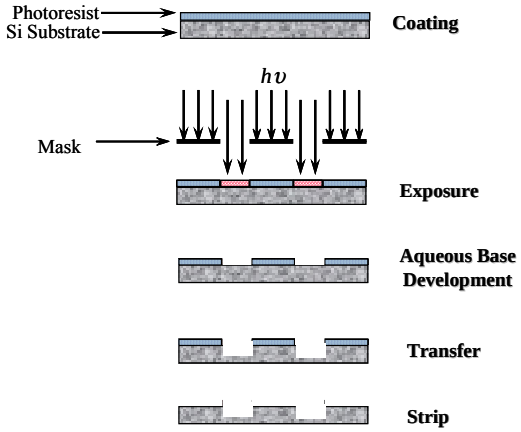

Figure 1.2: The microlithographic process.

Formulation, Spin-Coat and Post Apply Bake

First, the resist polymer is formulated with a particular photo active compound (PAC), and dissolved in an appropriate casting solvent such as propylene glycol methyl ether acetate (PGMEA), ethyl lactate, or 2-heptanone. This solution is then spin-coated onto a silicon substrate (wafer) resulting in a uniform film of a certain thickness. Film thickness can be altered by varying polymer concentration in the casting solvent and spin speeds. The coated wafer is then placed on a hot plate for a short time to drive off any remaining solvent and assure good adhesion between the film and the wafer.

Exposure and Post Exposure Bake

The film-coated wafer is then exposed by a light source of the proper wavelength (currently in the G-line, I-line, or deep-UV areas of the light spectrum). Areas of the resist film are selectively exposed through a mask which produces an optical image that will provide the desired pattern of relief images in

the resist. Upon exposure, the PAC in the resist formulation undergoes a photochemical rearrangement which induces a solubility switch in the resist. The exposed regions of the positive tone resist (negative tone not mentioned here) are rendered base-soluble, while the unexposed regions remain base insoluble. This induced chemical change is often facilitated with a "post exposure bake" (PEB), where the wafer is placed on a hot plate and heated for some amount of time.

Development, Etch and Strip

In the development step, the wafer is immersed in 0.26N tetramethylammonium hydroxide (TMAH) developer and the exposed regions of the resist are washed away, leaving the desired pattern of relief images in the resist. The exposed surface of the wafer is then eroded away in the transfer or etching step. This proceeds by inserting the wafer in a plasma etch chamber that generates free radicals and reactive ions that etch through the substrate. The remaining photoresist is less susceptible to etching, thereby protecting the areas of substrate that lay under it. Finally, after the desired pattern is transferred to the substrate, the resist is then removed by various plasma etching conditions, resulting in a desired circuit pattern that is etched into the silicon substrate.

Resolution limit of optical lithography

In order to keep pace with Moore's Law, the microelectronics industry is forced to use microlithography to create smaller and smaller feature sizes on chips. Underlying these efforts is the Rayleigh equation, stating:

$$F \propto \lambda/(NA) \qquad \textbf{(1)}$$

which relates the minimum feature size (F) that can be resolved with this lens to the wavelength of the exposure light (λ) and numerical aperture (NA): the sine of half of the angle of the image-forming cone of light at the image (figure 1.3).

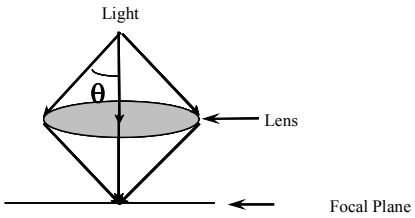

NA= n sin θ
n: index of refraction (for air, n ~ 1)

Figure 1.3: NA of an exposure lens system.

Therefore, minimum feature dimensions can be decreased by either reducing the wavelength of the exposure light, or increasing the NA of the imaging system. The majority of the advances in photolithography technology can be attributed to decreases in the exposure wavelength. The source of light for exposure tools has been either mercury arc lamps or excimer lasers. The mercury arc lamp emits a characteristic emission spectrum from ~200nm to 600nm. This type of light source has strong emission peaks at 436 nm (G-line) and 365 nm (I-line). As the lithography industry attempted to reduce exposure wavelengths to 248 nm in order to make yet smaller feature dimensions, it was found that the mercury arc exposure system's intensity was too low at this wavelength for suitable throughput. The first approach to this problem was to switch to an excimer laser, which has a significantly higher intensity in the deep-UV compared to a mercury arc lamp. The microelectronic industry currently uses a krypton-fluoride excimer laser for exposure at the 248 nm wavelength. The second

approach to this problem was to design a photoresist that could amplify the dose received within the film. Such a material is called a chemically amplified photoresist, and is discussed in a future section.

Novolac/Diazonapthoquinone Resist Systems

The "workhorse" photoresist for the microlithographic industry for 436 nm and I-line 365 nm (mercury ARC lamp) exposure is based on novolac and diazonapthoquinone (DNQ). Due to its phenolic character, novolac is sufficiently acidic to be soluble in aqueous base. Diazonapthoquinone is a photoactive compound (PAC) that interacts with novolac in such a way that the base polymer is rendered insoluble in base developer.[3,4] The nature of the substituent R, often a sulfonate, influences the solubility characteristics of the sensitizer molecule.[5] Upon exposure with light, DNQ undergoes the Wolff rearrangement to produce a ketene that reacts with water forming a carboxylic acid (figure 1.4). The unexposed regions of this novolac/DNQ formulation remain base insoluble, while the exposed regions have a dissolution rate in aqueous base that is equal to or greater than that of the novolac resin (figure 1.5).

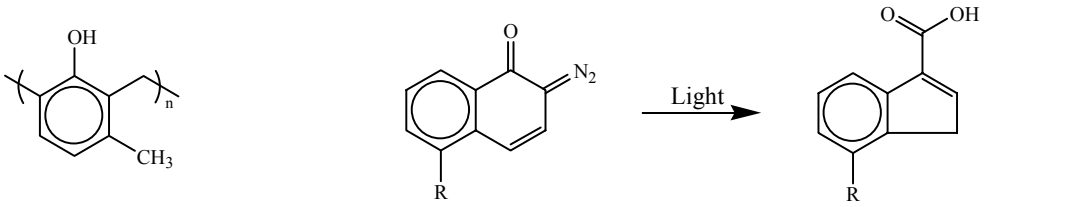

Figure 1.4: Novolac, DNQ and photoproducts

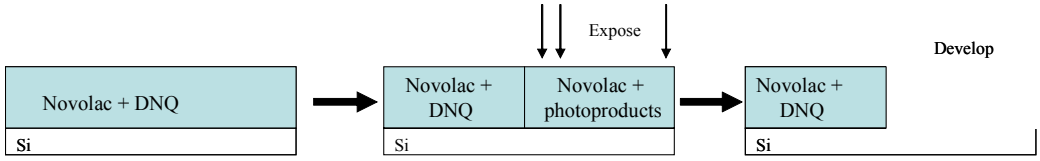

Figure 1.5: Schematic representation of Novolac/DNQ positive resist.

Chemically Amplified Resists and the Photoacid Generator

As exposure wavelengths were decreased to 248 nm in order to shrink dimensions of the most critical layers of the integrated circuit, a new resist was developed to amplify the low intensity of the mercury arc lamp at this wavelength. This resist relies on the addition of a photoacid generator (PAG) as opposed to the diazonapthoquinone PAC to the resist formulation. The base polymer of the chemically amplified resist (positive tone) has an acidic moiety that is masked with an acid labile protecting group. This renders the photoresist insoluble in base developer. Upon exposure to light, the PAG generates acid which cleaves off the protecting group, causing those areas of film to dissolve when exposed to TMAH developer. With each deprotection step, a new acidic molecule is regenerated that can catalyze cleavage of another protecting group (hence the name "chemical amplification").

The PAG that is formulated in a chemically amplified resist can be any of a number of materials that produce acid as a result of photolysis.[6] The most common PAGs utilized in photoresists are based on onium salts, originally designed for light-initiated cationic polymerization reactions.[7,8] An example of

such an onium salt is triphenyl-sulfonium nonaflate (TPS-Nf), shown in figure 1.6. Upon exposure to light, this material undergoes homolytic cleavage of the carbon-sulfur bond to give an aryl radical and a sulfur radical cation. The final Bronsted acid is generated by hydrogen abstraction by the sulfur radical cation, followed by protonation of the counter anion.[9]

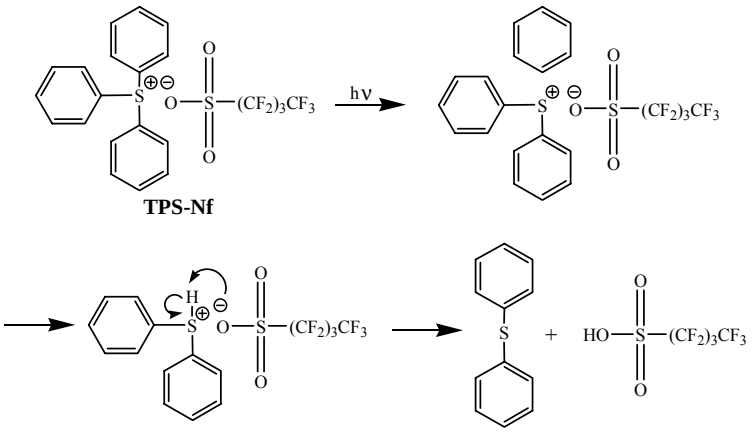

Figure 1.6: TPS-Nf and its photodecomposition.

The base polymer of a chemically amplified resist contains a base soluble moiety (carboxylic acid or acidic alcohol) that is protected by an acid-labile protecting group (*tert*-butyl ester, carbonate or acetal). The protecting group inhibits the polymer from being soluble in .26N TMAH, but when exposed to acid, it is cleaved, unmasking the acidic group, which results in a soluble polymer. Every deprotection results in the production of a new acidic molecule that can remove another protecting group. An example of a typical chemically amplified resist is shown in figure 1.7. The base resin with phenolic functionality is partially protected in order to inhibit solubility. Strong adhesion and wetability characteristics are retained by only partially deprotecting the polymer. As the PAG

produces acid, *t*-butyl carbonate protecting groups are cleaved, resulting in poly(hydroxystyrene), which is soluble in base developer. This process is facilitated by the formation of a stable tertiary carbocation through the *tert*-butyl group on the carbonate functionality. The volatile byproducts carbon dioxide and isobutene are produced, as is another molecule of acid, which re-enters the deprotection scheme to cleave another protecting group.

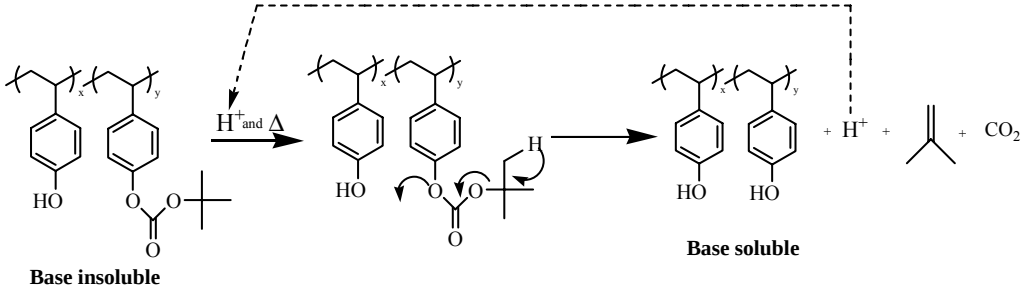

Figure 1.7: The acid catalyzed deprotection of a *t*-boc carbonate protected poly (4-hydroxystyrene).

The Onishi Paramater

An important characteristic of a polymer that is used as a chemically amplified resist is its ability to resist the reactive ion etch (RIE) step of the photolithographic process. The Onishi parameter, a well known empirical relationship between polymers and their resistance to the RIE step, states that etch rate is proportional to a polymer's carbon to hydrogen ratio (equation 2).[10]

$$\text{Rate}_{etch} \alpha \frac{N_T}{N_C - N_O} \qquad \begin{array}{l} N_C = \text{total number of carbon atoms} \\ N_O = \text{total number of oxygen atoms} \\ N_T = \text{total number of atoms} \end{array} \qquad (2)$$

Aliphatic materials have a relatively high etch rate, while pure carbon has the slowest. Both novolac and the polymer shown in 1.6 have relatively high carbon to hydrogen ratios, and therefore a slow etch rate (i.e., high etch resistance). Other polymers that display a relatively high etch resistance are those that incorporate norbornyl[11] and adamantyl[12] groups.

Resist Transparency

The four components of a polymer used for a chemically amplified resist have now been identified: the acidic moiety to provide good adhesion and wetability (carboxylic acid or acidic alcohol), the protecting group to inhibit dissolution and allow for chemical amplification (*t*-butyl ester, carbonate, or acetal), etch resistant group for the RIE phase (aromatic, norbornyl, or adamantyl rings), and a backbone to tether the polymer together. Once the photoresist polymer is "assembled," it then undergoes many stages of resist evaluation, which closely examine its performance in all of the steps of microlithographic fabrication. Before it can be considered for preliminary resist testing, the material must offer adequate transparency at the exposure wavelength for which it is intended. Figure 1.8 shows the drastic difference in image profile between a resist that is highly transparent at a given exposure wavelength and a resist that is highly absorbing at that wavelength. When the resist film is transparent, as is the case on the left, light is exposed down to the substrate, the appropriate photochemistry/deprotection occurs through the bulk of the film, and the all of the resist is removed during the development step. The substrate is now exposed and can be etched. When the film is highly absorbing, as is the case on the right, a

solubility switch occurs at only superficial areas of the film, and the majority of the resist remains after the development step. In this case, an etching step is ineffective.

Figure 1.8: The impact of photoresist absorbance on the photolithographic process.

Photoresists for 193 nm Lithography

As reductions in wavelength have been made to provide smaller feature sizes on chips, major changes had to be made in the structure of photoresist base polymers in order to meet transparency requirements. As researchers in the lithography community began to develop resist systems for 193 nm exposure, aromatic ring containing polymers, which were widely used for 248 nm lithography, were found to be too absorbing. The resist community was faced with the challenge of developing materials that did not contain opaque aromatic groups, but did have a relatively high carbon to hydrogen ratio in order to resist the RIE process. This was done by incorporating norbornyl and adamantyl rings into a variety of copolymers. For example, Allen et al.[13] developed a 193 nm photoresist system based on a methacrylate backbone known as "IBM Version 2" that contained a norbornane ester. This material had an etch rate that was only 1.2

times that of novolac and displayed excellent transparency and imaging quality at 193 nm (figure 1.9).

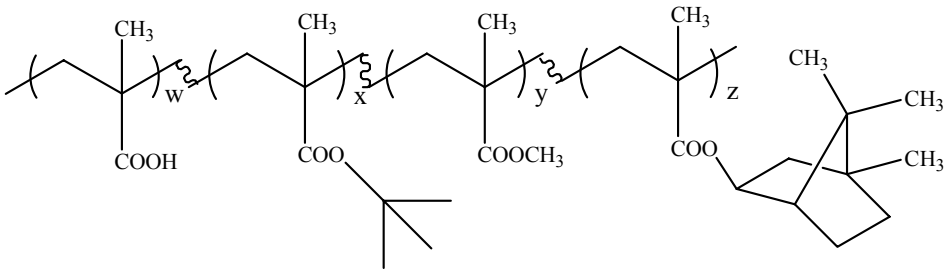

Figure 1.9: IBM Version 2.

Okoroanyanwu et al.[11] developed copolymers of functionalized norbornene and maleic anhydride, such as those shown in figure 1.10. These monomers could be copolymerized with radical initiators like azobisisobutyronitrile, thereby incorporating an etch-resistant norbornene group directly into the polymer backbone. The norbornene monomer was functionalized with a *t*-butyl ester which served as a protecting group for chemical amplification. Utilizing a polar comonomer like maleic anhydride enhances adhesion, wettability, and solubility in standard base developer. These non-phenolic materials had etch rates that were comparable to the resist polymer in figure 1.7, were extremely transparent, and provided good imagability with 193 nm exposure.

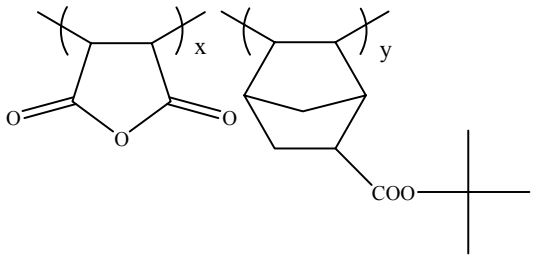

Figure 1.10: Maleic anhydride/norbornene resist copolymers.

Klopp et al.[12] developed an example of a resist polymer that utilizes an adamantyl group for its high carbon content. In this case, the adamantyl ester serves not only as an etch resist, but also as a protecting group for chemical amplification. Because the protecting group is a tertiary ester, a stable carbocation forms upon reaction with acid. The exposed regions of the film deprotect to the corresponding carboxylic acid, causing the desired solubility switch, while the unexposed regions retain the ester that will resist the etching step (figure 1.11). The adamantyl group has a very big impact on etch resistance as the copolymer shown in figure 1.11 had slower etch rates than most common deep-UV resist polymers.

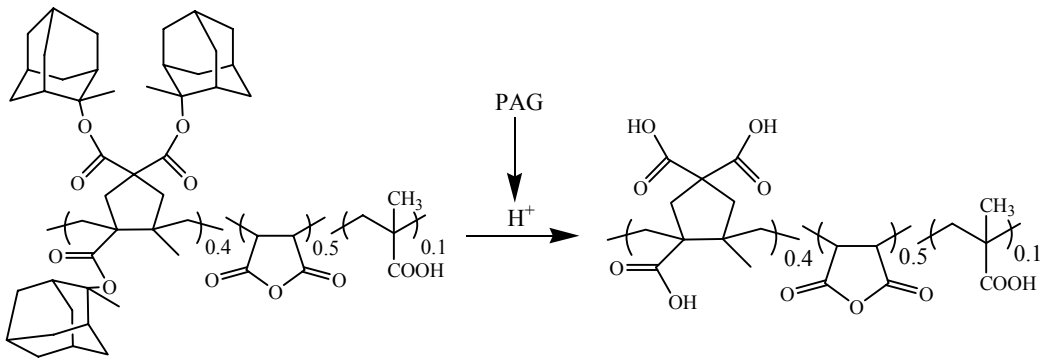

Figure 1.11: The adamantyl based resist by Klopp et al.

Airborne Amine Contamination and Base Additives

It should be noted that since chemically amplified photolithography relies on the production of acid, base contamination is an important issue that needs to be addressed. Even parts per million of amine contamination in the air can cause significant deformations in resist profile called "T-topping"[14,15] (figure 1.12).

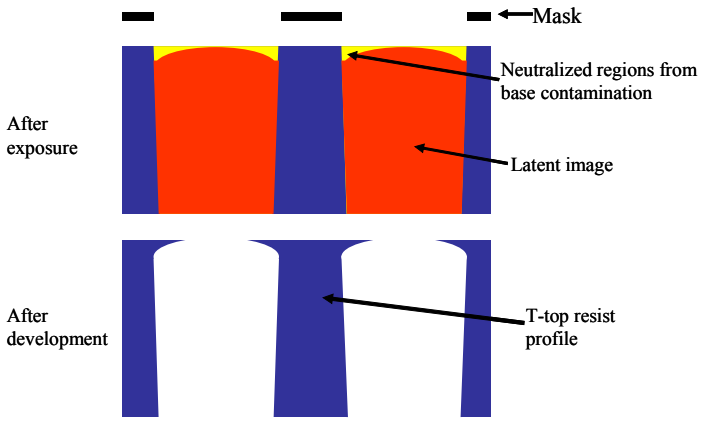

Figure 1.12: T-top formation due to airborne amine contamination.

Base contamination leads to unacceptable image profiles and linewidths after the etching step. So far, there have been many attempts to minimize airborne base contamination on the resist profile. Ito et al.[14] developed a polymer-annealing concept in 1995 that drastically reduced the effects these contaminants had on image profile. Protective overcoats have also been used to protect generated acid at the top of the film from being quenched.[16] An alternative way of protecting chemically amplified resists from base contamination, and the method used in the imaging experiments in this dissertation, is to use a known amount of base additive in the resist formulation.[17] If a resist formulation can properly

function with enough base formulated into it so any amount of airborne contamination is negligible, T-topping will be minimized. Generally, 10 weight percent of the amount of PAG added is enough base to effectively reduce any signs of image deformation due to airborne amine contamination but not enough to significantly affect the extent of deprotection by acid produced from the exposed PAG. Ultimately, a chemically amplified photoresist is comprised of four major components: casting solvent, base polymer, PAG, and base additive.

CHAPTER 2: DEVELOPMENT OF A RESIST POLYMER FOR 157 nm PHOTOLITHOGRPHY

The Advent of 157 nm Microlithography

Since the lithographic process was first invented, several generations of new exposure tools have been developed that utilize shorter and shorter wavelengths of light in order to minimize the dimensions of features on integrated circuits. Each new generation of exposure tools introduces wavelength reductions that limit the materials available for resist design. As was mentioned in Chapter 1, a variety of polymers have been developed for 193 nm lithography technology, and these materials have greatly improved transparency over their phenolic-based predecessors. Current 193 nm technology regularly produces devices with 0.13 μm minimum feature size, or critical dimension (CD). According to the 2001 update of the Semiconductor Industry Association (SIA) Roadmap, chips with 190 million transistors will be produced in 2005. This will require gatelengths as small as 70 nm. In order to produce such dimensions, a new generation of exposure tools have been developed that use fluorine (F_2) excimer lasers to provide exposures at the 157 nm wavelength, which is in the vacuum-UV (VUV) area of the light spectrum.

Polymer Absorbances at 157 nm

This new drop in exposure wavelength demands the development of a new class of polymers that fulfill the requisite characteristics of a photoresist resin and are highly transparent at 157 nm. Creating materials that fulfill such criteria is a

difficult task as air, water, oxygen gas, and even simple hydrocarbons like butane absorb strongly at this wavelength. Initial absorbance data by Kunz et al.[18] offered important insight into the absorbance characteristics of a variety of polymers at 157 nm (Table 2.1). For example, UV6-2D, a common DUV resist which has an absorbance of 0.37 μm^{-1} at 248 nm, has an absorbance of 6.84 μm^{-1} at 157 nm. This drastic absorbance increase is expected, as UV6-2D has aromatic character which is already too absorbing for use at 193 nm. The 193 nm resist PAR-101 (0.47 μm^{-1}at 193 nm) has an absorbance of 6.86 μm^{-1} at 157. At this transmittance, less than 10^{-5} % of the exposed light is getting through the entire resist film and reaching the substrate. This result was more surprising, as this material has no aromaticity associated with it. These materials, however, are fully *formulated* resists (polymer, PAG, base additive) so the absorbances of unfunctionalized homopolymers were examined in order to gain more insight as to how particular functional groups absorb in this part of the vacuum-UV spectrum. Even the most basic components of photoresist materials such as poly(methyl methacrylate) (PMMA) and poly(norbornene) are approximately one million times more absorbing at 157 nm than UV6-2D and PAR-101 at 248 and 193 nm, respectively.

	157 nm	**193 nm**	**248 nm**
UV6-2D	6.84		0.37
PAR-101	6.86	0.47	
PMMA	5.69		
Poly(norbornene)	6.10		
Poly(styrene)	6.20		
Fluorocarbon	0.70		

Table 2.1: Absorbances (μm^{-1}) of a number of materials at 157 nm.

Of all the carbon-backboned polymers tested, only those that were either fully or partially fluorinated offer improved transparency at 157. A 100 % fluorinated hydrocarbon polymer has an absorbance of 0.70 μm^{-1}at 157 nm, and a hydrocarbon that is 30% fluorinated has an absorbance of 1.34 μm^{-1}. This information set the tone for the synthesis of a wide range of fluorine containing materials by the resist community for utility at this new wavelength.

These reported absorbances raised many concerns, mainly dealing with the actual structure of a resist polymer for 157 applications. Since poly(norbornene) was far too absorbing at this wavelength, would this common alicyclic ring be unusable for a 157 resist? If PMMA was too absorbing, would the carbonyl group, a functionality that was incorporated into most of the resists for 248 and 193 nm lithography, be impractical at this wavelength? If fluorine offered transparency at 157, how much fluorine would be necessary? Would a perfluorinated version of a DUV photoresist be the answer?

Vacuum-UV Studies

In order to gain some perspective on the above questions, we decided to perform a gas phase study on certain fluorinated molecules. Gas phase studies are advantageous as they provide the absorbance spectra of single molecules, thereby avoiding the synthetic inconvenience of producing polymers. Furthermore, monomeric materials are often times less difficult to purify than polymers. This would be vital for vacuum-UV investigations, as any impurity could negatively effect the actual absorbance of a material. Vapor phase VUV spectra were measured using a custom built gas cell system. Samples were rigorously purified

by appropriate techniques, including column chromatography and vacuum distillation, degassed by a sequence of freeze/thaw cycles, and sealed in glass ampoules under vacuum. The ampoule was then placed in a chamber that was connected to the gas cell setup by flexible bellows which allowed the chamber to be shaken so that the glass ampoule shattered *in situ*. Further details on this setup are available in the literature.[19]

Absorbances of Fluroinated Norbornanes: 2,2-Difluoronorbornane and 2-Fluoronorbornane

To gain a better understanding of the effect that fluorination exerts on the absorbance of the norbornane skeleton, a systematic replacement of hydrogen atoms with fluorine was proposed[20] in order to measure the effect upon their absorbance at 157 nm. A number of synthetic pathways were pursued in order to produce a variety of substituted fluoro-norbornanes. The majority of these preparations required the use of the fluorinating reagent diethylaminosulfur trifluorinde (DAST)[21]. DAST converts primary, secondary, tertiary, allylic, and benzylic alcohols to monofluorides. Also, the carbonyl group of aldehydes and ketones can be converted to a 1,1-difluoro group in moderate to high yields. For fluorination in the 2-position in the norbornane ring, the commercially available starting material 2-bicyclo[2.2.1]heptanone (**2.1**) was reacted with DAST. The resulting product (**2.2**) was found to be stable to heat and vacuum. Interestingly, this was not the case for monofluorine substitution in the 2-position. Reaction of DAST with 2-*exo*-bicyclo[2.2.1]heptanol (**2.3**) afforded a high yield of the mono-substituted product (**2.4**). The crystallin product was purified by two sublimations

and sealed in a glass ampoule for VUV spectroscopic studies. However, after less than 48 hours in the glass container, the previously white crystals turned dark purple. The inside of the glass ampoule was also found to be etched. Analysis of the decomposition products showed that the 2-fluoronorbornane had been converted to dibicyclo[2.1.1]heptyl ether (**2.5**) in over 75% isolated yield (figure 2.1). This transformation was also observed when an attempt was made to distill the compound at ambient pressure. We believe that the compound undergoes facile dehydrofluorination and that the glass container is the oxygen source. This problem was overcome by loading the product into a steel ampoule for gas phase measurements. No decomposition was found when the molecule was placed in this environment, and a VUV spectrum was successfully acquired.

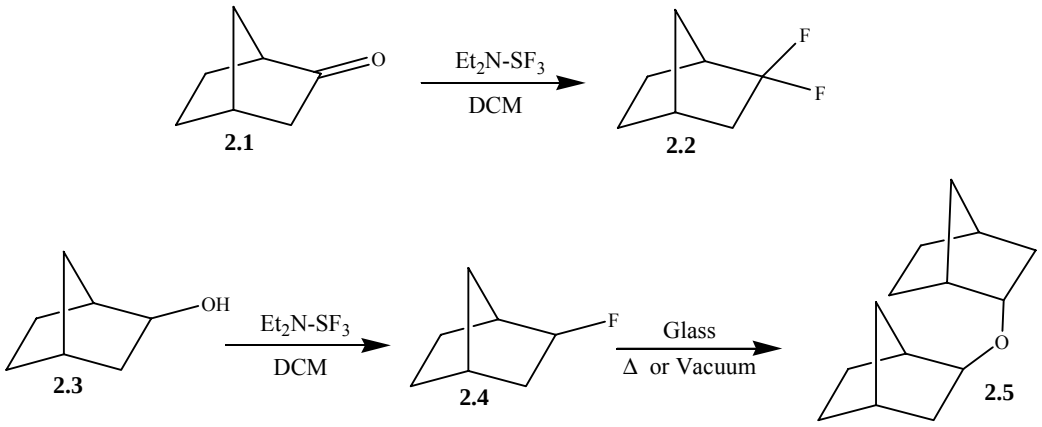

Figure 2.1: The synthesis of compounds **2.2** and **2.5**. To prevent decomposition, **2.2** was loaded into a steel ampoule for VUV analysis.

7,7-Difluoronorbornane

The synthesis of norbornanes with substitution in the 7-position of the ring required a different synthetic route. For di-substitution in the 7-position, 5,5-

dimethoxy-1,2,3,4-tetrachlorocyclopentadiene (**2.6**) was purchased and reacted with ethylene gas in a Diels-Alder cycloaddition to produce 7,7-dimethoxy-1,2,3,4-tetrachlorobicyclo[2.2.1.]hept-2-ene (**2.7**).[22] The cycloaddition product was dechlorinated with sodium metal and t-butyl alcohol generating 7,7-dimethoxybicyclo[2.2.1]hept-2-ene (**2.8**).[22] This reductive dehalogenation reportedly proceeds by electron transfer from 5 equivalents of sodium to chlorine to form a radical anion which then fragments. The resulting radical on the norbornane ring is then reduced to a carbanion by a second electron transfer from sodium and then protonated.[23] The dechlorinated norbornene was subjected to typical hydrogenation conditions using palladium metal on carbon support under hydrogen atmosphere[24] to produce the reduced product (**2.9**), which was hydrolyzed with acetic acid and HCl to produce bicyclo[2.2.1]hept-2-en-7-one (**2.10**).[25] The ketone was treated with DAST to produce 7,7-difluorobicyclo[2.2.1]hept-7-one (**2.11**). This molecule was extremely volatile, and great care had to be taken during its purification so it would not be lost by evaporation (figure 2.2).

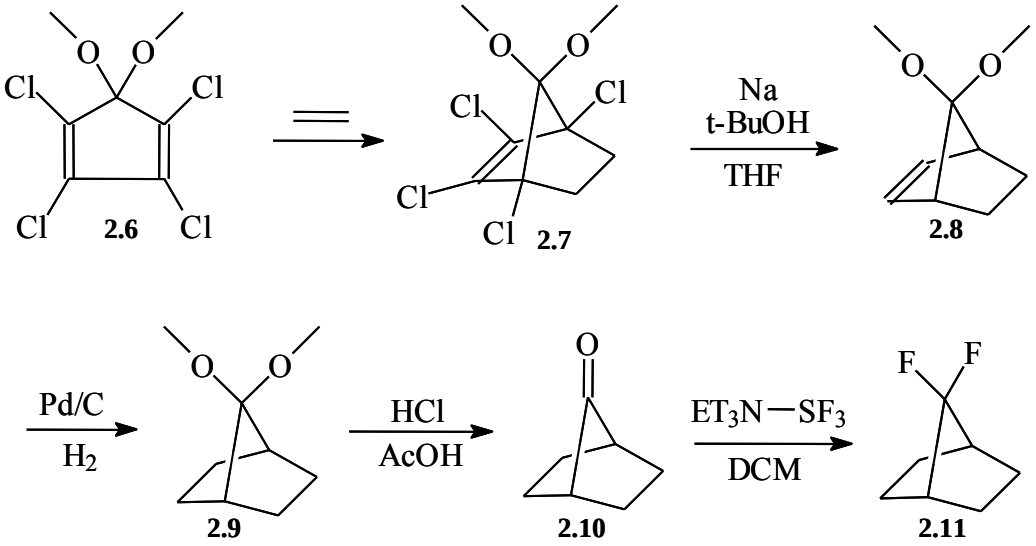

Figure 2.2: The synthesis of 7,7-difluronorbornane (**2.11**).

7-Fluoronorbornane

The last molecule to be synthesized in this series of fluorinated norbornanes was 7-fluoronorbornane. This molecule was prepared by modifying the synthesis for the di-substituted material. In order to reduce the amount of sodium required for the dehalogenation step, **2.7** was first reacted with triethyl amine and ethanol under hydrogenation conditions (palladium metal on carbon support under hydrogen atmosphere).[26] In one step, the olefin was reduced, chloride ion was eliminated, followed by reduction of the double bond that was formed, then another elimination, and finally another reduction, resulted in the dichloronorbornane (**2.12**). This new material, which had fewer chlorines than **2.7**, could be dehalogenated using fewer equivalents of sodium metal. Hydrolysis

under acidic conditions afforded the ketone (**2.10**), which was then reduced to the alcohol using sodium borohydride (**2.13**).

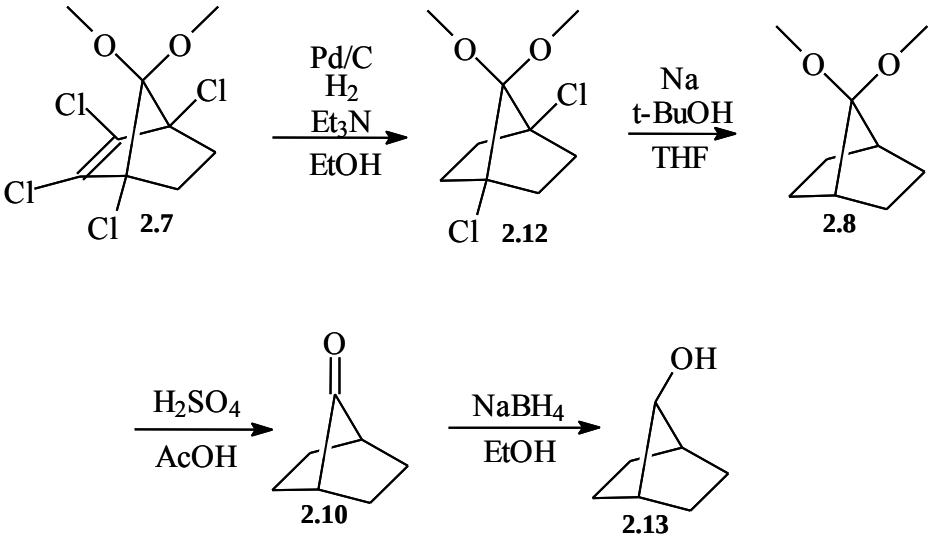

Figure 2.3: The synthesis of bicyclo[2.2.1]heptan-7-ol (**2.13**).

Many attempts were made to convert the alcohol to the monofluoride. Due to the success of DAST with molecule **2.4**, it was hoped that the reaction of **2.13** with this fluorinating reagent would be as fruitful. Unfortunately, this was not the case. The reaction was closely monitored by gas chromatography by extracting aliquots of the reaction mixture and quenching it with 5% sodium hydroxide. There were three predominant peaks on the GC chromatograph: the starting material (**2.13**, t_R=3.1 min), the monofluoride product (t_R=2.1 min) and an impurity with a relatively high retention time (t_R=9.8). These three peak areas varied depending on temperature of the reaction. At temperatures below -30ºC, the formation of the target molecule was limited, and the GC chromatograph showed

peaks for starting material and the impurity. When the reaction mixture was warmed to room temperature, the peak area of the impurity decreased and the amount of both the starting material and target molecule increased. Investigations of the impurity by ^{1}H NMR, ^{19}F NMR (no peak found) and high resolution mass spectroscopy revealed the impurity to be bicyclo[2.2.1]hept-7-yl-*N*,*N*-diethylsulfinamate (**2.15**). This observation is rationalized by considering the DAST mechanism[27] shown in figure 2.4. Due to the fact that *some* of the target molecule was formed, the reaction was repeated on a larger scale. However, it was impossible to remove other impurities from the low boiling monofluoride by either distillation or column chromatography.

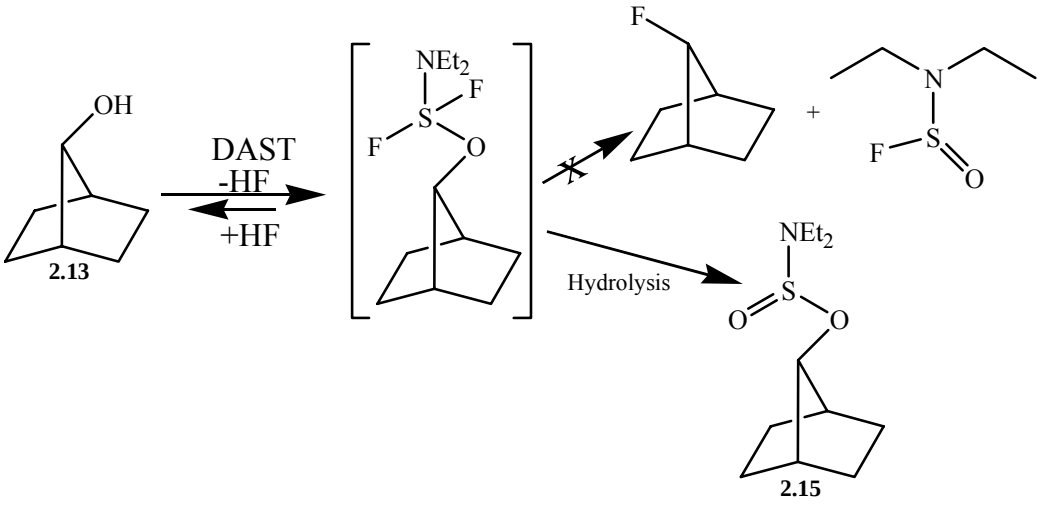

Figure 2.4: Reaction mechanism of fluorination by DAST.

Due to the discouraging results with the DAST reagent, we turned to another fluorinating reagent: (2-chloro-1,1,2-trifluoroethyl)diethylamine (**2.16**). This reagent has been reported to convert alcohols, such as cetyl alcohol and 2-

adamantanol, to fluorides in good yield.[28] This material was synthesized using a literature procedure.[29] Unfortunately, when **2.13** was treated with **2.16** at room temperature**,** GC analysis showed no evidence of the desired product. The reaction was repeated at elevated temperatures, and a variety of unidentifiable side products were formed. From the reaction that took place at room temperature, we were able to isolate a compound with a high retention time (t_R=5.7 minutes) in 46% yield. This material was determined to be bicycle[2.2.1]hept-7-yl chlorofluoroacetate (**2.17**) through spectroscopic analysis. This result can be explained by considering the mechanism by which **2.16** converts alcohols to fluorides.[30] The driving force to cleave one of the carbon-fluoride bonds of **2.16** relies on the equilibrium between the reagent and the iminium fluoride. The iminium fluoride then reacts with the alcohol of the starting material to produce the alkyl fluoride and 2-chloro-*N*,*N*-diethyl-2-fluoroacetamide (**2.17**). In the case of **2.13**, we postulated that the alcohol from the starting material reacted with the iminium fluoride, and this intermediate was hydrolyzed during workup, resulting in the formation of **2.17** (figure 2.5).

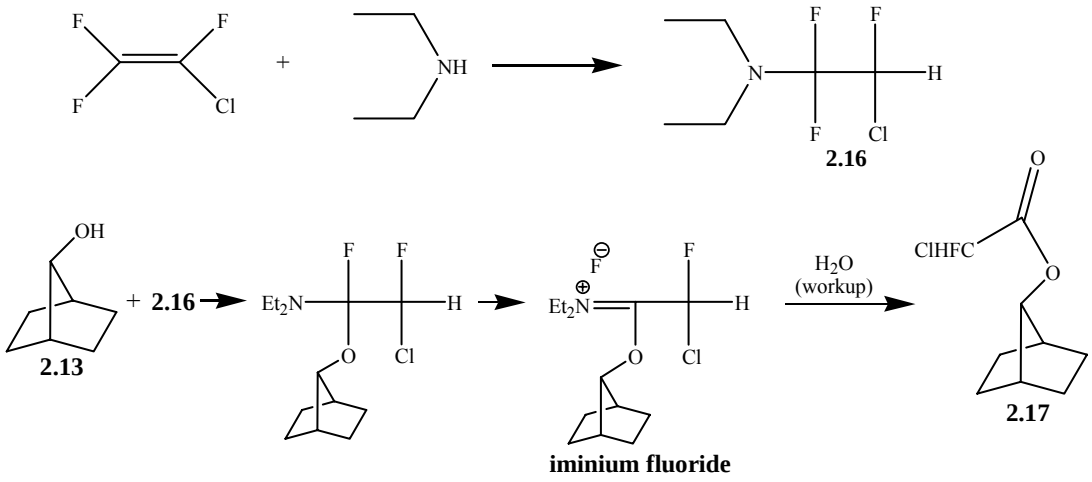

Figure 2.5: The synthesis of **2.16** and the formation of **2.17**.

It should be noted that **2.13** was reacted with 70% hydrogen fluoride / 30% pyridine reagent, which has been reported[31] to successfully convert a variety of secondary and tertiary alcohols to the alkyl fluoride. No reaction took place with this reagent.

After attempts to fluorinate **2.13** with three different fluorinating reagents were unsuccessful we reviewed the reactivity of the 7 position of bicyclo[2.2.1]heptane system and found that "7-chloronorbornane is legendary in its inertness to normal ionization conditions."[32] With this information in mind, we thought that the desired substitution would be facilitated with the replacement of the hydroxyl group with a better leaving group. Norbornane **2.13** was reacted under conventional conditions in order to synthesize the triflate **2.18**. The triflate was then treated with dry cesium fluoride at elevated temperatures in order to produce the desired 7-fluorobicyclo[2.2.1]heptane (**2.19**, figure 2.6). Cesium fluoride was chosen as the fluorinating reagent in attempts to minimize side reactions. Great care in purification by column chromatography and sublimation,

including solvent removal by vacuum distillation, allowed isolation of this extremely volatile product in its purest form.

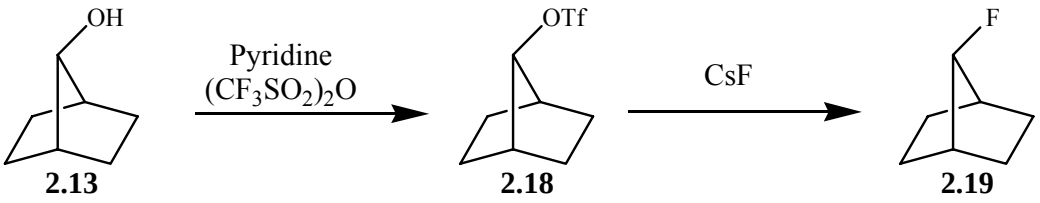

Figure 2.6: The successful synthesis of 7-fluorobicyclo[2.2.1]heptane (**2.19**).

Due to the discovery of the surprising lability of the monofluoro derivatives to "glass catalyzed" elimination, vicinal substitution was determined to be less attractive from a practical synthetic perspective than the more stable, geminally disubstituted isomers. Such model compounds were not prepared.

V-UV Absorbances of Fluorinated Norbornanes

The VUV spectra of all of the fluorinated model compounds are presented in figure 2.7. This study has demonstrated that absorbance in this region relies not only on the number of fluorines substituted on the norbornane ring but also, and perhaps more importantly, on the position of the substitution. As seen in figure 2.7, substituting two hydrogens for two fluorines leads to a higher transparency at 157 nm than substitution with only one fluorine. This was to be expected, since Kunz et al.[18] reported that a 100 % fluorinated hydrocarbon polymer had a significantly lower absorbance than a hydrocarbon polymer that was 30% fluorinated. The VUV spectra show that introduction of geminal

fluorosubstituents on the 2-carbon bridge (**2.2**), rather than the 7-carbon bridge (**2.11**) is the most effective substitution pattern. From a polymer synthesis standpoint, the important implication from this data is that perfluorination is not necessary in order to synthesize a relatively transparent polymer for use as a 157 nm resist material.

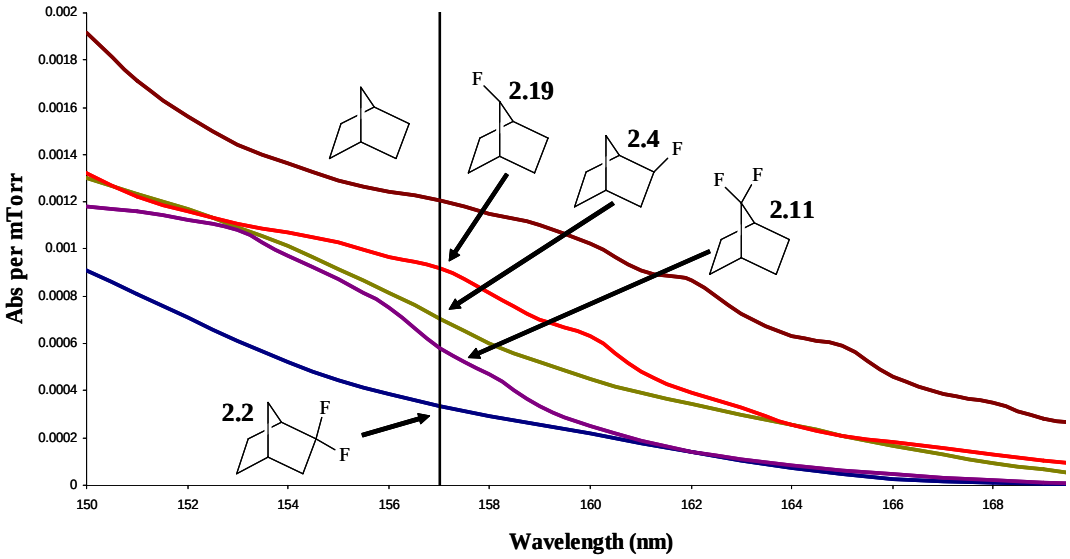

Figure 2.7: The VUV absorbances of various fluorinated norbornanes.

The Hexafluoroisopropanol Group

The spectroscopic study above demonstrated that although poly(norbornane) has a very high optical density at 157 nm, the possibility of incorporating a norbornane unit into a resist polymer existed if the alicyclic ring took advantage of key substitution patterns. Therefore, a candidate for the etch

resistant moiety of a 157 resist had been established. While this was encouraging progress, but there were still unknowns in this area. The backbone, acidic group, and protecting group moieties for a 157 resist had yet to be recognized. With the provided spectroscopic data at hand, further work by others in this group identified fluorinated materials that could be incorporated into each of the modules of the photoresist polymer. The hexafluoroisopropanol group, like **2.2**, contains geminally-substituted groups (trifluoromethyl) that are strongly electron-withdrawing, and when incorporated into a polymer greatly enhances transparency at 157 nm[20]. Furthermore, the hexafluoroisopropanol group is an example of a hydroxyl group that is fairly acidic as a result of inductive stabilization of the conjugate base. The two trifluoromethyl groups adjacent to the alcohol moiety result in acid strengths near that of phenol ($pK_a \sim 11$).[33] Our group extended this information in the development of a fluorinated, norbornane-based photoresist that utilized the hexafluoroisopropanol moiety as its acidic group, which was based on a material originally developed for 193 nm imaging.[34] The hexafluoroisopropanol group was acetal protected in order to provide a protection group for chemical amplification. It was also believed that since the ethyl acetal protecting group contained no carbonyl functionality, transparency at 157 could be maximized. The material was incorporated into a copolymer and preliminary 193 nm imaging studies[20] demonstrated its utility in a chemically amplified resist setting (figure 2.8).

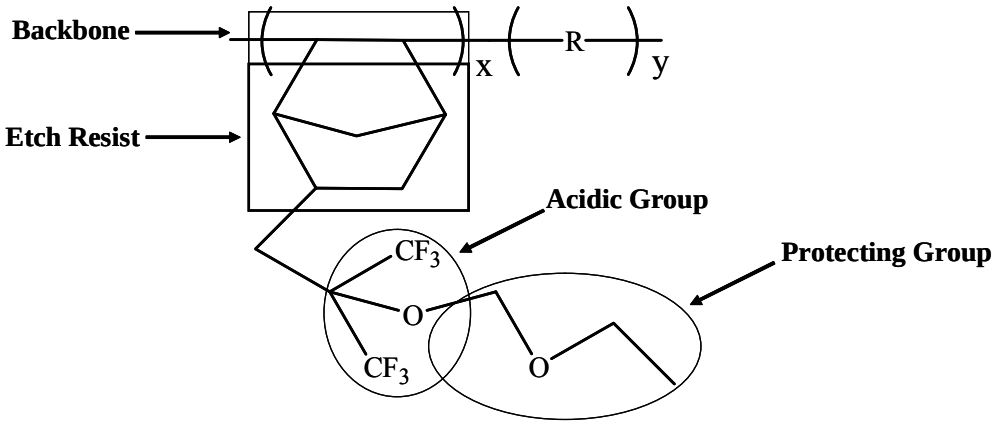

Figure 2.8: A fluorinated photoresist polymer based on a norbonane backbone/etch resist, a hexafluoroisopropanol moiety to serve as the acidic group, and an acetal protecting group for chemical amplification. The geminal trifluromethyl groups significantly enhance transparency at 157 nm. For prelimnary 193 nm imaging, this material was copolymerized with maleic anhydride (R).

While candidates for all of the four basic modules for a 157 nm photoresist had been established, it was still important to explore other transparent platforms. The high absorbance of PMMA at this wavelength implied that the carbonyl functional group would be unusable. However, all previous 248 and 193 nm photoresists utilize the carbonyl group in either the backbone, acidic group, or protecting group. Was it possible to increase the transparency of the highly absorbing carbonyl group with fluorine substitution as it was with the norbornane ring?

Modeling Studies of the Effect of Fluorine Substitution

Subsequent to the proposal to investigate the effect of fluorine on the norbornane ring at 157 nm, Matsuzawa et. al[35] released important results in which the VUV absorbances of certain fluorinated compounds were derived from

quantum mechanical calculations. It was predicted that the incorporation of trifluoromethyl groups into a molecule with ester functionality would have an extreme impact on absorbance at 157 when compared to its hydrocarbon analogue (figure 2.9). This was important information as it predicted that the high absorbance of a carbonyl group could be overcome with the incorporation of a strongly electron-withdrawing α-trifluoromethyl group.

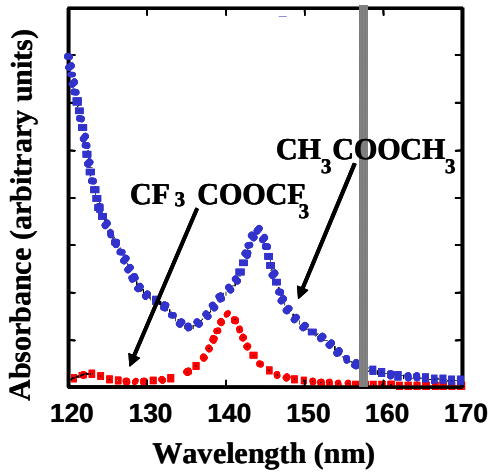

Figure 2.9: The calculated absorbance spectra of methyl acetate and its fluorinated derivative.

V-UV Studies of Fluorinated Esters

These calculations inspired us to acquire a set of esters of trifluoroacetic acid and 3,3,3-trifluoropropioic acid and to measure their absorbance at 157 nm. While trifluoromethyl trifluoroacetate can be synthesized by a photochemical reaction[36], we decided that commercially available ethyl acetate derivatives could be used to confirm Matsuzawa's prediction. We believed that the esters **2.20** and **2.21** were appropriate model compounds, and, when compared to the spectra of

ethyl acetate, would corroborate these theoretical calculations. As predicted, the addition of the trifluoromethyl group to the ester functionality causes a peak shift and dramatically improves transparency in the VUV (figure 2.10).

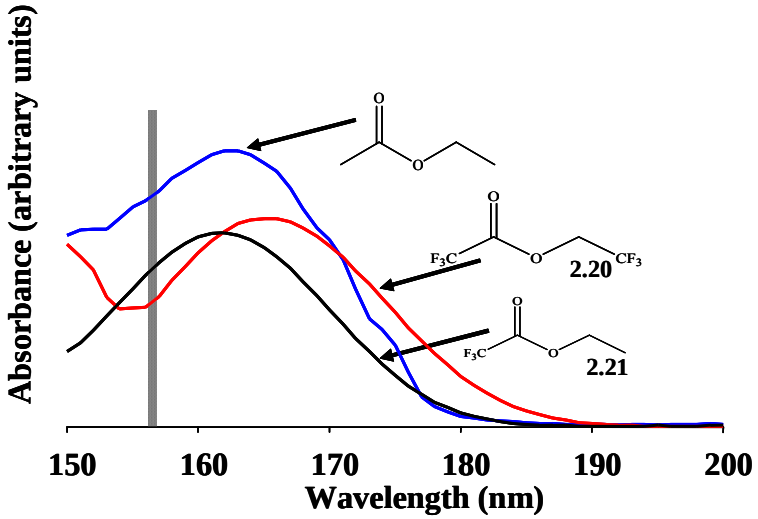

Figure 2.10: Absorbances of fluorinated ethyl acetates.

With this data at hand, it was then necessary to consider the end goal of producing a relatively transparent polymer. Ultimately, we hoped to use this gas phase data to design a backbone moiety for a 157 resist. The aforementioned ethyl acetate derivatives do demonstrate the importance of a trifluoromethyl group, but it was difficult to extend these molecules to a polymer backbone design. Knowing that a methacrylate backbone was commonly used in 193 nm resist technology, we were inspired to synthesize molecules that could be indicative of the absorbance of a fluorinated PMMA. The model compound 2,2,2-trifluoroethyl 3,3,3-trifluropropionate (**2.22**) was prepared from the corresponding acid and alcohol with dicyclohexylcarbodiimide (DCC) and dimethylamino pyridine (DMAP). Since even a small impurity can affect absorbance spectra, solvent was not used in

the reaction because its complete removal was difficult due to the low boiling point of the product. As shown in figure 2.11, β-fluorination of the alkyl ester generates a hypsochromic shift that reduces absorbance at 157.

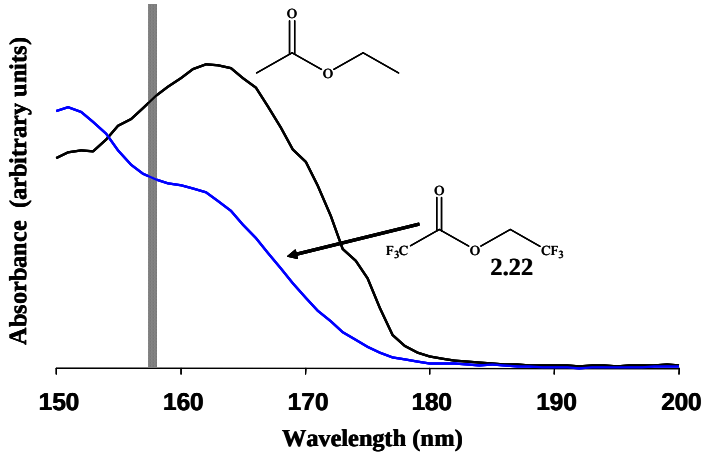

Figure 2.11: Absorbances of fluorinated esters.

Model compound **2.22** is a unique molecule with a structure that inspires a monomeric species. We envisaged that if this trifluoroethyl trifluropropionate was relatively transparent at 157 nm, then the polymer of a 2-trifluoromethylacrylate should be relatively transparent as well (figure 2.12). The next chapter will describe efforts to synthesize poly(methyl 2-trifluoromethylacrylate) and various resist polymers with 2-trifluromethacrylates in the backbone moiety for exposure at 157 nm.

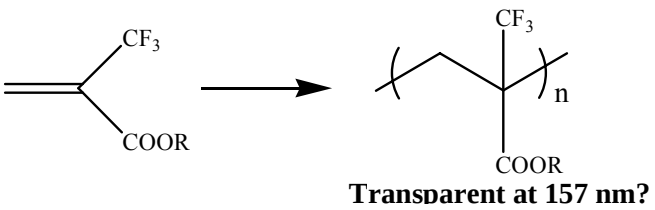

Figure 2.12: A 2-trifluromethylacrylate and its homopolymer.

CHAPTER 3: 2-TRIFLUOROMETHYLACRYLATES AS BACKBONES FOR 157 nm PHOTORESIST POLYMERS

Poly(methyl 2-trifluoromethylacrylate) received much attention in the early 1980's as a resist material for electron beam (e-beam) lithography. Resist polymers for e-beam lithography must undergo main-chain scission upon exposure to radiation.[37] This drastic decrease in molecular weight causes the exposed regions of resist, which were insoluble in developer before exposure, to become soluble. PMMA, the most common e-beam resist, has a number of advantageous processing characteristics but lacks the radiation sensitivity necessary for high production throughput.[38] Considerable effort[39-41] has been focused on placing strong electron withdrawing groups on the main-chain of PMMA in order to increase its sensitivity to radiation. One of the most successful examples of such an effort was the development of poly(methyl 2-trifluoromethylacrylate).[42] The introduction of the trifluoromethyl group in the main-chain significantly increases e-beam sensitivity when compared to PMMA, but does not render the material susceptible to cross-linking as it does when the methacrylate main-chain is substituted with only a single halogen atom[39].

Methyl 2-Trifluoromethylacrylate Reactivity

The trifluoromethyl group also effects the reactivity of methyl 2-trifluoromethylacrylate (MTFMA) toward polymerization. Ito et al.[42] reported that attempts to homopolymerize this monomer with free radical initiation with either azobis(isobutronitrile) (AIBN) or benzoyl peroxide (BPO) were unsuccessful. However, while this material would not radically homopolymerize, MTFMA

could be free-radically copolymerized with methyl methacrylate. The reactivity of these two monomers (MTFMA: M_1 and methyl methacrylate: M_2) were determined assuming the terminal model of copolymerization[43] (figure 3.1). The reactivity values were determined to be $r_1 = 0$ (MTFMA does not self propagate) and $r_2 = 2.36$. In order to obtain a copolymer with almost 1:1 alternation, a high concentration (~ 80%) of MTFMA was required in the feed.

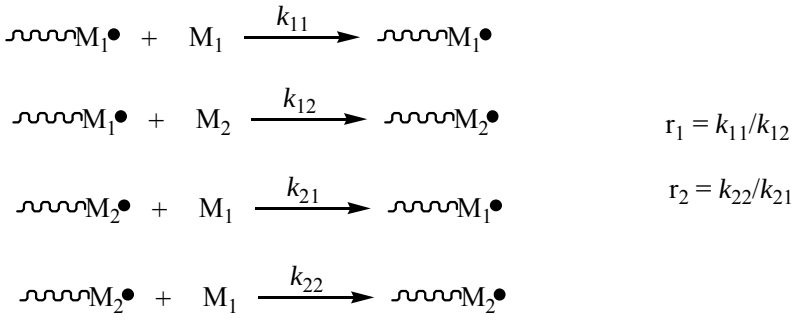

Figure 3.1: The terminal model of copolymerization, where $M_1\cdot$ represents a propagating chain ending in M_1, k_{11} is the rate constant for a propagating chain ending in M_1 adding to M_1, and so on. Since MTFMA (M_1) does not self propagate, $r_1 = 0$.

It should be noted that shortly after Ito's results were published, Iwatsuki et al.[44] reported some success with the free radical homopolymerization of MTFMA with AIBN and PBO, although polymer conversion to was low, the required reaction time was long (~8 days), and molecular weights were moderate (M_n ~ 9000). The determined reactivity ratios for the copolymerization of MTFMA and methyl methacrylate were $r_1 = 0.1 \pm 0.1$ and $r_2 = 2.3 \pm 0.2$, which are in good agreement with the values determined by Ito et al.[42]

While copolymers of MTFMA and methyl methacrylate would be more sensitive to e-beam radiation than poly(methyl methacrylate), a homopolymer of MTFMA would, in principle, take the most advantage of a strongly electron withdrawing group on the main chain of an e-beam resist polymer. Ito et al. reported the anionic homopolymerization of MTFMA with pyridine initiation[42] and then later with bases such as potassium cyanide, potassium acetate and potassium *tert*-butoxide.[45] Interestingly, typical anionic initiators for methyl methacrylate, such as *n*-BuLi and phenyl magnesium bromide, result in a very sluggish polymerization of MTFMA. When these organometallic reagents were reacted with MTFMA, GC/MS analysis showed that the *n*-butyl group adds to the β-carbon of MTFMA, and the adduct further reacts with *n*-BuLi resulting on attack of the trifluoromethyl moiety.[45]

Synthesis of Poly(Methyl 2-Trifluoromethylacrylate)

Due to the interesting VUV spectroscopic results of the model compound 2,2,2-trifluoroethyl-3,3,3-trifluropropionate (**2.22**), we proceeded to synthesize MTFMA using a modification of the published method of Buxton et al.[46] Trifluoroacetone (**3.1**) was reacted with sodium cyanide under acidic conditions to form the corresponding cyanohydrin (**3.2**), which was then reacted with methanol and one equivalent of water to convert the cyano group to the methyl ester (**3.3**). The hydroxyl group of the methyl ester was converted to the acetate (**3.4**), which was then slowly fed down a custom built pyrolysis column filled with pieces of quartz tubing and wrapped in heating tape which was heated to 500ºC. The ester acetate was converted to MTFMA (**3.5**) with acetic acid as a side product. This

was a highly successful reaction scheme with a total yield of over 50%, and could provide large quantities of this monomer at one time. Finally, MTFMA was anionically homopolymerized with potassium acetate and 18-crown-6 to form poly(methyl 2-trifluoromethylacrylate) (**3.6**).

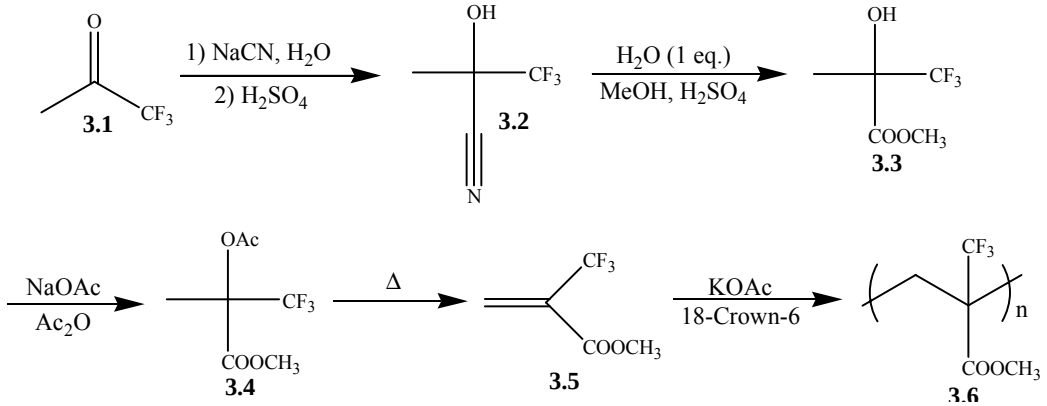

Figure 3.2: The synthesis of MTFMA. The overall yield of this monomer was over 50%.

Once the polymer was prepared, its transparency at 157 nm was investigated using variable angle spectroscopic ellipsometry (VASE). This spectroscopic technique is used to examine the absorbance of polymeric films in the VUV by spin-coating the polymer onto a silicon wafer and placing it in an evacuated chamber. The tool measures changes in the polarization state of light reflected from a sample surface, and this polarization change can be used to measure film thickness and absorbance.[47] VASE measurements showed that poly(methyl 2-trifluoromethylacrylate) had an absorbance of 2.76 μm^{-1} at 157 nm. As we had hoped, the substitution of the trifluoromethyl group had a significant

effect on the absorbance of this material: its hydrocarbon analogue, PMMA, had an absorbance of 5.69 μm^{-1} (figure 3.3).

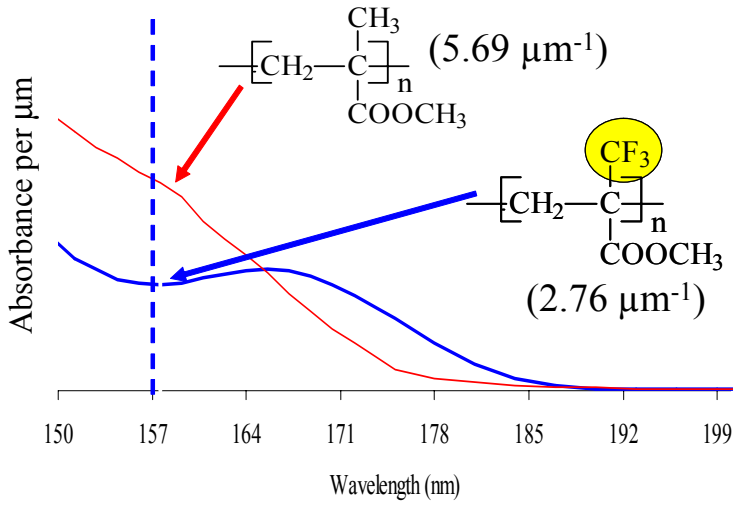

Figure 3.3: The absorbance of poly(methyl 2-trifluoromethylacrylate) at 157 nm**.**

Now that a candidate for the backbone moiety of a 157 nm resist was identified, we next had to determine how to develop a resist polymer utilizing the relatively transparent 2-trifluoromethylacrylate backbone. What immediately came to mind were the IBM Version 1 and Version 2 193 nm resist polymers[48] that were mentioned in Chapter 1, which were based on a methacrylate backbone. These materials possessed good processing characteristics and resulted in high contrast features upon exposure. It was hoped that a 2-trifluoromethylacrylate version of such a resist would possess similar attributes.

Esters of 2-Trifluoromethylacrylate

In order to create a resist polymer based on a 2-trifluoromethylacrylate backbone, it would be necessary to prepare other esters of the fluorinated acrylate besides methyl. The *tert*-butyl ester was needed for chemical amplification. A carboxylic acid needed to be incorporated into the resist polymer for aqueous base development, but any monomer containing such a group had to be protected for base initiated anionic polymerization, and then deprotected. Since the pyrolysis route in figure 3.1 afforded large quantities of MTFMA, we tried to hydrolyze the methyl ester to the carboxylic acid, which could then, in principle, be esterified using a wide variety of techniques. Soaponification reactions were run in D_2O with either sodium bicarbonate or sodium carbonate at 50ºC for 1 hour and monitored by ^1H NMR. Neither reaction produced the carboxylic acid. The developments of peaks at δ 3-4 and the reduction of peaks at δ 6-7 was indicative of a hydrated monomer and oligomers (figure 3.4).

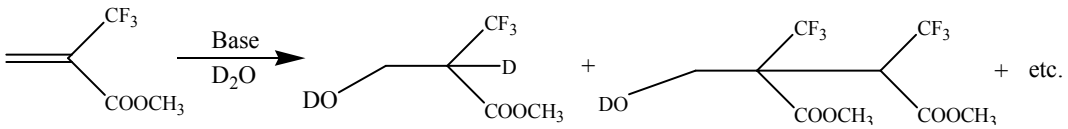

Figure 3.4: Possible ^1H monitored reaction of MTFMA with base.

Reaction with lithium iodide in DMF (S_N2) also resulted in the formation of oligomeic products. We then focused our attention to protecting the double bond with a Diels-Alder cycloaddition, hydrolyzing to the carboxylic acid, and then heating to induce the retro Diels-Alder, resulting in the desired 2-trifluoromethylacrylic acid. The cycloaddition between MTFMA and

cyclopentadiene was a success, but the subsequent hydrolysis did not proceed cleanly. Attempts to perform the Diels-Alder between MTFMA and furan were also unsuccessful due to extremely slow rates of reaction.

After many ineffective attempts to hydrolyze the methyl ester to 2-trifluoromethylacrylic acid, we explored alternative ways to prepare the desired molecule. Fuchikami et al.[49] reported the preparation of the carboxylic acid by the palladium complex catalyzed carbonylation of 2-bromo-3,3,3-trifluoropropene (figure 3.5). This procedure was successfully repeated, and thus afforded a method to produce reasonable quantities of the needed monomer (**3.7**).

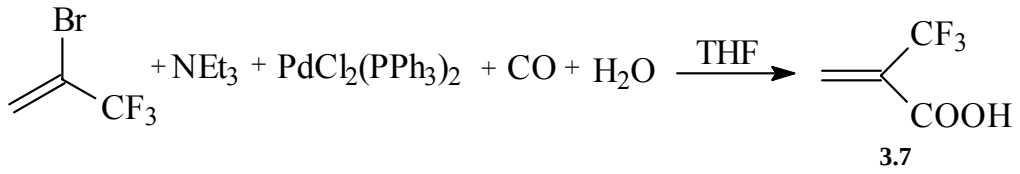

3.7

Figure 3.5: The palladium catalyzed carbonylation synthesis of 2-trifluoromethylacrylic acid reported by Fuchikami et. al.

Once quantities of the acid could be prepared, the next goal was esterification. Monomer **3.7** could be easily converted to the *tert*-butyl ester (**3.8**) by reaction with isobutene and a catalytic amount of H_2SO_4 (figure 3.6)

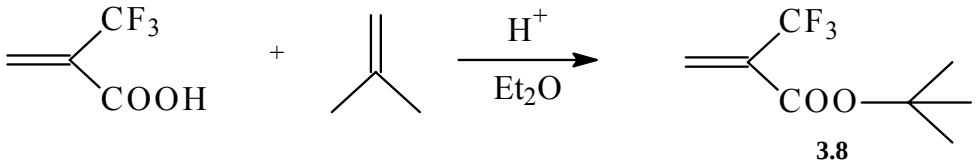

3.8

Figure 3.6: *Tert*-butyl 2-trifluromethylacrylate (**3.8**).

The carbonylation of 2-bromo-3,3,3-trifluoropropene was repeated, using benzyl alcohol instead of water in the hope of synthesizing the benzyl ester, which could be used as the protecting group for base catalyzed anionic polymerization. Unfortunately, only dibenzyl ether and benzyl 2-phenylacetate were obtained and none of the expected product was formed.

We also looked to modify the pyrolysis route used to synthesize MTFMA. In this case, only the most robust esters could be considered, as the last step in the synthesis was exposure to a 500ºC glass column. We envisaged that a benzyl ester could withstand such conditions. This monomer could be incorporated into a copolymer and then subjected to traditional hydrogenation conditions to deprotect the benzyl ester, resulting in the desired carboxylic acid. The synthesis of benzyl 2-trifluoromethylacrylate was accomplished by reacting the cyanohydrin of trifluoroacetone (**3.2)** with methanol and an excess of water under acidic conditions to give the carboxylic acid (**3.9**). The alcohol of **3.9** was converted to the acetate (**3.10**), and the carboxylic acid was deprotonated with 1-8-diazabicyclo[5.4.0]undec-7-ene (DBU) and reacted with benzyl chloride to form the benzyl ester (**3.11**). This molecule was then subjected to pyrolysis conditions to form the desired benzyl ester (**3.12**). While not as highly yielding as the process in figure 3.2, this procedure produced an important component in the development of resist polymer based on a 2-trifluoromethylacrylate backbone (figure 3.7).

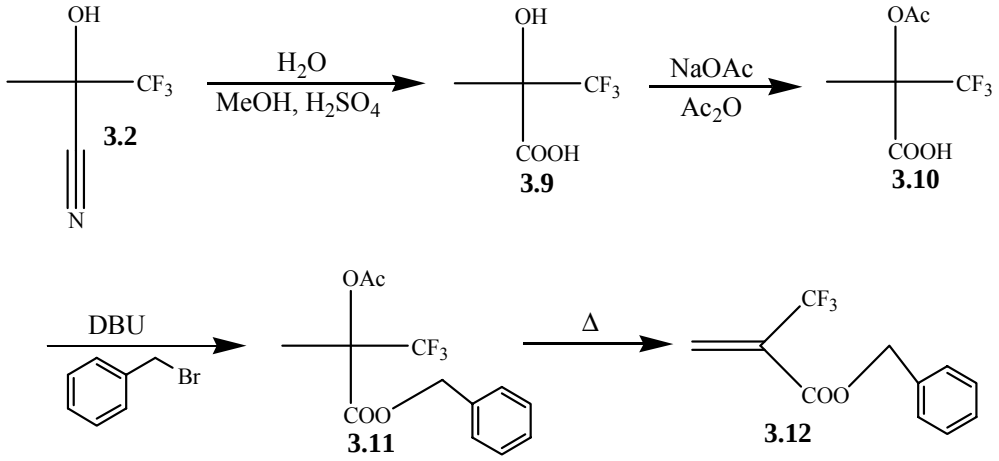

Figure 3.7: The synthesis of benzyl 2-trifluromethylacrylate.

A 157 nm Resist Polymer with a 2-Trifluoromethylacrylate Backbone

Once all of the desired monomers were obtained, they could be incorporated into a copolymer. MTFMA (**3.5**), *tert*-butyl trifluoromethacrylate (**3.8**) and benzyl 2-trifluoromethacryate (**3.12**) were copolymerized in bulk using potassium acetate and 18-crown-6. The resulting viscous solution was dissolved in THF and precipitated into hexanes, affording a white polymer (figure 3.8). The monomer composition can be determined by ^{1}H NMR by examining methyl ester (-C$\underline{H}_3$), *tert*-butyl ester (-C(C$\underline{H}_3$)$_3$), and benzyl ester (-C$\underline{H}_2$(Ph)) peaks. The copolymer was then redissolved with ethyl acetate and treated under typical hydrogenation conditions using palladium on carbon under hydrogen atmosphere. The hydrogenated copolymer was precipitated affording a white powder (**3.14**) which has a glass transition temperature (T_g) of approximately 95ºC.

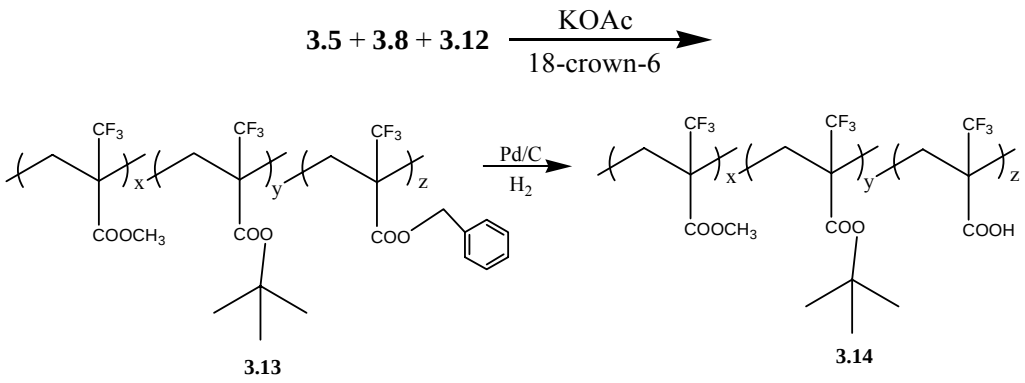

Figure 3.8: The synthesis of a fluorinated resist polymer with a 2-trifluoromethylacrylate backbone.

As expected, VASE spectroscopy showed promising results. Copolymer **3.14** has an absorbance of 3.0 μm^{-1}. As shown in figure 3.9, the 2-trifluoromethylacrylate copolymer had an absorbance that was many orders of magnitude less than UV-6, a 248 nm photoresist that was used at the time to qualify the first 157 nm exposure tools.

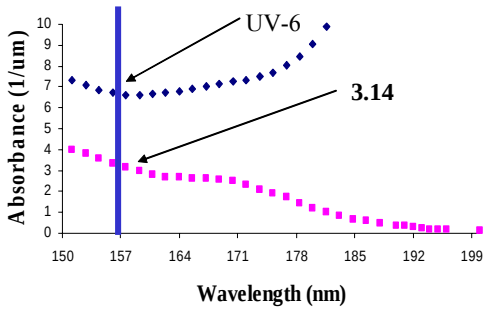

Figure 3.9: The VASE spectra of copolymer **3.14**. UV-6 is a 248 nm photoresist that was used to test the first 157 nm steppers.

157 nm Imaging

The final "test" for the 2-trifluoromethylacrylate backbone as a resist polymer was to examine its imagability. This was a daunting task as the monomer loading in the copolymer had to be tuned so as to provide proper resist behavior.

For example, the first 2-trifluoromethylacrylate backbone resist polymers to be imaged were prepared with less than 35% *tert*-butyl ester and more than 25% carboxylic acid in the polymer backbone ($y < .35$ and $z > .25$). Any structures produced from imaging these copolymers displayed very poor contrast. Due to the high amount of soluble carboxylic acid and low amount of protecting group, unexposed areas of the resist actually developed away. When the polymer was prepared with too little of the acidic group ($y > .44$, $z < .14$), it was so highly inhibited that all of the exposed regions did not develop away. Ultimately, the material that exhibited the most successful imaging properties consisted of 31 % methyl ester, 50 % *tert*-butyl ester, and 19 % carboxylic acid. As shown in figure 3.10, 157 nm exposure using the x=31, y=50, and z=19 version of **3.14** as a resist polymer resulted in structures with dimensions as low as 120 nm. However, these materials still show somewhat poor contrast, and structure quality can probably be improved with further imaging studies.

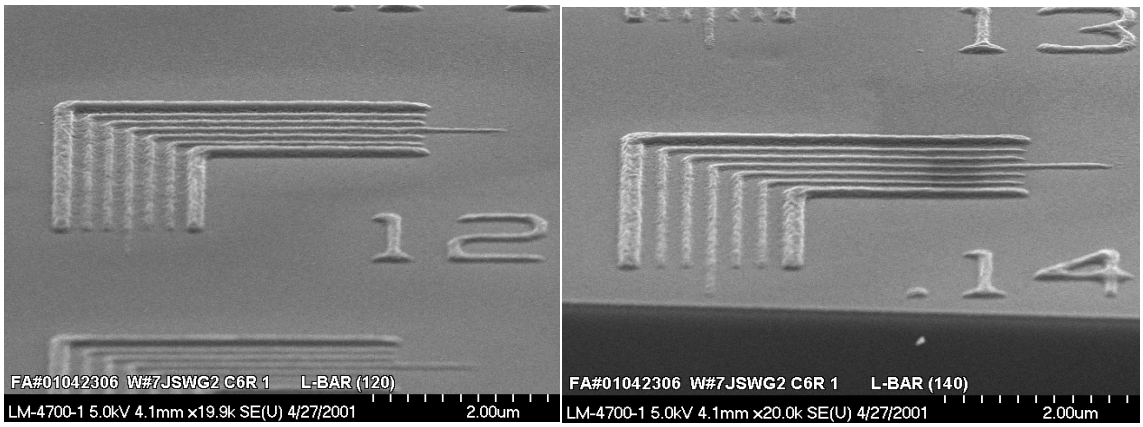

Figure 3.10: SEM pictures of the images produced with resist polymer **3.14** (x=31, y=50, and z=19). The structures on the left have 120nm dimensions, while the structures on the right are 140 nm. The film thickness is 130 nm.

An Etch Resistant 2-Trifluoromethylacrylate Resist Polymer

While the above resist polymer did show promise, it was not a "resist" in the true sense of the word as it had no etch resistant component. The next logical step in the acrylate platform was to design a material with an etch resistant ester that could be copolymerized into a resist material. In order to do so, we were again faced with the task of preparing esters of 2-trifluoromethylacrylate. Since the carbonylation reaction could produce quantities of 2-trifluoromethylacrylic acid, we chose to try traditional esterification methods on that molecule. Conversion of the acid to the acid chloride followed by reaction with a primary and secondary alcohols was most successful. An excess of phthaloyl dichloride was reacted with 2-trifluromethacrylic acid to form the acid chloride (**3.15**). The high boiling phthaloyl dichloride reagent was chosen because the target molecule could be easily removed from it by distillation. The 2-trifluoromethylacryloyl chloride (**3.15**) could then be reacted with norborneol (**3.16**) and adamantanol (**3.17**) to provide etch resistant esters, as well as benzyl alcohol (**3.12**) for the protected ester for anionic polymerization.

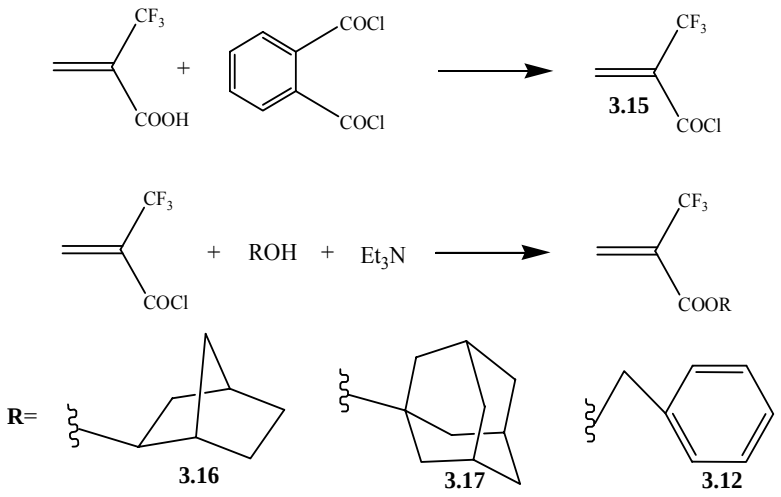

Figure 3.11: The synthesis of 2-trifluromethylacryloyl chloride (**3.15**), norbornyl 2-trifluoromethylacrylate (**3.16**), adamantyl 2-trifluromethacrylate (**3.17**), and benzyl 2-trifluromethacrylate (**3.12**).

While **3.16** and **3.17** were certainly necessary to incorporate into a 2-trifluoromethylacrylate based resist polymer in order to achieve any degree of etch resistance, their high carbon content was sure to increase the optical density of any material they were integrated into. To solve this problem, we sought to synthesize a fluorinated alcohol that had high etch resistance characteristics. To achieve this, 1-(trifluoromethyl)ethenyl acetate (**3.18**) was reacted in a Diels-Alder fashion with cyclopentadiene to form the 2-trifluoromethyl-bicyclo[2.2.1]hept-5-en-2-yl ester (**3.19**), which was hydrolyzed with methanol and 1M NaOH to afford 2-trifluoromethyl-bicyclo[2.2.1]hept-5-en-2-ol (**3.20**). The alkene was then reduced with palladium catalyst under hydrogen pressure to give 2-trifluoromethyl-bicyclo[2.2.1]heptan-2-ol (**3.21**), which was reacted with **3.15** to give **3.22** (figure 3.12).

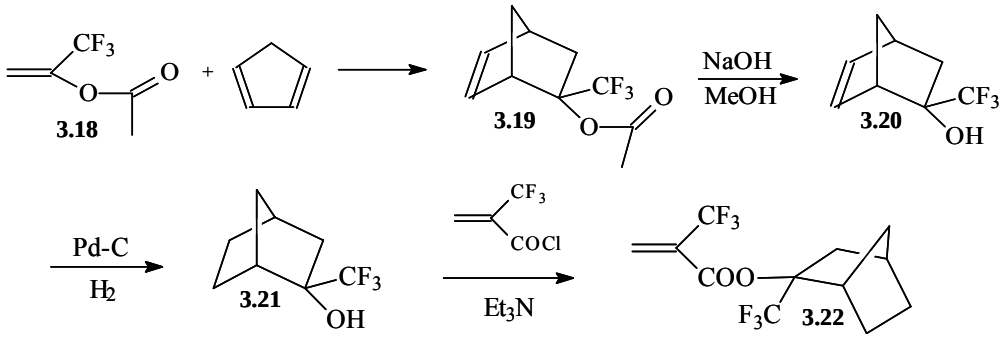

Figure 3.12: The synthesis of **3.22**.

Polymer Synthesis

Using the same polymerization/deprotection procedures used to synthesize resist polymer **3.14**, copolymers were synthesized that contained both fluorinated and non-fluorinated norbornane esters. As shown in figure 3.12, the use of the 2-trifluoromethylacrylate with the trifluoromethyl group geminal to the ester linkage has a significant effect on polymer transparency. Resist copolymer **3.23,** which incorporates acrylate **3.16**, has an absorbance of 3.1 μm^{-1} at 157 nm. Terpolymer **3.24**, which incorporates acrylate **3.22**, has an absorbance of 2.5 μm^{-1} at 157 nm. The additional trifluoromethyl group on the norbornane ring has a profound effect on polymer transparency: even with the added alicyclic ring and *tert*-butyl esters, which have significantly more carbons, copolymer **3.24** still manages to be more transparent than poly(methyl 2-trifluoromethylacrylate) (2.76 μm^{-1}).

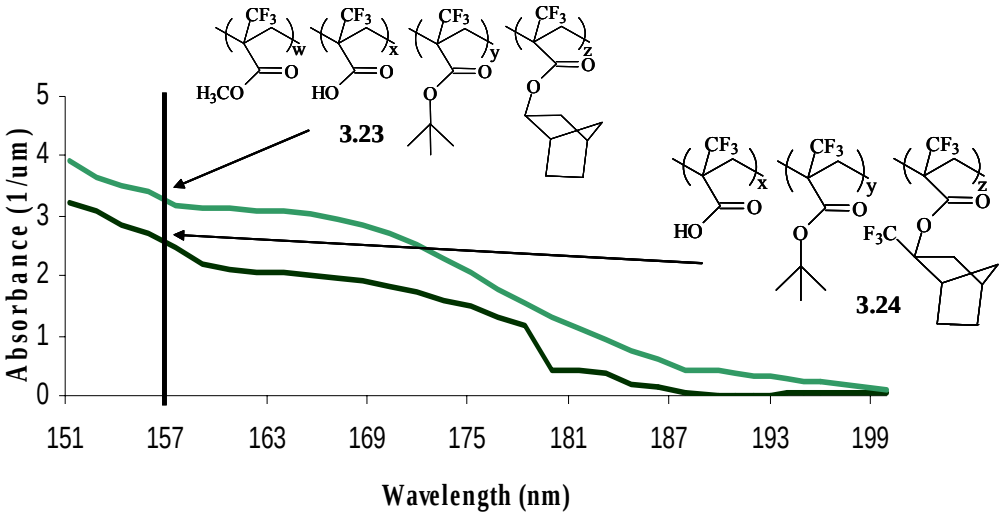

Figure 3.13: The absorbances of norbornane containing copolymers **3.23** and **3.24**.

157 nm Imaging

Imaging experiments of an etch resistant 2-trifluormethacrylate resist polymer were focused on **3.24** due to its high transparency at 157 nm. Exposure of this material at 157 nm successfully produced positive tone images. Figure 3.14 shows structures with dimensions of 190 nm. As was the case with the material that produced the images in figure 3.9, monomer incorporation has not been optimized to the point where the best image profiles are obtained. However, it was immediately apparent from initial imaging studies of terpolymer **3.24** that the norbornane incorporating copolymer demonstrated improved contrast over resist copolymer **3.14**. Another advantage of the incorporation of the norbornane ester is its steric bulk: the relatively large alicyclic ring hinders crankshaft rotation around the polymer backbone and raises the T_g of the material to approximately 135°C. This is in the preferable range for optimal lithographic performance.

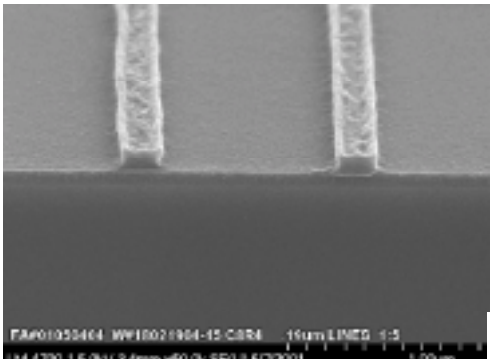

Figure 3.14: SEM images of 190 nm structures produced from resist terpolymer **3.24**. Film thickness is 120 nm.

The above examples of the 2-trifluoromethylacrylate platform show much progress in the development of resist polymers for 157 nm exposure. These materials incorporate a fluorinated backbone, which has a very low absorbance at 157 nm compared to their hydrocarbon analogues. These polymers have the ability to produce positive tone images with 157 nm exposure. Both transparency and T_g can be improved with the incorporation of a fluorinated etch resistant group. However, there are significant drawbacks, most noticeably the protection and deprotection steps that are necessary for anionic copolymerization of these monomers. The deprotection step is slow: hydrogenation to remove the benzyl ester takes over 48 hours at 50°C. Furthermore, once preparation conditions are finally worked out, extensive imaging studies are required to determine optimal imaging conditions, which invariably leads to repeating the polymer synthesis in order to produce a resist material with the desired properties (more/less inhibition, base solubility, etch resistance, etc.). Another drawback that should be mentioned

is the rapid vaporization that this polymer undergoes when examined in the scanning electron microscope (SEM). This comes as no surprise, however, since the backbone of the material is very sensitive to electron induced main chain scission.[42]

Radical Copolymerizations of 2-Trifluoromethylacrylate and Norbornene

In light of the above drawbacks, we recognized the value of the 2-trifluormethyl acrylates to 157 nm resist development, and decided to investigate how they could be incorporated into a resist copolymer backbone without the use of base catalyzed anionic polymerization. Around this time, Ito et al.[50], who were also studying the utility of 2-trifluoromethylacrylates as 157 nm resists, first demonstrated the synthesis of a radically polymerized 2-trifluoromethylacrylate/norbornene copolymer. While the homopolymerization of 2-triflouromethacrylates with radical initiators such as AIBN is at best sluggish, these materials radically copolymerize with various norbornenes in moderate yield. The most surprising fact, however, was not that the 2-trifluoromethylacrylates *do* radically copolymerize, but rather, *how*. Ito et al. reported that with even large variations in comonomer loading in the reaction, the resulting polymer displayed a nominally 2:1 (2-trifluoromethylacrylate:norbornene) polymer incorporation. The copolymerization tolerated a variety of esters of 2-trifluoromethylacrylates and a diverse range of fluorinated norbornenes. The most obvious advantage that this polymerization scheme had is that no protection step is required for successful synthesis. Also, norbornene is directly incorporated into the polymer backbone, giving the

opportunity to include many interesting, transparent functional groups to the backbone ring.

Application of Gas Phase Studies

The 2:1 radical copolymerization also afforded us with the opportunity to take advantage of the knowledge gained from the fluorine substitution study done in the gas phase that was discussed in Chapter 2. This would allow us to position strongly electron withdrawing groups on the backbone norbornane ring in such a way that polymer transparency could be maximized at 157 nm. This principle is demonstrated in figure 3.15. Two norbornane rings, each with trifluoromethyl and methyl ester functionalities were synthesized. Molecule **3.25** was previously synthesized during efforts to protect the double bond of MTFMA from oligomerizing during hydrolysis. Norbornane **3.28** was prepared by Dr. Raymond Hung by deprotonating carboxylic acid **3.26** with DBU followed by reaction with methyl iodide. The consequent olefin was reacted in a Diels-Alder with cyclopentadiene, resulting in methyl ester **3.28**. As shown in the gas phase spectrum of these two materials, norbornane **3.25** is significantly more transparent at 157 nm than **3.28**. Since both molecules have the same number of atoms, and for that matter identical functional groups, the difference in transparency must be attributed to the substitution pattern. The more transparent **3.25** has these electron withdrawing functional groups geminal to one another, which, as explained from the VUV data in figure 2.15, is the most advantageous substitution pattern Norbornane **3.28**, which has these groups vicinally substituted, does not take advantage of the most beneficial substitution pattern.

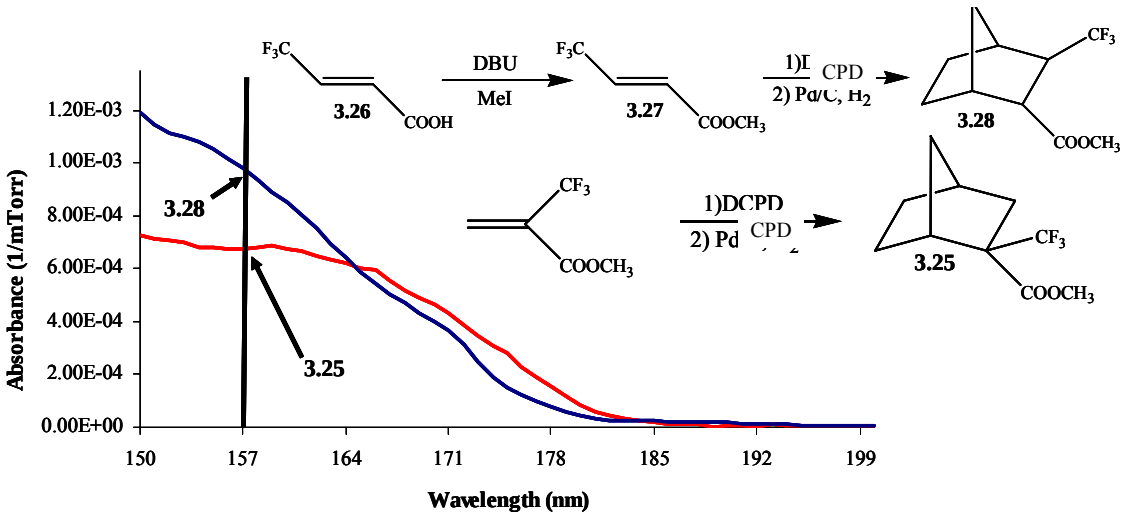

Figure 3.15: The synthesis and gas phase absorbance spectra of fluorinated norbornanes **3.25** and **3.28**.

Other Fluorinated Norbornanes

Another interesting fluorinated norbornene that could be incorporated into a "2:1" backbone is **3.20.** Originally intended as a precursor to an etch resistant ester of 2-trifluoromethylacrylate, this geminally substituted norbornene contains a trifluoromethyl group for transparency and an alcohol for increased polarity. While not acidic enough to be soluble in aqueous base developer, this material should provide adequate adhesion characteristics to any polymer it is incorporated into. The gas phase data in figure 3.16 show that the hydrogenated version of this material is quite transparent in the VUV.

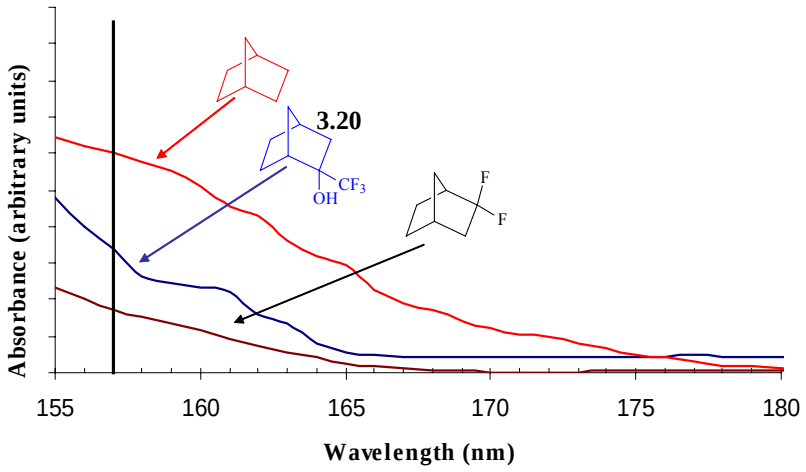

Figure 3.16: The VUV spectra of norbornane **3.20**.

The hexafluoroisopropanol norbornene (**3.29**) that was mentioned in Chapter 2 is also an attractive candidate for incorporation into a radical copolymer with a 2-trifluoromethylacrylate. As opposed to fluorinated norbornol **3.20,** this alcohol has a second trifluoromethyl group that can inductively stabilize a negative charge on the oxygen, rendering this molecule soluble in aqueous developer. The alcohol can also be *t*-boc protected (**3.30**). Exposure to acid generated from PAG will cleave off the protecting group, rendering the otherwise base insoluble material soluble (figure 3.17)

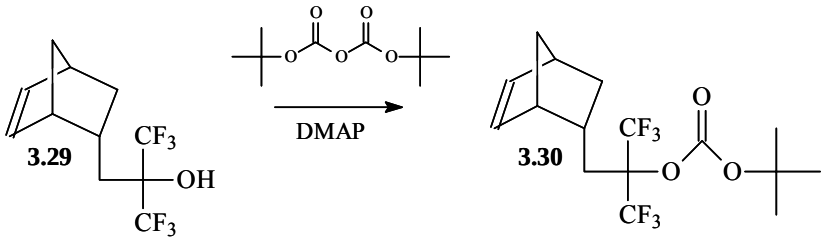

Figure 3.17: *t*-BOC protected norbornene hexafluoroisopropanol.

Novel 2-Trifluoromethylacrylates

This new radical copolymerization platform also affords the opportunity to incorporate newly functionalized 2-trifluoromethylacrylates into copolymers. In particular, we hoped to incorporate a highly fluorinated alcohol in the ester position that would serve some function as a resist component and also increase transparency at 157. The commercially available diol **3.31** is highly fluorinated, and one alcohol can be linked to an acrylate while the other can serve as an acidic group for aqueous base development. Before this was done, however, the aromaticity of **3.31** needed to be dealt with if a transparent monomer based on this material was to be designed. The aromatic ring was hydrogenated under aggressive conditions (600 psi hydrogen pressure) using rhodium on carbon support according to a literature procedure.[51] Unfortunately, this synthesis was attempted many times with little initial success. Catalysts from a number of chemical suppliers were used, but it was not until the use of rhodium on carbon supplied from Aldrich Chemical Co. that any reaction took place. Once the hydrogenated material was obtained, it was reacted with 2-trifluromethylacryloyl chloride to obtain the highly fluorinated acrylate. The target molecule could be separated from the bis-adduct and starting material by flash chromatography.

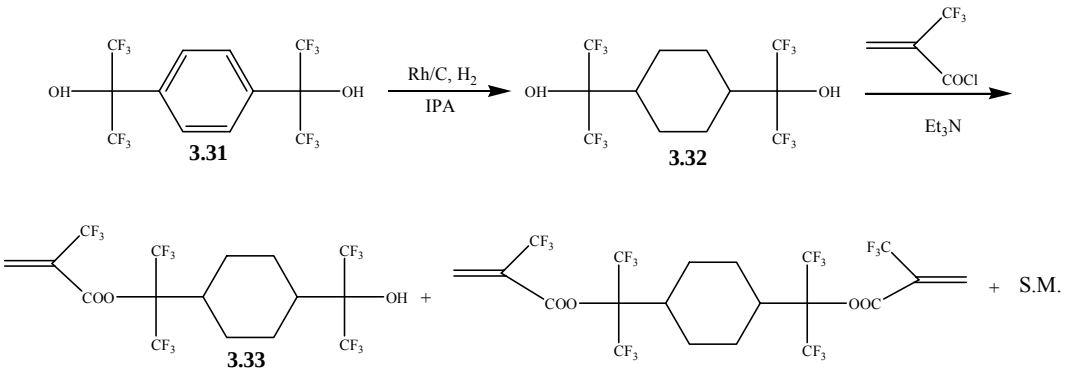

Figure 3.18: The synthesis of 2-trifluromethylacryalte of **3.33**.

Radical Copolymers

Once candidates for the 2:1 2-trifluormethacryalte/norbornene radical copolymerizations were identified, the actual polymerizations were attempted. The monomers were loaded into the reaction vessel in a 1:1 ratio with AIBN and no solvent, stirred at 80ºC, and then precipitated into a non-polar solvent. This resulted in a white polymers with molecular weights ranging from 3,000-6,000. The structures and VASE spectra of the first copolymers of this sort to be prepared in our labs are shown in figure 3.19.

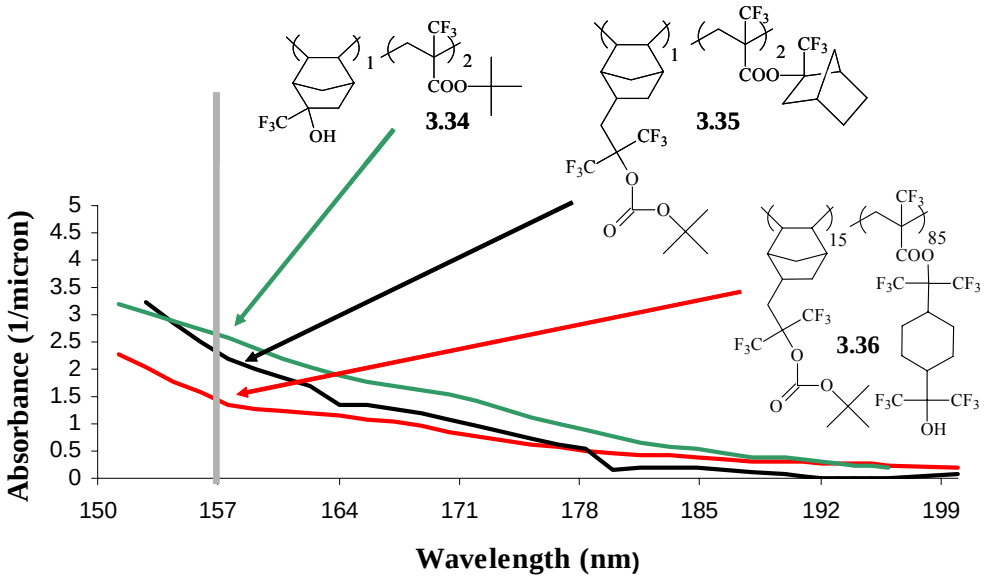

Figure 3.19: Structure and VASE spectra of initial 2-trifluormethacryalte/ norbornene radical copolymerizations.

Copolymer **3.34** incorporates *tert*-butyl 2-trifluoromethylacrylate (**3.8**) and the trifluoromethyl norobornenol **3.20**. As expected, the copolymer has 66% 2-trifluoromethylacrylate incorporation and 33% norbornene incorporation. This material has a relatively low absorbance of 2.7 μm^{-1} at 157 nm. Resist material **3.35** is a 66:33 copolymer, which has the 2-trifluoromethylacrylate designed with the fluorinated norbornane for etch resistance (**3.22**) and the boc-protected norbornene hexafluoroisopropanol (**3.30**). These monomers have a higher fluorine content than those used for copolymer **3.34**, so it was expected that **3.35** has a higher transparency at 157 nm (2.18 μm^{-1}). While **3.35** is a relatively transparent 2:1 radical copolymer, its lack of hydroxyl or carboxylic functionality prevented it from properly adhering to the silicon substrate and further imaging studies were not pursued with this material. The value of geminally substituted trifluoromethyl

groups is easily observed when one considers the 157 absorbance of resist copolymer **3.36**. This material also incorporates the boc-protected norbornene hexafluoroisopropanol (**3.30**) and the highly fluorinated acrylate **3.33.** Both of these monomers contain pairs of geminally-substituted trifluoromethyl groups (2 pairs in the case of acrylate **3.33**), and as a result copolymer **3.36** has an absorbance of 1.35 μm^{-1}. This absorbance at 157 nm is extremely low, even when compared to the most successful fluorinated metal catalyzed-based resist polymers used for 157 nm lithography.[52] Interestingly, **3.36** is an example of a 2-trifluoromethylacrylate/norbornene resist copolymer that significantly deviates from the "usual" 2:1 incorporation ratio. The synthesis of **3.36** was repeated a number of times with 1:1 loadings of each monomer, and in each case the incorporation of 2-trifluoromethylacrylate **3.33** remained constant at approximately 85 %.

157 nm Imaging

Preliminary 157 nm imaging experiments with copolymer 3.34 produced structures with 120 and 130 dimensions (figure 3.20). Compared to the lithographic results of the anionic 2-trifluoromethylacrylate resist polymers, these materials produced high contrast images that left no residue in the unexposed areas. The biggest drawback to this platform is the high PAG loading (15 wt%) and high exposure dose (74mJ/cm^2) necessary to attain these images. This is most likely due to a number of factors. While 33% of the copolymer is unprotected, the exposed alcohol is not acidic enough to offer any initial base solubility. The remainder of the polymer is 66% protecting group in the form of a *tert*-butyl ester.

Similar copolymers of this 2-trifluoromethylacrylate have been reported[53] to have a very poor contact angle with water, which leads to poor base solubility after exposure. As expected, a film of copolymer 3.34 had a high contact angle (75º) with water. Since the resist polymer is relatively hydrophobic before exposure, the majority of these protection sites must be cleaved to expose a high amount of carboxylic acid in order to invoke a base solubility switch. To do so may require a high amount of acid and energy to make the exposed regions base soluble.

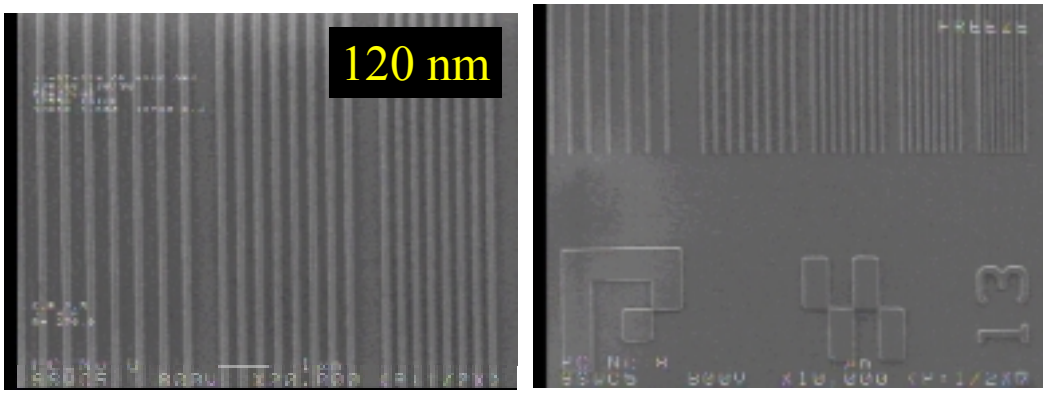

Figure 3.20: SEM images of 120 nm (left) and 130 nm (right) structures of resist polymer **3.34** produced with 157 nm exposure. The images are 130 nm thick.

Next, resist polymer 3.36 was formulated in order to investigate its lithographic capabilities. This material is extremely transparent, and hopes for its lithographic performance were high. However, when this material was exposed to 157 nm light, the exposed regions of the film remained base insoluble. This was a very surprising result. While the material is a copolymer of two different monomers, each monomer contained the hexafluoroisopropanol moiety which is sufficiently acidic to be base soluble. The copolymer was only 15% boc-

protected, and in most instances this would not be enough protecting group to *inhibit* dissolution. But in this case, no film dissolution occurred at all. Since the polymer consisted of 85% monomer 3.33, we chose to investigate this material's solubility in base developer.

Investigation of Polymer Solubility

In order to see how the highly fluorinated 2-trifluoromethylacrylate 3.33 was affecting copolymer solubility, we decided to make its homopolymer. This was done by *t*-boc protecting one of the alcohols of the hydrogenated bis-hexafluoroisopropanol cyclohexane, reacting the second alcohol with 2-trifluromethylacryloyl chloride, anionically polymerizing the acrylate, and then deprotecting with trifluoroacetic acid (TFAA) to give the unprotected homopolymer (3.37, figure 3.21).

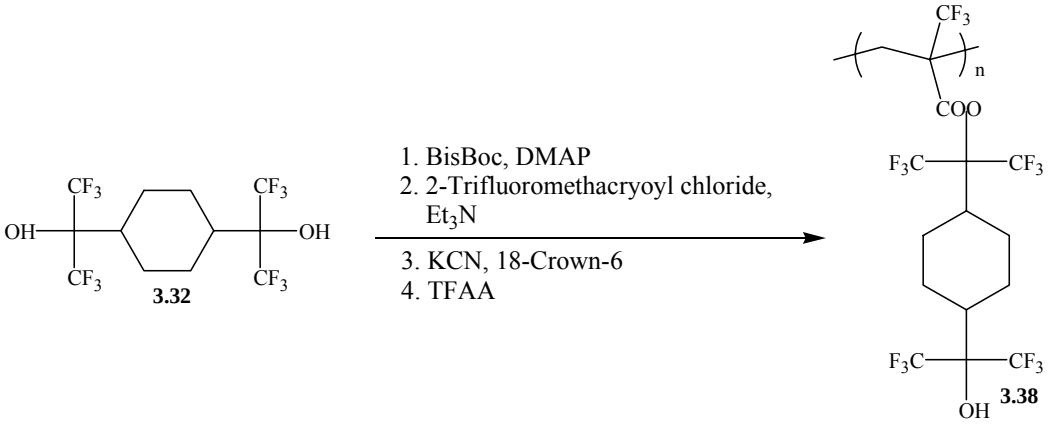

Figure 3.21: The synthesis of the homopolymer of 2-trifluromethylacrylate **3.33.**

Once the polymer was prepared, its dissolution rate in aqueous base developer could be observed. This was done by coating an approximately 600 nm thick film of homopolymer **3.38** on a silicon wafer, pouring industry standard base developer on the film, and monitoring the change in film thickness over time. The entire experiment was done using an ellipsometer which can detect slight changes in film thickness even when the film is submerged in developer. The results of the experiment are shown in figure 3.22. For comparison, the dissolution rates of homopolymer **3.38** and the homopolymer of norbornene hexafluoroisopropanol (**3.29**) are provided. As expected, the hexafluoroisopropanol homopolymer film, which was initially 600 nm thick, fully developed away in less than 3 seconds. This was not the case for the 2-trifluoromethylacrylate homopolymer. After more than 50 seconds in .26 N base developer, there was little change in film thickness. The film thickness remained unchanged for several minutes, after which time it lifted off the wafer due to adhesion failure. The data clearly demonstrate that the bis-hexafluoroisopropanol cyclohexane 2-trifluoromethylacrylate (**3.33**) is insoluble in base developer.

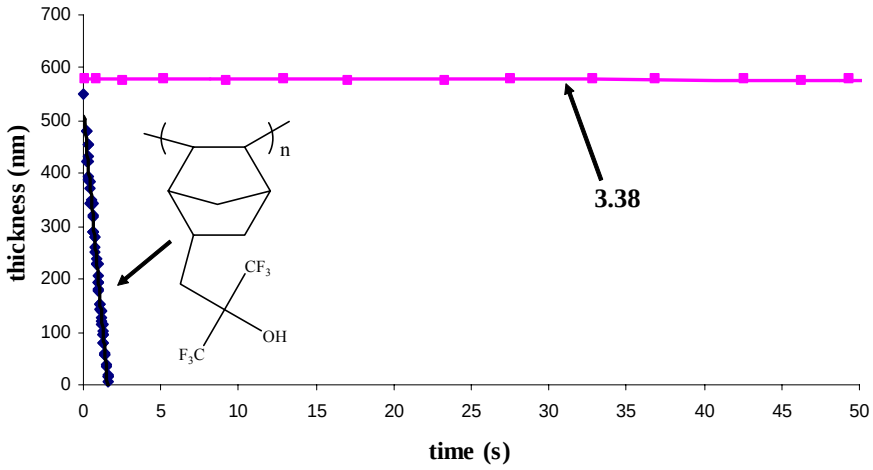

Figure 3.22: Film thickness changes in homopolymer **3.38** compared to the homopolymer of norbornene hexafluroisopropanol (**3.29**) in .26 N TMAH developer.

The Carboxylic Acid Moiety to Increase Base Solubility

Although the polymer derived from monomer **3.33** is insoluble, we still recognized its value from a transparency standpoint. The two pairs of geminal trifluoromethyl groups have a profound effect on transparency, as evidenced by the 1.35 μm^{-1} 157 nm absorbance of copolymer **3.26**. Since little could be done to increase the base solubility of the monomer, we looked to adjust the functional groups on the norbornene copolymer in order to increase the acidity of the entire resist. Upon exposure to acid, the **3.26** copolymer was deprotected, exposing an acidic alcohol (pKa ~ 11). If the deprotection exposed a more acidic carboxylic acid, then the insolubility of the highly fluorinated 2-trifluoromethylacrylate **3.33** might be overcome, rendering the exposed portions of the film soluble.

In order to incorporate a carboxylic functional group on a norbornane ring, we elected to exploit the Diels-Alder cycloaddition between 2-trifluoromethylacrylates and cyclopentadiene. This allowed for geminal substitution of a trifluoromethyl group and a protected carboxylic acid, and takes advantage of substitution patterns mentioned in figure 3.14. *Tert*-butyl 2-trifluoromethylacrylate (**3.8**) reacted rapidly with cyclopentadiene to afford the norbornene **3.39** (figure 3.23).

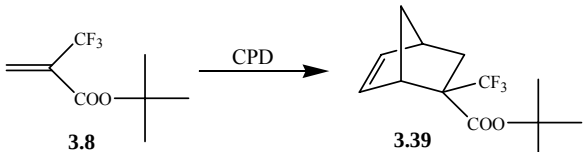

3.8 **3.39**

Figure 3.23: The synthesis of monomer **3.39.**

This monomer was then radically copolymerized with 2-trifluoromethylacrylate **3.33**, resulting in resist copolymer **3.40**. The monomer incorporation for this material was 66:33 (2-trifluoromethylacrylate:norbornene). While using a protected carboxylic acid of this type may be advantageous because it increases copolymer solubility, there is a transparency price to be paid. VASE spectroscopy showed that copolymer **3.40** has an absorbance of 2.15 μm^{-1} at 157 nm. This is substantially higher than the 157 absorbance of copolymer **3.26** (1.35 μm^{-1}). While both materials contain the highly fluorinated monomer **3.33**, the incorporation of norbornene monomer **3.39,** which has only one trifluoromethyl group, does not have the impact on absorbance that geminally-substituted trifluoromethyl groups (norbornene hexafluoroisopropanol) have.

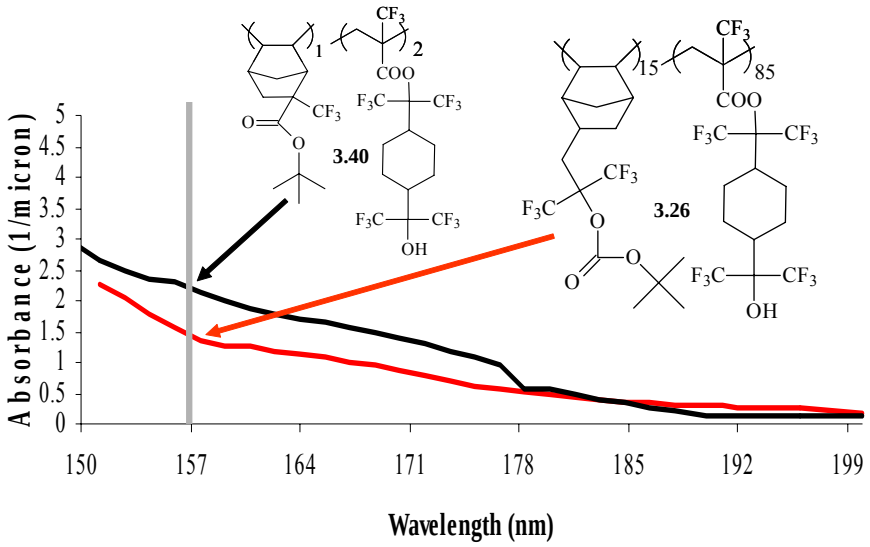

Figure 3.24: VASE spectroscopy of copolymer **3.40**. The impact on absorbance of geminally disubstituted trifluromethyl groups compared to just one trifluromethyl group is immediately apparent.

157 nm Imaging

Imaging experiments with copolymer **3.40** were successful. Preliminary lithographic studies at 157 nm produced positive tone structures (figure 3.23). The exposed regions of the resist film completely developed away, and the unexposed regions were inhibited from base development. Replacing the hexafluoroisopropanol moiety with a carboxylic acid successfully increased the acidity of the exposed polymer. This system did, however, require an exposure dose of 52 mJ/cm^2. While this is certainly an improvement over resist copolymer **3.34** (74mJ/cm^2), it is still a relatively high dose to image. In the case of **3.40**, the 2-trifluoromethylacrylate comonomer is base insoluble, and a film of the copolymer had a contact angle of 73º with water. This is only a slight

improvement over the hydrophobic **3.34** resist copolymer. Again, since little could be done to adjust the structure of the highly fluorinated acrylate, we focused our efforts on adjusting the nature of the norbornene comonomer.

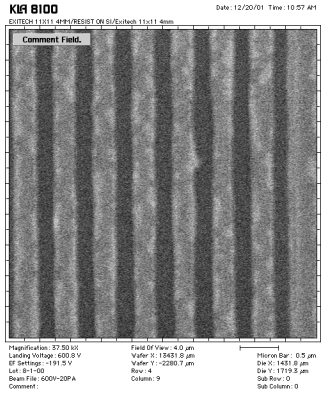

Figure 3.25: Initial imaging experiments with resist copolymer **3.40.** The exposed regions of the resist completely developed away.

Acetal Protecting Group

Since the dose required to image copolymer **3.40** may be partially attributed to the hydrophobicity of the tert-butyl ester group, we chose to seek an alternative acid-labile ester for chemical amplification. As mentioned in Chapter 2, previous studies in our group[54] demonstrated the use of an ethyl acetal protecting group for chemical amplification. To see if an acetal protecting group would improve the dose required to image a copolymer, a trifluoromethyl norbornane ester with this functional group was synthesized. Cyclopentadiene was reacted with 2-trifluormethacrylic acid, and this cycloaddition product (**3.41**) was deprotanated with butyl lithium and reacted with chloromethyl ethyl ether to give the desired monomer (**3.42**). This monomer was then radically copolymerized

with 2-trifluoromethylacrylate **3.33** to give the desired acetal protected resist copolymer (**3.43**, figure 3.26). VASE spectroscopy of a polymer film of **3.43** demonstrated no transparency advantage for an acetal protected resist over the same resist that was *tert*-butyl protected. Both copolymers **3.40** and **3.43** had absorbances of 2.15μm^{-1} at 157 nm.

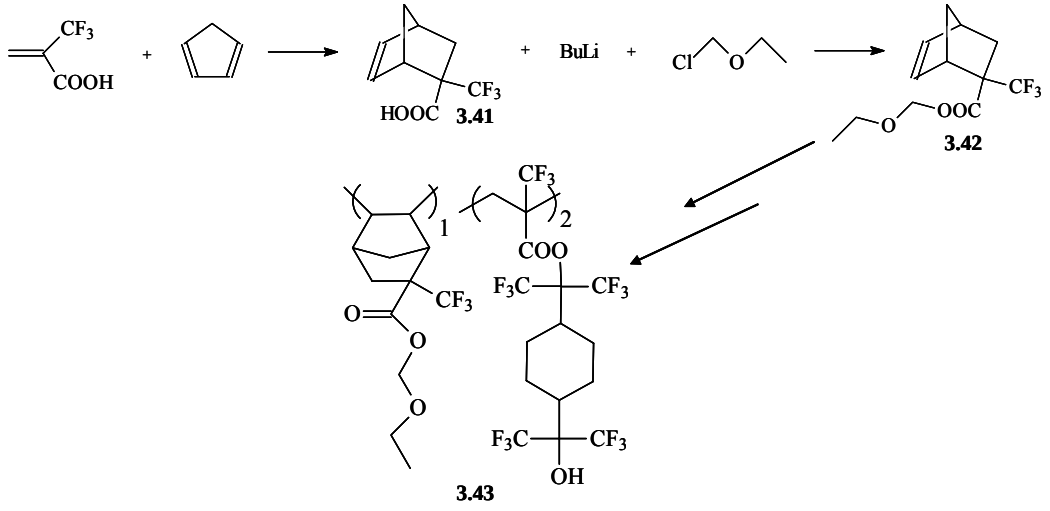

Figure 3.26: The synthesis of acetal-ester norbornene **3.42** and acetal-protected resist copolymer **3.43**.

157 nm Imaging

Preliminary 157 nm imaging experiments showed very encouraging results. Figure 3.27 shows high contrast structures with 130 nm dimensions produced with resist copolymer **3.43**. The exposed regions of the resist film were completely removed after development with base. Most importantly, the exposure dose required to produce these images was 19 mJ/cm^2. This is a significant improvement over resist copolymer **3.40** which has an identical structure with the

exception of a *tert*-butyl protecting group. As expected, the copolymer with an acetal protecting group is much less hydrophobic than the *tert*-butyl protected copolymer (contact angle with water: 68º and 73º, respectively). By any measure, copolymer **3.43** offers imaging characteristics that are superior to any other resist polymer that incorporates a 2-trifluoromethylacrylate in its backbone.

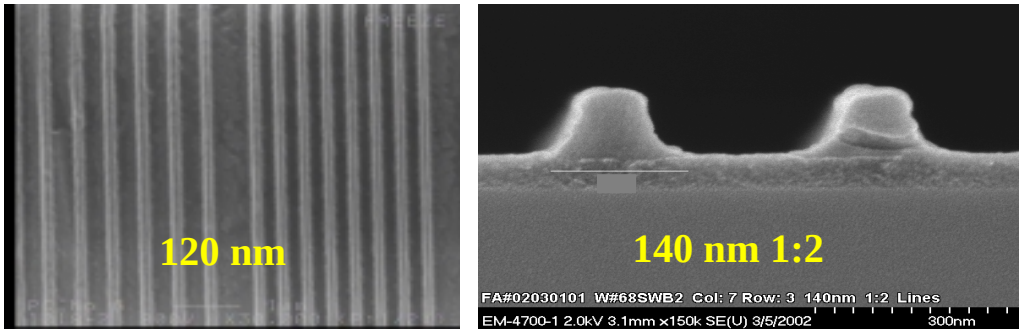

Figure 3.27: SEM pictures of structures produced with resist copolymer **3.43**. The images on the left are structures with 120 nm dimensions, and the structures on the right are cross sections of structures with 140 nm dimensions. The film thickness is 125 nm.

While the above 2-trifluoromethylacrylate/norbornene radical copolymers offer improved 157 nm transparency and superior imaging capabilities over their anionic-initiated predecessors, there are still drawbacks to these materials from a lithography standpoint. For these systems, the amount of the functional moieties (acidic group, protecting group, etc.) in the resist polymer is not adjustable due to the nature of this radical copolymerization. Traditionally, the varying of the monomer incorporation into a resist copolymer is vital in order to maximize lithographic performance. Even resist polymer **3.43**, which offers the best

lithographic capabilities of all the 2-trifluoromethylacrylate-based resists discussed in this dissertation, suffers from poor sidewall angles and resist residue in the exposed region of the film. Such residue is certainly due to the highly fluorinated, yet base insoluble, **3.33** co-monomer. While many of the radical copolymers discussed in this section are as transparent as the most successful norbornane-based 157 resist polymers to come out of our group[52], they do not possess the important imaging characteristics of straight sidewalls and good contrast between exposed and unexposed areas. Our norbornane-based 157 resist polymers do display such characteristics because monomer incorporation can be tuned so as to maximize lithographic capabilities. Because the 2-trifluoromethylacrylate/ norbornene radical platform does not allow for such tuning, printing sub-100 nm lines would seem improbable.

CHAPTER 4: REACTIVITY STUDEIS OF 2-TRIFLUROMETHYL ACRYLATES TOWARD RADICAL POLYMERIZATIONS

Chapter 3 describes an assortment of 2-trifluromethylacrylate based resist polymers that were prepared by anionic and radical copolymerizations. Studies of these materials demonstrated that they were relatively transparent at 157 nm and produced positive-tone images when exposed at this wavelength. During these studies, radical copolymerizations between 2-trifluromethylacrylates and various norbornenes were reported, and these copolymers displayed a curious 2:1 (2-trifluromethylacrylate:norbornene) monomer incorporation. This chapter focuses on efforts to study this peculiar radical copolymerization.

The rate at which a polymerization proceeds, the molecular weight and composition of the resulting copolymer, and the formation of sideproducts are factors that one must consider during the synthesis of a resist material. The study of polymerization kinetics aims to give insight into these factors so that predictions can be made as to a monomer's reactivity toward copolymerization with other monomers. Such studies are fruitful because knowledge of the microstructure of a material can help explain certain behaviors that occur during the photolithographic process, such as the dissolution characteristics of a resist polymer during the development step.

THE TERMINAL MODEL OF COPOLYMERIZATION

The kinetics of radical polymerization are often studied assuming the terminal model of copolymerization.[55] This model assumes that the chemical reactivity of the propagating chain in a copolymerization is dependent only on the

identity of the monomer unit at the end of the growing chain and independent of polymer composition preceding the last monomer unit. Consider, for example, the case for the radical copolymerization of MTFMA and methyl methacrylate[56] discussed in Chapter 3. As was shown in figure 3.1, four rate constants must be considered when determining the reactivity ratios for such a copolymerization: the rate at which a growing chain ending in MTFMA reacts with either another MTFMA monomer or a methyl methacrylate monomer (k_{11} or k_{12}, respectively) and the rate at which a growing chain ending in methyl methacrylate reacts with either a MTFMA monomer or another methyl methacrylate monomer (k_{21} or k_{22}, respectively).

The Penultimate Model of Copolymerization

While continuing studies of copolymers for 157 nm resist applications, Ito et al.[57,58] reported that the radical copolymerization of 2-trifluoromethylacrylate and norbornene monomers could not be treated with the terminal model of copolymerization. Using this model to study the radical copolymerization of *tert*-butyl 2-trifluromethylacrylate (M_1) and norbornene (M_2), the authors found that derived reactivity ratios (r_1=0.53 and r_2=0.0) failed to fit experimentally determined feed-composition plots. However, reactivity ratios that were determined using the penultimate model of copolymerization (r_1=0.17, r_1'=1.91 and r_2=r_2'=0.0) gave a significantly better fit to experimentally determined feed-composition ratios.

The penultimate model differs from the terminal model in that it considers how the penultimate, or second to last, unit on the growing polymer chain effects

the reactivity of the chain end radical toward another monomer.[55] The reactivity of a propagating radical chain is often affected by the penultimate unit in many radical copolymerizations where the monomers contain highly bulky or polar substituents. For example, this behavior has been observed in the copolymerization of styrene and fumaronitrile.[59] Growing polymer chains having styrene as the last added unit and fumaronitrile as the penultimate unit show greatly decreased reactivity toward a fumaronitrile monomer, perhaps due to steric and polar repulsions between the fumaronitrile in the penultimate unit on the chain and the incoming fumaronitrle monomer.[55]

Reactivity Ratio Determination Using the Penultimate Model

When the composition of both the terminal and penultimate units on a growing polymer chain must be considered when studying reactivity toward another monomer, the mathematical determination of reactivity ratios using the penultimate model becomes more complex as eight propagating reactions and four reactivity ratios must be considered (figure 4.1).

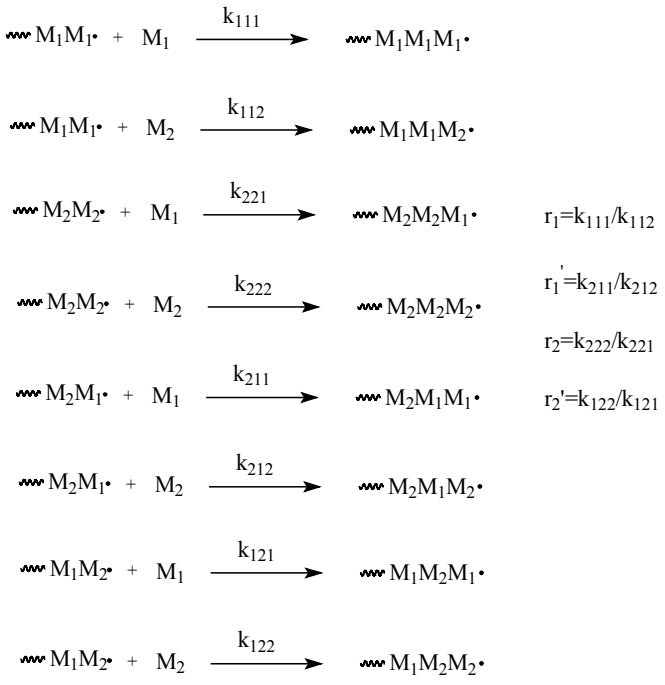

Figure 4.1: The eight propagating reactions and four reactivity ratios of the penultimate model of copolymerization.

In the case of the copolymerization between norbornene and *tert*-butyl 2-trifluromethylacrylate,[57,58] the norbornene monomer reacts with the 2-trifluro-methacrylate polymer radical 6 times faster than the 2-trifluromethylacrylate when the penultimate group is a 2-trifluromethylacrylate ($r_1 = k_{111}/k_{112} = .017$). However, when the penultimate group is norbornene, the growing 2-trifluoromethylacrylate radical reacts with a 2-trifluromethylacrylate monomer ~2 times faster than with another norbornene monomer ($r_1' = k_{211}/k_{212} = 1.91$). In both of the above instances, the most likely (faster) addition of a growing radical polymer chain to a monomer unit will lead to the 2:1 2-trifluoromethylacrylate:norbornene monomer incorporation that has been observed for such radical copolymerizations (figure

4.2). Since norbornene does not self-propagate with radical initiators such as AIBN,[60] $k_{222}= k_{212}=0$ and $r_2=r_2'=0$.

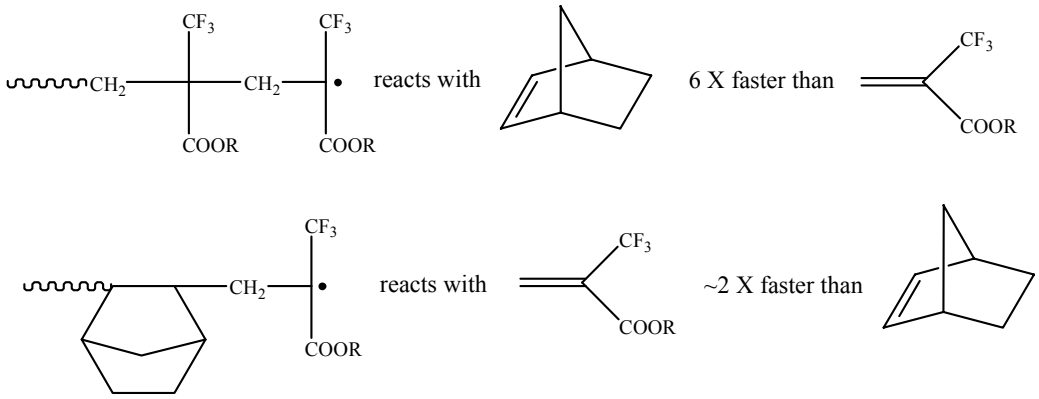

Figure 4.2: With the determined reactivity ratios $r_1=0.17$ and $r_1'=1.91$ determined by Ito et al., the most likely reaction of a propagating polymer chain and monomer will lead to a 2:1 (2-trifluoromethylacrylate:norbornene) monomer incorporation. (R= *t*-butyl)

In a collaboration with Dr. Hiroshi Ito of the IBM Almaden Research Center, our group examined the reactivity ratios of a 2-trilfuoromethacrylate/ norbornene monomer pair. Since the mathematical treatment used to determine monomer reactivity ratios assumes no change in feed composition, copolymerizations were stopped at less than 12% conversion. However, enough copolymer must be produced (~500 mg) in order to properly analyze the material by various spectroscopic methods. Therefore, we needed to select monomers that were readily available. The acrylate monomer that we chose was 2-trifluoromethylacrylic acid, which was being produced commercially in large quantities by this time. Initially, we wanted to look at a norbornene monomer that

had a geminally substituted trifluoromethyl group, such as norbornene monomer **3.42**.

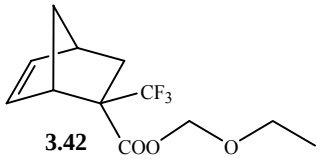

3.42

Unfortunately, the copolymerization of this pair was too low yielding, perhaps due to the low electron density of the norbornene double bond, and therefore impractical. We then turned to a *tert*-butyl ester substituted norbornene as a comonomer. While this monomer is not fluorinated, it plays a major role in our norbornane based metal-catalyzed 157 resist program.[61] It is also available from a commercial supplier.

Reactivity ratio determinations proceeded by performing a number of radical copolymerizations with various monomer loadings. The reactions were stopped at under 10% conversion, and their copolymer composition was determined by ^{13}C NMR. As expected, analysis of the copolymerization of these monomers could not be treated by the terminal model, as the reactivity ratios determined using the Kelen-Tudos[62] terminal model produced a plot that was an extremely poor fit with experimental data. However, when the copolymer composition curve was modeled using the penultimate model, the fit with the experimental data was very good. The copolymer composition with a kinetic penultimate effect is obtained as:

$$\frac{d[M_1]}{d[M_2]} = \frac{1+\dfrac{r_1'X(r_1X+1)}{(r_1'X+1)}}{1+\dfrac{r_2'X(r_2X+1)}{(r_2'X+1)}}$$

where $X = [M_1]/[M_2]$. For the 2-trifluoromethylacrylate/norbornene system, norbornene is incapable of self propagation ($r_2=r_2'=0$), and the above equation simplifies to:

$$\frac{d[M_1]}{d[M_2]} - 1 = 1+\frac{r_1'X(r_1X+1)}{(r_1'X+1)}$$

As shown in figure 4.3, this equation gives a good fit of the experimental copolymer composition data with $r_1 = 0.172$ and $r_1' = 0.278$.

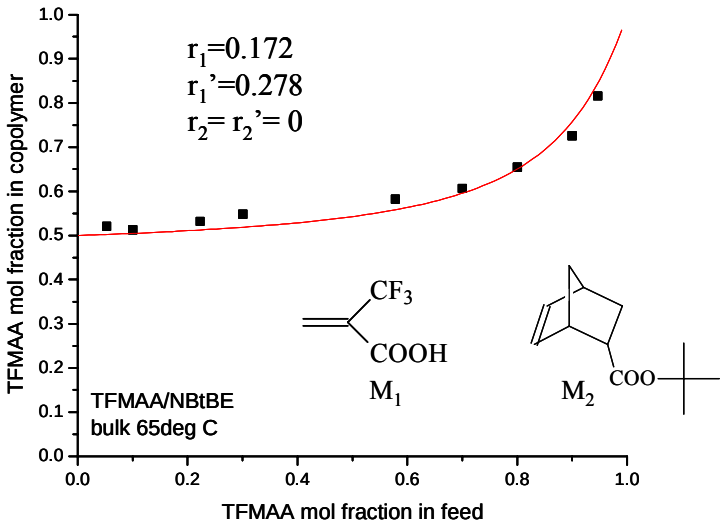

Figure 4.3: The copolymer composition curve for 2-trifluoromethylacrylic acid and norbornene *t*-butyl ester.

An r_1 value of 0.172 indicates that the 2-trifluoromethylacrylic acid polymer radical reacts with norbornene *t*-butyl ester 6 times faster than another 2-trifluromethylacrylate monomer when the penultimate group is a 2-trifluromethylacrylate. This result is consistent with the observed 2:1 incorporation ratio for such systems. Interestingly, an r_1' value of 0.278 indicates that the 2-trifluoromethylacrylic acid polymer radical reacts with norbornene *t*-butyl ester 3.5 times faster than another 2-trifluromethylacrylate monomer when the penultimate group is norbornene *t*-butyl ester. This is somewhat inconsistent with the expected 2:1 monomer incorporation. This system displays a small penultimate effect (r_1'/r_1= 1.6) compared to that observed for the copolymerization of *t*-butyl 2-trifluoromethylacrylate and norbornene (r_1'/r_1= ~11).[58] In the case of r_1'/r_1= ~11, a penultimate 2-trifluoromethylacrylate group significantly retards reaction of a 2-trifluoromethylacrylate radical with another acrylate monomer, while a penultimate norbornene unit accelerates such a reaction. This is in accordance with the expected 2:1 monomer incorporation. In the case studied here, a smaller penultimate effect (r_1'/r_1= 1.6) shows that the effect of a penultimate 2-trifluoromethylacrylate is not as pronounced, but is nevertheless indicative of a system where 2-trifluoromethylacrylate radicals preferentially react with norbornene when the penultimate group is a 2-trifluoromethylacrylate. Furthermore, the polymer incorporation of 2-trifluoromethylacrylic acid ester never reaches less than about 55% in this system, even at 5% loading (figure 4.3). Therefore, this system is dominated by reactions that perpetuate the expected 2:1 2-trifluoromethylacrylate:norbornene incorporation (i.e., the reaction of a 2-

trifluoromethylacrylic acid polymer radical with a norbornene *t*-butyl ester when the penultimate group is a 2-trifluromethylacrylate).

Copolymerization Studies Using ^{1}H NMR

This radical copolymerization was also monitored by ^{1}H NMR. This provided an opportunity to monitor this copolymerization while it was occurring. Varying concentrations of 2-trifluoromethylacrylic acid and norbornene *tert*-butyl ester were loaded into NMR tubes using AIBN as the initiator and 1,4-dioxane-d_8 as the NMR and polymerization solvent. The sample was heated to 70ºC, and scans were taken of the sample approximately every 25 minutes. Monomer consumption curves are presented for the copolymerization of a 1:1 equivalent of 2-trifluoromethylacrylic acid and norbornene *tert*-butyl ester with 4 wt.% AIBN in figure 4.4. As time proceeds at 70ºC, twice as much 2-trifluoromethylacrylate monomer is consumed as norbornene monomer. This is consistent with the observation of a "2:1" monomer incorporation in the copolymer. At any point during the copolymerization, the mole % 2-trifluoromethylacrylic acid in the feed never significantly deviates from 50%.

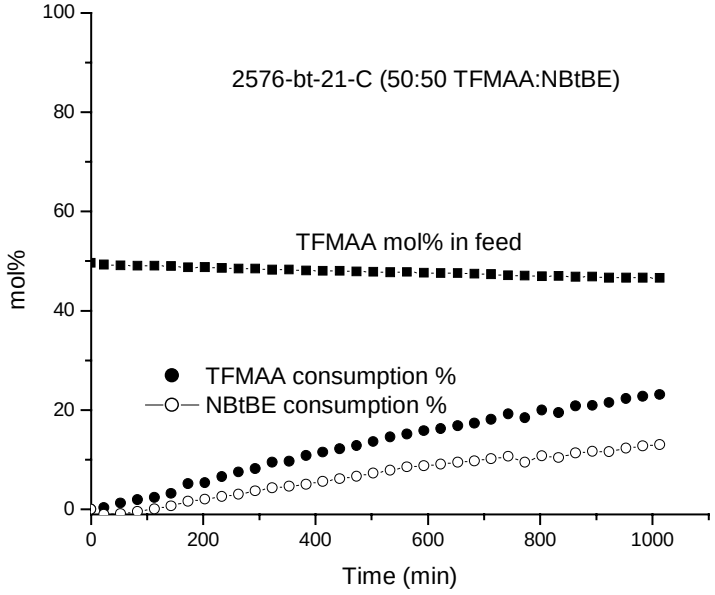

Figure 4.4: *In situ* ^{1}H NMR analysis of a 2-trifluromethylacrylic acid/*tert*-butyl norbornene (1:1) radical copolymerization.

The comonomer composition was adjusted to 70:30 2-trifluoromethylacrylic acid:norbornene *tert*-butyl ester, and the changes in consumption % and mole fraction of 2-trifluoromethylacrylate in the copolymer can be seen in figure 4.5. In this case, the monomer loading in the feed is the same as the predicted monomer incorporation in the copolymer. Due to the increased loading of 2-trifluoromethylacrylic acid, the mole fraction of this monomer in the copolymer is close to 70%. This is consistent with the feed-composition data in figure 4.3, which shows that the 2-trifluoromethylacrylate monomer incorporation can be as high as 80% at 95% monomer loading. At any point during the copolymerization, the consumption % of both monomers is virtually identical

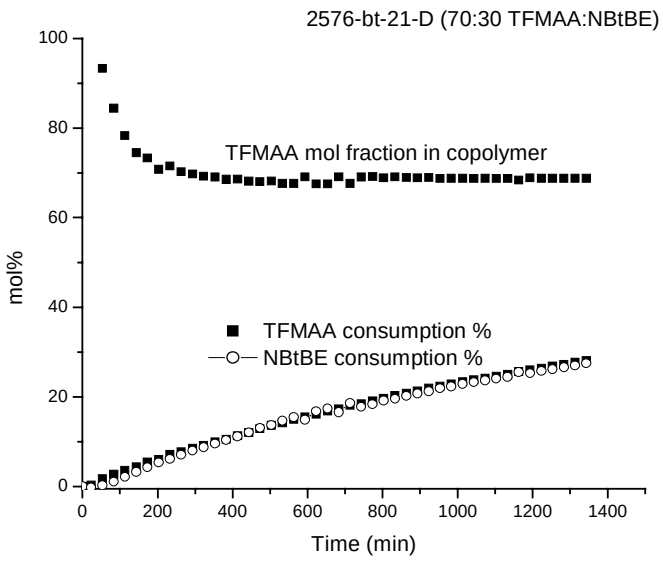

Figure 4.5: *In situ* ^{1}H NMR analysis of a 2-trifluromethylacrylic acid/*tert*-butyl norbornene (70:30) radical copolymerization.

The polymerization kinetics of a 30:70 loading of 2-trifluoromethylacrylic acid and norbornene *tert*-butyl ester were also observed, the results of which are shown in figure 4.6. This data is consistent with what had already been observed in both of the previous NMR experiments and the feed-composition graph. With a decreased loading of 2-trifluoromethylacrylic acid, the mole fraction of this monomer in the copolymer never exceeds 57%. Also, the limited amount of 2-trifluoromethylacrylate monomer in the feed results in an increased % consumption of this monomer. The abundance of the norbornene monomer has the opposite effect on the % consumption of this material in the feed.

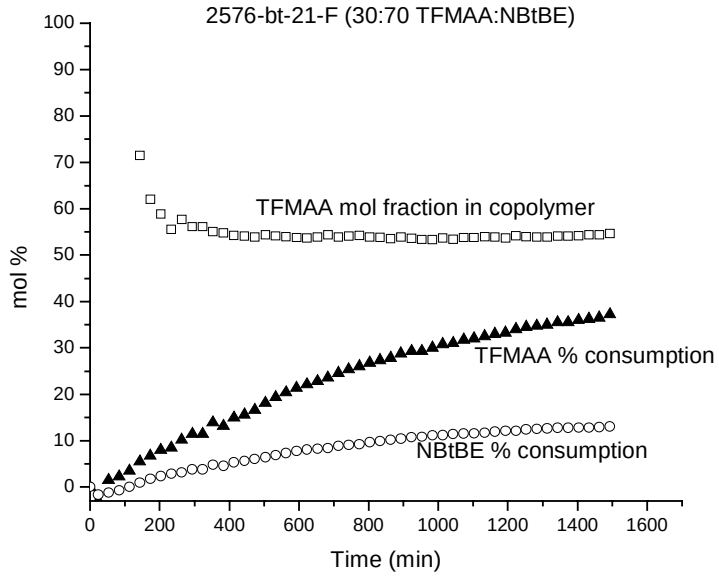

Figure 4.6: *In situ* ^{1}H NMR analysis of a 2-trifluromethylacrylic acid/*tert*-butyl norbornene (30:70) radical copolymerization.

The above studies are important because they give credence for the 2:1 2-trifluoromethylacrylate:norbornene radical copolymerization that was originally observed by Ito et al.[63] While analysis of a copolymer synthesized from two monomers can only show the end result of that copolymerization, the ^{1}H NMR studies show a direct observation of the copolymerization from its inception. Monomer loadings were adjusted in order to observe how monomer consumption could change during the course of the reaction. Feed-composition graphs were used to determine reactivity ratios of comonomers, which were used to explain how monomers are reacting during copolymerization, including how propagating radicals interact with incoming monomers. Most importantly, such studies demonstrated that the penultimate unit on the propagating radical chain is the determining factor in this interaction.

While these studies have been extremely important as to explain *how* this radical copolymerization is taking place, we were eager to conduct investigations that might explain *why* such behavior was being observed. The feed-composition data gathered for the 2-trifluoromethylacrylate/norbornane system was indicative of a penultimate effect. Like the hypothesized explanation for the styrene fumaronitrile system,[55,59] we rationalized that the strongly electron-rich trifluoromethyl group of the 2-trifluoromethylacrylate in the penultimate position on the propagating radical induced electronic repulsion with the electron-rich trifluoromethyl group of an incoming 2-trifluromethylacrylate monomer. This led to a suppression in reactivity between a propagating radical with a 2-trifluoromethylacrylate in the penultimate position and another 2-trifluoromethylacrylate monomer. Remember that the 2-trifluoromethylacrylic acid polymer radical reacts with norbornene *t*-butyl ester 6 times faster than another 2-trifluromethylacrylate monomer when the penultimate group is 2-trifluoromethylacrylic acid (figure 4.3). However, the above rationalization is speculation, and we wanted to conduct an experiment that would prove that an electron rich penultimate group of a propagating radical could suppress reactivity with an incoming monomer with an electron rich substituent. Such experiments would be part of our continued collaboration with Dr. Hiroshi Ito from the IBM Almaden Research Center.

The Mercury Method

The reactivities of a number of olefins toward a variety of radicals has been studied using the "mercury method." [64,65] In this method, an alkyl mercuric halide is reduced with sodium borohydride, generating an alkyl radical. This radical can react with one of two different olefins, and subsequent hydrogen abstraction forms a 1:1 adduct (figure 4.7).

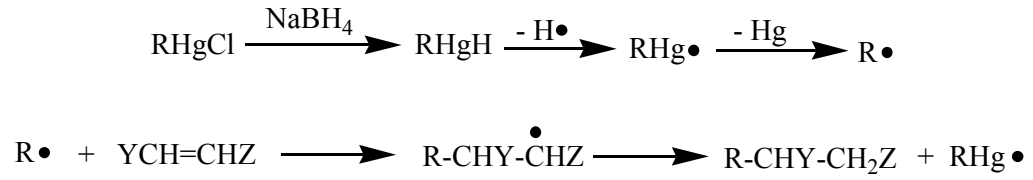

Figure 4.7: The reaction of an alkyl mercuric halide with $NaBH_4$ to form an alkyl radical, and subseuent reaction with an olefin.

This method has been useful in determining the reactivity of both MTFMA and acrylonitrile toward a cyclohexyl radical.[66] A competitive addition of MTFMA and acrylonitrile toward the cyclohexyl radical was performed by reacting cyclohexyl mercuric chloride with sodium borohydride in the presence of an excess of the two monomers. The procedure was repeated a number of times with varying concentrations of monomer, and in each case the ratio of the resulting adducts was measured by GC. The feed ratio of each monomer was plotted against the product ratio of the resulting adducts, and the slope of the linear plot (0.089) corresponded to the ratio of the rate constant k_4 to the rate constant k_2, indicating that MTFMA is approximately 11 times more reactive toward the cyclohexyl radical than acrylonitrile (figure 4.8).

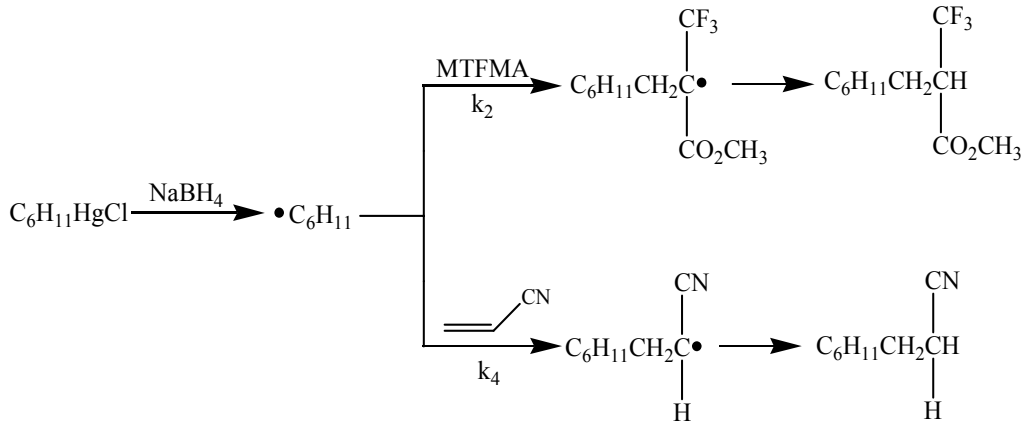

Figure 4.8: The competative reaction of the cyclohexyl radical with MTFMA and acrylonitrile. The mercury method was used to determine that MTFMA is 11 times more reactive than acrylonitrile toward the cyclohexyl radical.

Previous Studies of the Penultimate Effect Using the Mercury Method

Similar competitive reaction studies using the mercury method were used to study penultimate effects in the radical copolymerization between styrene and acrylonitrile.[67] In this case, a number of competitive reaction studies were conducted between these monomers with varying alkyl mercuric halides in order to model different "penultimate" units. Since penultimate effects alter the reactivity of a radical toward a monomer, Jones et al.[67,68] proposed that the mercury method could be used to show that the selectivity of addition of olefins to alkyl radicals is sensitive to the nature of substituents placed in a position that was γ (or penultimate) to the radical center. The authors reported a significant difference in reactivity between radicals (formed from the reaction of alkyl mercuric bromides and sodium borohydride) with phenyl and cyano substituents in the position that is penultimate to the radical center. The 3-cyanopropyl radical

preferentially reacts with acrylonitrile over styrene, but this preference is reduced by a factor of 3.5 when compared to competitive reactivity studies with the 3-phenyl propyl radical (figure 4.9). Since a substituent that was γ (penultimate) to the radical center could have such an effect on radical reactivity, the authors concluded that the penultimate model is an appropriate description of the radical copolymerization of styrene and acrylonitrile.

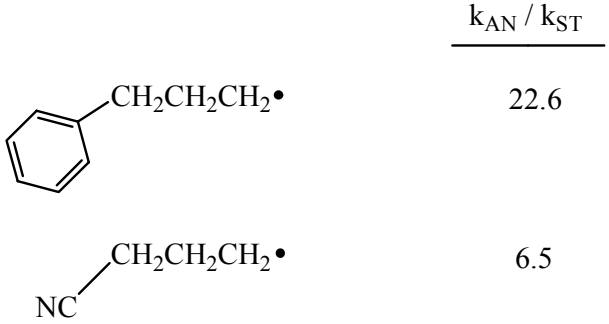

Figure 4.9: Relative rates of addition of styrene (ST) and acrylonitrile (AN) to substituted alkyl radicals as determined by Jones et al.

Monomer Candidates

In order to substantiate the claim that the penultimate model of copolymerization was an accurate description of the radical copolymerization of 2-trifluoromethylacrylates, we set out to use the mercury method to show that the electron rich trifluoromethyl group could effect radical reactivity when in a position that is penultimate to a propagating radical. Ideally, competitive reaction studies similar to those discussed above could be performed using a 2-trifluoromethylacrylate and norbornene as the monomers. However, the norbornene monomer is virtually unreactive toward the alkyl radical formed from the reaction of an alkyl mercuric halide and sodium borohydride.[69] We therefore

chose *tert*- butyl 2-trifluromethylacrylate and *tert* butyl methacrylate as the monomers for the competitive study. While these monomers are not a direct model of the norbornene/2-trifluromethylacrylate copolymerization, they will still give good insight into the reactivity of different propagating radicals with monomers that do and do not contain trifluoromethyl groups.

Alkyl Mercuric Halide Synthesis

Once monomer candidates were identified, alkyl mercuric halides that could be converted to propagating radicals had to be chosen. Here, it was necessary to choose molecules that would provide propagating radials that were the same in structure with the exception of the penultimate group. Inspired by the aforementioned efforts by Jones et al.,[67,68] we determined that the alkyl mercuric halides shown in figure **4.10** would provide propagating radicals that were analogous to a methyl acrylate propagating radical with methyl and trifluoromethyl penultimate units.

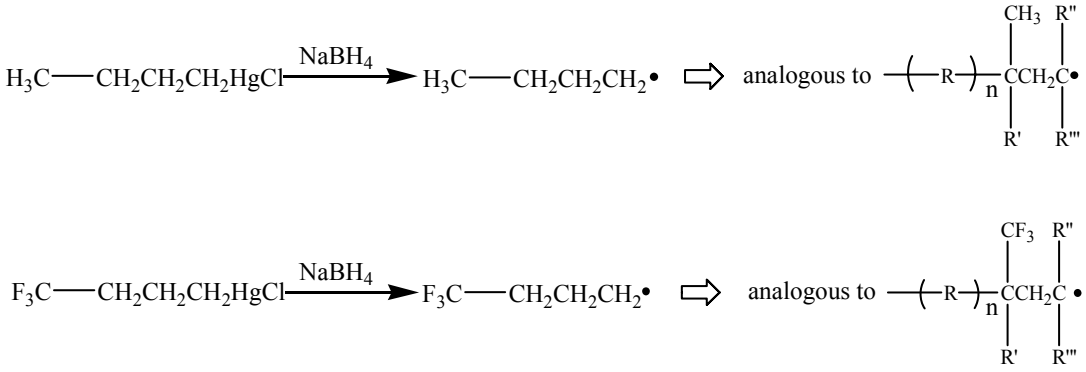

Figure 4.10: Propagating radicals with methyl and trifluoromethyl penultimate groups for mercury method competitive studies.

The synthesis of such compounds was relatively straightforward and based on procedures described in other reports.[67,70] Commercially available butyl magnesium bromide was reacted with mercuric chloride to form the desired butyl mercuric chloride. The alkyl halide with a trifluoromethyl group in the penultimate position was prepared by reacting 4-bromo-1,1,1-trifluro-butane with magnesium to form the Grignard reagent, followed by reaction with mercuric chloride to give the desired fluorinated mercuric chloride (figure 4.11).

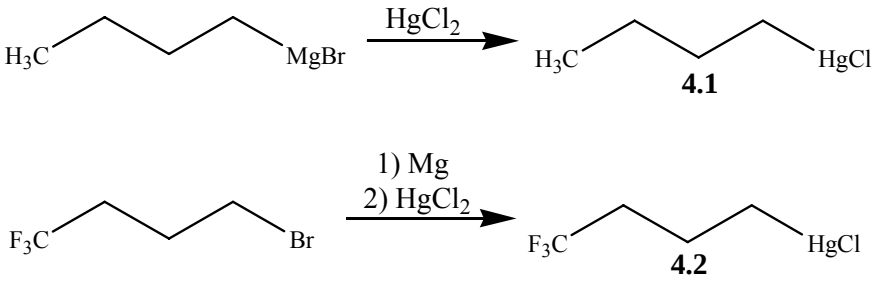

Figure 4.11: The synthesis of alkyl mercuric halides **4.1** and **4.2**.

Adduct Synthesis

Once the desired mercuric halides were synthesized, it was necessary to react them with each of the monomers to be used in the competitive reaction study. Both **4.1** and **4.2** were reacted with *tert*-butyl 2-trilfuoromethacrylate and *tert*-butyl methacrylate, and the adducts were obtained in moderate yields (figure 4.12). Once the adducts were prepared and characterized, they were used for GC calibration using either *t*-butyl benzene or dimethoxybenzene as the internal standard. The amount of each adduct formed during the competitive reactions

would be determined by GC, so it was vital to know how % area of a particular peak on a GC chromatogram related to the number of moles of an adduct.

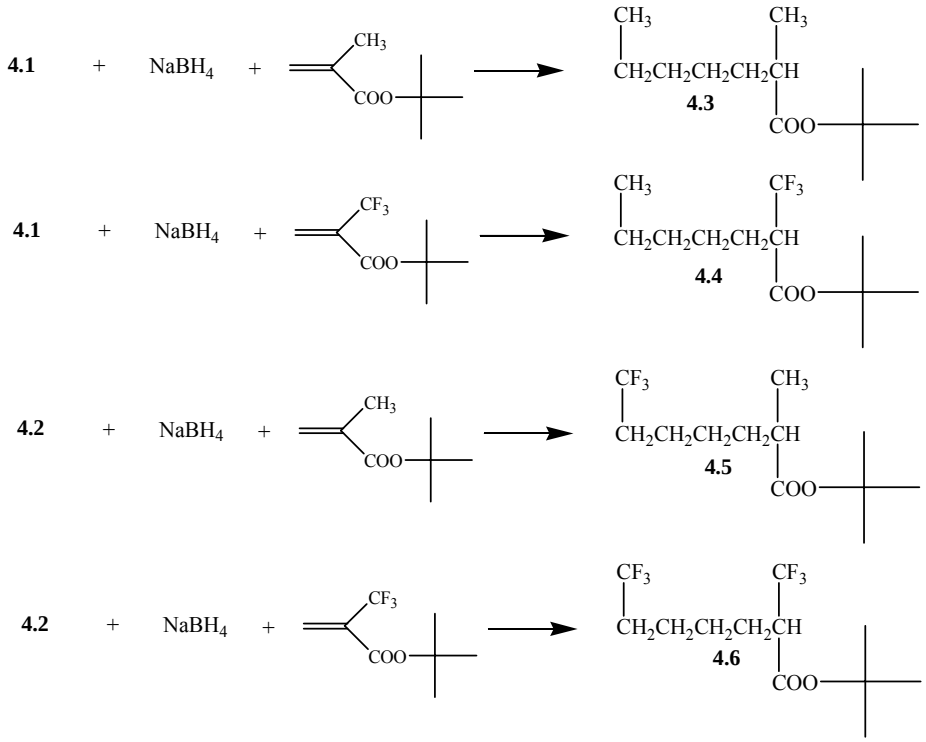

Figure 4.12: The synthesis of the alkyl mercuric halide/acrylate adducts (**4.3**-**4.6**).

Competitive Reaction Studies

Once GC calibration was accomplished, we proceeded with the competitive reaction studies. This was performed by reacting the alkyl mercuric halide with at least a 10-fold excess of the two monomers in the presence of sodium borohydride. In the first study, the propagating radical with a methyl penultimate group (generated from **4.1**) was reacted with varying ratios of *tert*-

butyl 2-trifluoromethylacrylate and *tert*-butyl methacrylate. Table 4.1 summarizes the results of the competitive addition of these monomers, and figure 4.13 demonstrates the plot of the product ratio [**4.3**]/[**4.4**]. The slope of the linear plot (0.0414) in figure 4.13 indicates that *tert*-butyl 2-trilfuoromethacrylate is about 24 times more reactive than *tert*-butyl methacrylate toward this radical. This high selectivity is to be expected, as it is well known that alkyl radicals tend to add faster to olefins substituted with strong electron withdrawing groups than to electron rich π-systems.[65,71] For example, Ito et al. extrapolated results from the mercury method study of MTFMA and acrylonitrile to determine that MTFMA is 54 times more reactive toward the cyclohexyl radical than methyl methacrylate.[66]

Feed (mmol)		Feed ratio	Product ratio
t-butyl TFMA	*t*-butyl MA	[TFMA]/[MA]	[**4.3**]/[**4.4**]
1.39	7.00	5.04	0.29
1.25	12.46	9.98	0.43
1.55	21.89	14.10	0.57
1.26	24.83	19.72	0.89
1.18	35.52	30.02	1.25

Table 4.1: Competitive addition of *tert*-butyl 2-trifluoromethylacrylate (*t*-butyl TFMA) and *tert*-butyl methacrylate (*t*-butyl MA) to propagating radical with methyl penultimate group (from **4.1**).

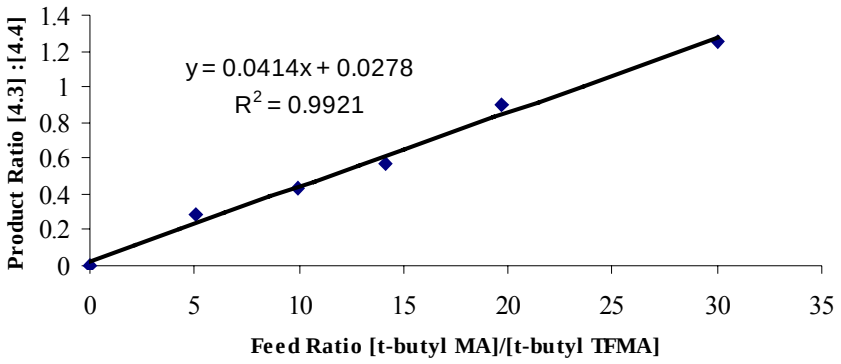

Figure 4.13: Correlation between product ratio and the feed ratio data shown in table 4.1.

In the second study done using the mercury method, a propagating radical with a trifluoromethyl penultimate group (generated from **4.2**) was reacted with varying ratios of *tert*-butyl 2-trilfuoromethylacrylate and *tert*-butyl methacrylate. Table 4.2 summarizes the results of the competitive addition of these monomers, and figure 4.14 demonstrates the plot of the product ratio [**4.5**]/[**4.6**]. The slope of the linear plot (0.0797) in figure 4.14 indicates that *tert*-butyl 2-trilfuoromethacrylate is about 12 times more reactive than *tert*-butyl methacrylate toward this radical. Again, we observed a preference of a propagating radical to react more quickly with the olefin that had less electron density. However, the affinity of this propagating radical for the 2-trifluromethylacrylate monomer is suppressed by a factor of 2 when compared to the reactivity of the radical generated from **4.1** (slope of 0.0414 vs. slope of 0.0797, respectively). This difference in selectivity can only be attributed to the substituent that is penultimate

to the propagating radical center. This data clearly shows that selectivity toward the 2-trifluoromethylacrylate monomer is suppressed when that penultimate group is trifluoromethyl. This is likely explained by the development of repulsive forces of the electron rich trifluoromethyl groups on the radical and incoming monomer. Such conclusions were also drawn by Giese et al.[72] and Jones et al.[67,68] when considering penultimate effects of other functional groups. Additionally, ab initio molecular orbital calculations also demonstrated that the origin of penultimate effects of series of γ-substituted propyl radicals to various alkenes is best described by polar effects.[73] We believe our results lend strong support to the suggestion that the radical copolymerization between various norbornenes and 2-trifluromethylacrylates is best described by the penultimate model.

Feed (mmol)		Feed ratio	Product ratio
t-butyl TFMA	*t*-butyl MA	[TFMA]/[MA]	[**4.5**]/[**4.6**]
1.46	7.31	5.02	0.19
0.93	9.30	10.00	0.59
0.83	12.56	15.10	1.08
0.83	15.33	18.40	1.36
0.89	19.37	21.70	1.48
0.89	26.89	30.08	2.30
0.81	24.63	30.37	2.35

Table 4.2: Competative addition of *tert*-butyl 2-trifluoromethylacrylate and *tert*-butyl methacrylate to propagating radical with methyl penultimate group (from **4.2**).

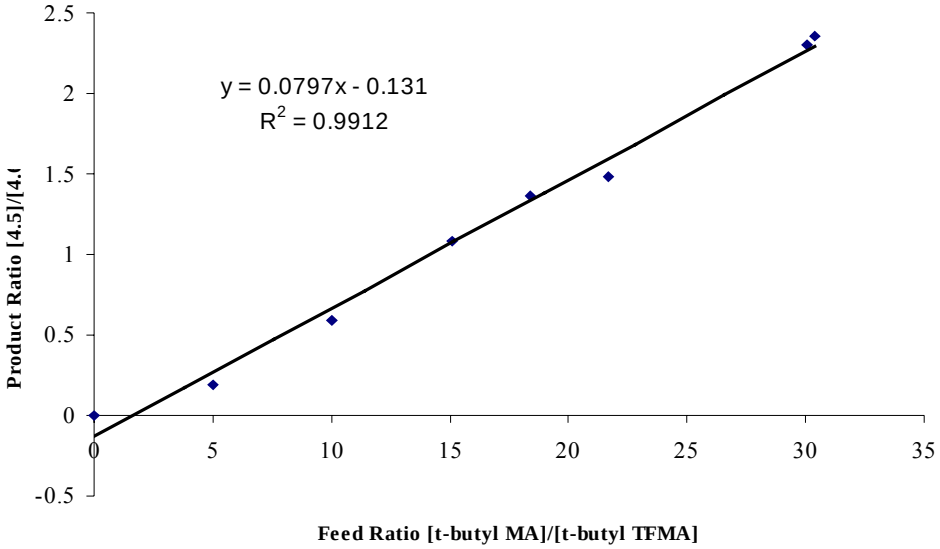

Figure 4.14: Correlation between product ratio and the feed ratio data shown in table 4.2.

ESR Studies of 2-Trifluoromethylacrylate Radicals

After executing experiments that gave insight to the reactivity of a propagating radical that involves a 2-trifluromethylacrylate, we looked to perform experiments that might give insight to the structure of such a radical. In order to do this, we attempted to examine these radicals using electron spin resonance spectroscopy (ESR) in a collaboration with Dr. Paul Kasai of the IBM Almaden Research Center. ESR is a spectroscopic technique that measures the resonance transition of the unpaired electron of a free radical. It is therefore very similar to NMR, except that electron spin is aligned in a magnetic field instead of nuclear spin. This technique was used to examine the conformation of free radicals trapped in photopolymerized 1,6-hexanediol dimethacrylate (HDDMA).[74] HDDMA is a good material with which to study free radicals because a dense,

cross-linked network quickly forms upon photopolymerization which can trap a large amount of free-radicals for evaluation. While a cross-linked network is an excellent way to rapidly capture free-radicals for ESR, it was an impractical approach for a 2-trifluromethylacrylate due to its sluggish radical homopolymerization. However, 2-trifluoromethylacrylates do radically copolymerize with methacrylates. We therefore proposed blending *tert*-butyl trifluoromethacrylate with HDDMA to generate a strong ESR signal. While this would be a mixture of spectra to 2 different radicals, the background spectra of HDDMA could be "subtracted" out, resulting in the spectra of a 2-trifluoromethylacrylate radical signal.

Using the photoinitiator α,α-dimethoxy-α-phenylacetophenone (DMPA) to generate radicals upon UV exposure, the ESR spectra of HDDMA was first acquired. The results of this effort are shown in figure 4.15. The spectra displays the "5+4" line pattern that is indicative of the propagation radical indicated in the figure.

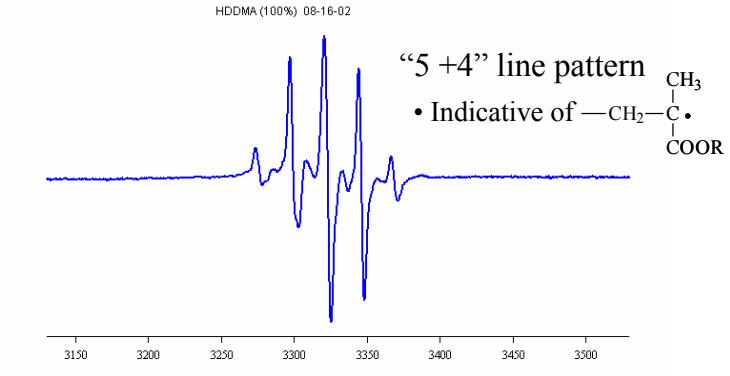

Figure 4.15: The ESR spectra of HDDMA.

We then prepared blends of *tert*-butyl 2-trifluoromethylacrylate, HDDMA, and DMPA. The sample was UV exposed, but unfortunately, did not give an adequate ESR signal. This may have been due to an impeded rate of copolymerization due to the steric bulk of the *t*-butyl group. We thence prepared a blend of methyl 2-trifluoromethylacarylate (MTFMA), HDDMA and DMPA. A strong ESR signal was observed when this blend was exposed to UV (Fig. 4.16A). When the signal due to the propagation radical of the HDDMA system (Fig. 4.15) was subtracted, the spectrum shown in Fig. 4.16B was obtained. Here a sextet pattern with the relative intensity of binomial coefficients and successive spacing of ~25 gauss was discerned as indicated. The spectrum thus revealed is assigned to the propagation radical of the MTFMA system. The sextet pattern is ascribed to the hyperfine coupling interactions of (roughly) equal magnitude to 5 nuclei of spin ½. It has been shown that the average isotropic coupling constant of both β-protons and β-fluorine nuclei of alkyl radicals are in the range of 20 ~ 30 gauss.[75]

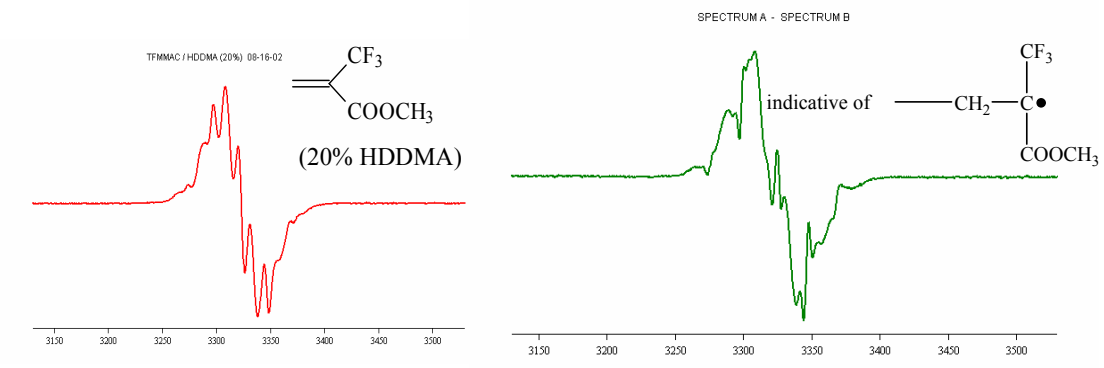

Figure 4.16: The ESR spectra of MTFMA and HDDMA (left) and the spectra with the HDDMA background removed.

Finally, we were eager to investigate how the addition of a norbornene unit to the above mixture might affect the ESR spectra of MTFMA. While 2-trifluoromethylacrylates and norbornenes do radically copolymerize, it was thought that this copolymerization would not ensue quickly enough to form the dense network necessary to trap radicals. We therefore blended these materials with HDDMA in the hopes of getting an adequate signal. The strong signal shown in figure 4.17 was observed. It is clearly different from that observed from the mixture without norbornene. The difference must be due to the presence of additional radicals involving the norbonene moiety. Detailed analysis of the spectrum was hampered by the extreme broadness of the spectrum.

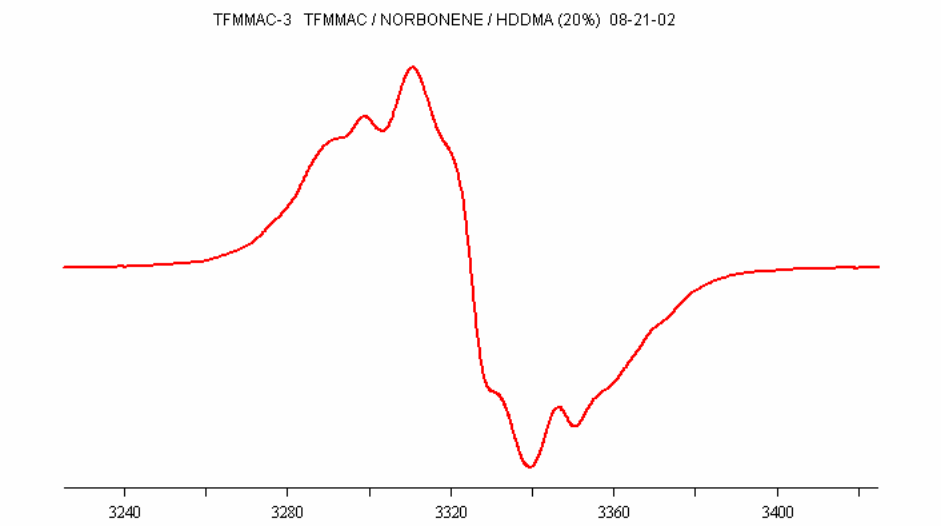

Figure 4.17: The ESR spectra of MTFMA, norbornene and HDDMA.

Conclusions and Future Work

Through analysis of model calculations and gas phase absorbance measurements, 2-trifluromethylacrylates have been identified as important monomer candidates for use in 157 nm photoresist development. Utilizing a variety of novel 2-trifluoromethylacrylates and norbornenes, novel resist polymers have been produced via anionic and radical copolymerizations. These materials were significantly more transparent than their hydrocarbon analogues at 157 nm. Radical copolymers were prepared that incorporate norbornene rings with fluorine-substituents in the polymer backbone in order to maximize transparency. Preliminary lithographic studies produced positive-tone structures with 157 nm exposure, but image quality can certainly be improved with further process and formulation optimization.

The interesting "2:1" monomer incorporation displayed in radical copolymerizations of various 2-trifluoromethylacrylates and norbornenes was also studied. Reactivity ratio determinations of the copolymerization of 2-trifluoromethylacrylic acid and *tert*-butyl ester norbornene confirmed work by Ito et al.[58] who reported that this reaction follows the penultimate model of copolymerization in which the rate of the propagation reaction is affected by both the terminal and penultimate units of the propagating radical. This reaction was also monitored using ^{1}H NMR to confirm a "2:1" incorporation of these monomers. Competitive reactions utilizing the mercury method were employed to confirm a selectivity difference between propagating radicals with penultimate trifluoromethyl substitution toward monomers with and without trifluoromethyl

groups. These studies showed a suppression in selectivity between radicals with a trifluoromethyl group in the penultimate position and *tert*-butyl 2-trifluoromethylacrylate, which was attributed to polar repulsive forces between the penultimate trifluoromethyl group on the propagating radical and the trifluoromethyl group on the incoming monomer. These findings demonstrated that the penultimate model is an appropriate description of the radical copolymerization of these two monomers. ESR experiments were also used to study the mid-chain propagating radical of methyl 2-trifluoromethylacrylate.

Future work in this area involves further investigation of this interesting radical copolymerization. While the mercury method experiments show that a penultimate trifluoromethyl group of a propagating radical does indeed have an effect on selectivity toward a 2-trifluoromethylacrylate, further, more extensive experiments can be performed that might better model the radical copolymerization between this monomer and norbornene. For example, Cywar et al.[76] designed two different ^{13}C labeled bisazo radical initiators which had phenyl and cyano substitution in positions that would become penultimate to the propagating radical. These molecules were used in a competitive polymerization reaction between acrylonitrile and styrene and, through the use of ^{13}C NMR, showed that the selectivity of the radical with a penultimate cyano group toward acrylonitrile was suppressed, thereby lending further support to the proposed penultimate model of polymerization between these two monomers. This work has advantages over the mercury method experiments by Jones et al.[67,68] in that it more accurately models the macroradicals involved in such a copolymerization.

One could imagine performing an analogous experiment with a 2-trifluoromethylacrylate and norbornene using ^{13}C labeled bisazo radical initiators which had methyl and trifluoromethyl substitution in positions that would be penultimate to the propagating radical.

While the ESR experiments discussed in this chapter did not successfully give insight into the characteristics of the radical in copolymerization between 2-trifluoromethylacrylate and norbornene, precedent has been set by others to use this technique to examine penultimate effects using this spectroscopic technique. By preparing bisazo compounds with various substituents that were penultimate to the propagating radical followed by reaction with sulfenyl acrylates, Tankana et al.[77] used ESR to demonstrate that the cyano group in a penultimate unit of a radical leads to suppression of the rate of addition of an olefin to the radical. Perhaps such a study could be done to examine the reactivity of a propagating radical with a penultimate trifluoromethyl group.

Finally, extensive ab inito molecular orbital calculations have been performed by Coote et al. in order to elucidate reaction barriers[78,79] and propagation rate coefficients[80] of copolymerizations that are best described by the penultimate model of copolymerization. While extensive study (certainly not executed by this author alone) of the reaction between 2-trifluormethacrylate and norbornene has been mentioned in this thesis, theoretical investigations have yet to be done. Perhaps such studies will give important insight into this intriguing and fairly new radical copolymerization.

APPENDIX I: A NEGATIVE TONE RESIST POLYMER FOR 157 nm LITHOGRAPHY

Thus far, this dissertation has dealt with materials for positive-tone lithography, where exposed regions of an insoluble resist material undergo a chemical change that renders it soluble in base developer. While this technology plays a crucial role in the development of the integrated circuit, many components of the modern semiconductor are fabricated through the use of negative tone photolithography. In this case, exposed regions of a soluble resist film undergo a chemical change, often a cross-linking reaction, which renders these regions insoluble in base developer (figure I.1). Resist simulations have shown that while narrow resist lines are best printed with a positive tone process, a negative tone process is advantageous for producing narrow trench geometries.[81] This section focuses on the development of a fluorinated negative-tone resist for 157 nm exposure.

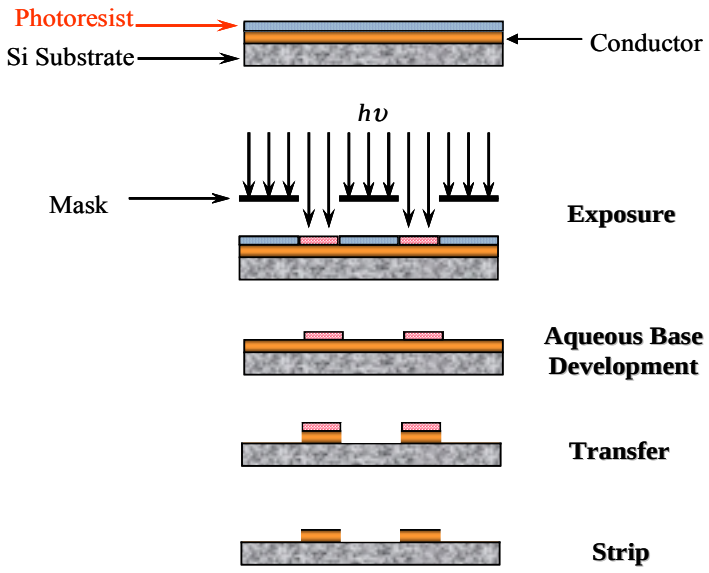

Figure I.1: The negative tone resist process.

In order to design a resist for 157 nm lithography with requisite transparency requirements, we first looked toward poly(3-bicyclo[2.2.1]hept-5-en-2-yl)-1,1,1-trifluoro-2-(trifluoromethyl)propan-2-ol) (PNBHFA). This material has a very low absorbance at 157 nm(1.2 μm^{-1}), and is the basis for our group's most successful 157 resist materials.[82] We envisaged that a base soluble analogue of PNBHFA could be formulated with a cross-linker, that, when exposed to acid, would crosslink with the base resin, forming an insoluble network. The cross-linker that we elected to study was tetramethoxymethyl glycouril (TMMG). This material has been used previously as a cross-linker for *i*-line and DUV applications.[83,84] While the TMMG cross-linker would appreciably increase absorbance at 157 nm, it could be used for proof of concept experiments.

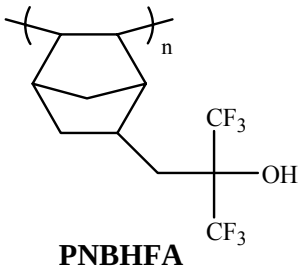

PNBHFA

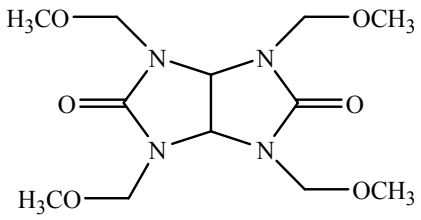

TMMG

Figure I.2: PBNHFA and TMMG.

In the DUV application[83], exposure of a poly(hydroxystyrene) (PHOST), PAG, and TMMG formulation generated acid that protonated the methoxy group of TMMG. The electrophilicity of the methylene unit was substantially increased, and subsequently reacted with the aromatic ring of PHOST via an electrophilc aromatic substitution mechanism, resulting in a cross-linked resin. Extending this chemistry to 157 would be nontrivial because the high absorbance of aromatic rings precludes their use.[85] Hence, the primary pathway for this reaction with aromatic substituents, is not available. PNBHFA has an alcohol functional group that could conceivably serve as a nucleophile in an ether forming reaction with such a crosslinker. However, the highly electron withdrawing trifluoromethyl substituents and the steric bulk of these groups makes such an attack unlikely. We therefore sought to move the alcohol functionality away from the geminal trifluoromethyl groups to a primary position. Such a modification would increase the nucleophilicity of the alcohol by both increasing its electron density and reducing steric hindrance.

Norbornene hexafluoroalcohol (NBHFA) monomer was reacted with sodium hydride and bromoethanol in order to produce the primary alcohol by a Williamson ether synthesis. Unfortunately, these efforts resulted in the recovery of starting material. We therefore sought out molecules that were more susceptible to nucleophilic attack in order to achieve such an addition. NBHFA reacted with sodium hydride and bromomethyl acetate to give the adduct **I.1**. This material was subsequently reduced with lithium aluminum hydride to give the desired monomer norbornene hexafluoro-primary alcohol (NBHFPA, **I.2**).

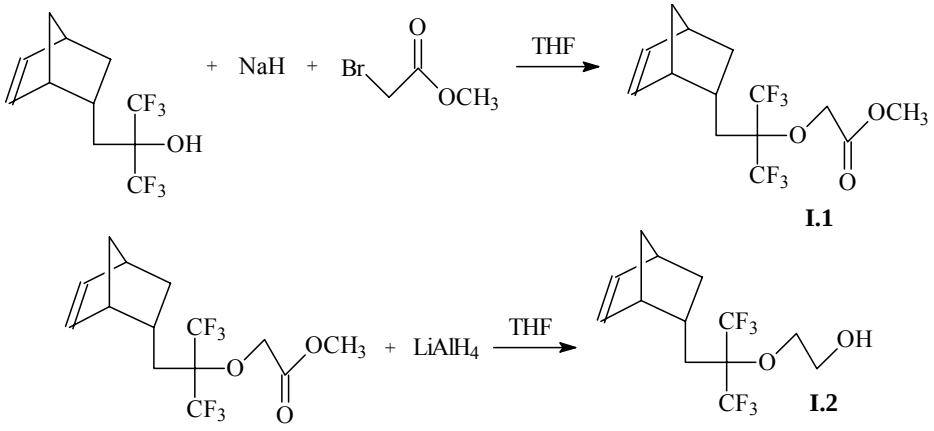

Figure I.3: The synthesis of **NBHFPA** (**I.2**).

While the synthesis of NBHFPA allows for interaction with a cross-linker, moving the alcohol away from the trifluoromethyl groups decreases the acidity of this material. The pKa of the hexfluoroalcohol starting material is around 11[86], but repositioning the alcohol two methylene units away from the inductive effect of the trifluoromethyl groups renders this new monomer insoluble in base developer. However, PNBHFPA could still be incorporated into a base soluble resist if it were

copolymerized with a highly acidic comonomer. To achieve this, the norbornene monomer was radically copolymerized with 2-trifluoromethylacrylic acid resulting in the copolymer **I.3** which displayed the 2:1 (2-trifluoromethylacrylate : norbornene) monomer incorporation first described by Ito et al.[87] (figure I.4).

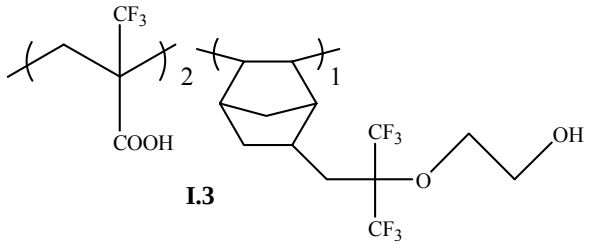

I.3

Figure I.4: Copolymer **I.3**.

Copolymer **I.3** was formulated with PAG and TMMG. This formulation was spin-coated on a silicon wafer and exposed at 157 nm. As shown in figure **I.5**, this experiment resulted in negative tone structures. The unexposed regions of the resist showed no residues, proving that **I.3** is sufficiently soluble in base developer. The exposed regions of the resist did not develop away, demonstrating that some degree of cross-liking occurred in the system. One drawback to this resist system is that the exposed regions did exhibit some degree of swelling. This is at least partially due to the incorporation of carboxylic acid in the copolymer. Future work involves using Ni and Pd vinyl addition catalysts[82] to synthesize a negative tone copolymer of norbornene hexafluoroalcohol and NBHFPA. The hexafluoroalchol moiety provides solubility in base developer, so incorporation of a very acidic carboxylic acid functional group would not be necessary, thereby decreasing swelling in the exposed regions of the resist. As opposed to the above

radical copolymer, an all-norbornene backbone also allows for tuning of monomer incorporation in order to improve resist properties. Also, one might consider the synthesis a fluorinated version of a methoxymethyl glycouril that could be formulated into a negative tone resist without adding absorbance at 157 nm.

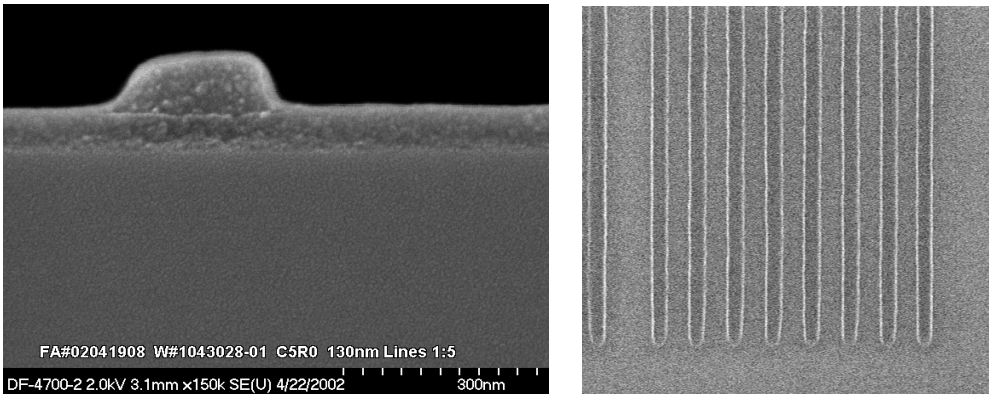

79.6% polymer, 14% x-linker , 6.1% TPS-Nf, .3% TBAH, 157 nm exposure (43 mJ/cm^2), binary mask, 125 nm thick on 82 nm of ARC, 100˚C-60s PAB, 100˚C-90s PEB, 30s development (0.26N TMAH)

Figure I.5: Negative-tone 157 nm imaging experiments with copolymer I.3.

APPENDIX II: DIRECT MEASUREMENT OF THE REACTION FRONT IN CHEMICALLY AMPLIFIED PHOTORESISTS

As semiconductor device geometries continue to shrink to sub-100 nm critical dimensions, new constraints are placed on photoresist development. The feature sizes created at the dawn of chemically amplified resist technology did not demand concern over phenomena such as degree of polymerization, the radius of gyration of resist polymers, or the path length of a photoacid generator as it moves through a resist film. To achieve sub-100 nm sizes, however, critical dimensions must be controlled to tolerances at the 2 to 5 nm length scales. Interestingly, this is comparable to the diameter of a novolac monomer (1nm) and the radius of gyration of a typical novolac polymer chain (3-5 nm).[88] The development of small feature sizes also calls for careful control of the PAG used for chemical amplification. The generated acid must be mobile enough to protect an adequate amount of protecting groups on the resist polymer, but not diffuse so far as to cause image deformation (i.e., deprotect unexposed areas of resist). In order to meet transparency requirements for next generation photolithography, film thicknesses will be decreased, increasing the probability that these aforementioned factors will have an impact on resist performance. A quantitative understanding of these properties in thin resist films is critical in order to successfully produce such small dimensions. Such an understanding demands the study of the reaction-diffusion process at the nanometer length scale.

In a collaboration between Sean Burns, Dr. Eric K. Lin of the National Institute of Standards and Technology and Dr. Dario L. Goldfarb of the IBM T. J.

Watson Research Center, we measured the deprotection front profile of a resist film utilizing neutron reflectivity. Neutron reflectivity is a spectroscopic technique that can provide angstrom-level resolution of the thickness, density, and surface roughness of a film. The manner in which a neutron reflects off a surface is very similar to the way that light reflects off a surface, and the same laws apply to both instances (refractive index, for example). In a neutron reflectivity experiment, a polarized beam of neutrons is focused onto a polymer film and the reflected intensity of those neutrons is measured as a function of momentum transfer (Q). The extremely small wavelength of the neutron beam (0.2-2.0 nm) allows for exceptionally high resolution spectroscopy, permitting the examination of very thin (less than 100nm) resist films (figure II.1).

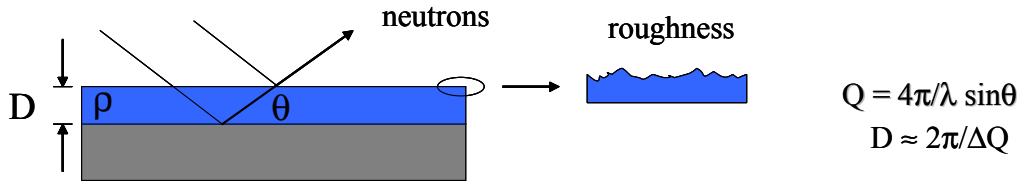

Figure II.1: A schematic of a neutron reflectivity experiment. Momentum transfer (Q) is used to measure changes in film thickness. Such measurements give insight into surface roughness.

In order to measure the shape of a deprotection profile of a chemically amplified resist using neutron reflectivity, a bilayer experiment was proposed. In this experiment, a film of a completely protected homopolymer (in this case, *tert*-butyl carbonate protected poly[p-hydroxystyrene]) was coated on a silicon wafer. Then, a completely *deprotected* homopolymer (poly[hydroxystyrene]) formulated

with PAG was spin-coated on top of the protected layer. Upon exposure to light and a post-apply bake, photo-generated acid diffuses through the top film to the bottom film where it deprotects regions of the protected homopolymer. Neutron reflectivity was used to measure the contrast between the protected and deprotected areas of film. A development step washed all of the unprotected areas of film away, and neutron reflectivity could again be used to measure the thickness and roughness of the resulting profile.

Neutrons are scattered by nuclear interactions. Unfortunately, there does not exist a significant difference in neutron scattering intensity between *tert*-butyl carbonate protected poly(hydroxystyrene) (PBOCST) and poly(hydroxystyrene) (PHOST). Fortunately, there is a large difference in the neutron scattering cross section between deuterium and hydrogen nuclei (figure II.2).[89] We could therefore create strong contrast between PBOCST and PHOST by slightly modifying the protected polymer by incorporation with deuterium.

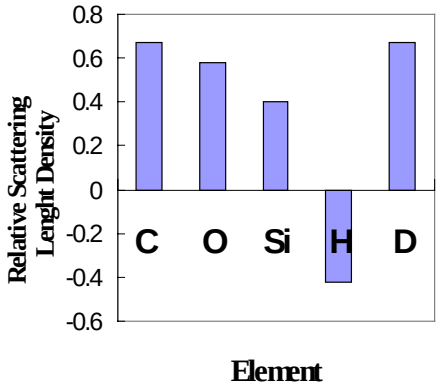

Figure II.2: The neutron scattering intensity of different elements. There is a strong difference between hydrogen and deuterium.

PHOST is routinely converted to PBOCST by treatment with di-*tert*-butyl dicarbonate and dimethyl amino pyridine (DMAP). If a deuterated version of di-*tert*-butyl dicarbonate were used in the protection of PHOST, the resulting polymer would contain enough deuterium to offer good contrast between it and the reaction product to enable neutron reflectivity bilayer experiments. To that end, 2-methyl-2-propanol-d_{10} was purchased, and then reacted with potassium metal in dry THF to form potassium *tert*-butoxide-d_{10} (the reaction was considered to be complete when all of the potassium appeared to dissolve in the THF; this generally took about 48 hours). This salt was then used as starting material for the published procedure[90] for making di-*tert*-butyl dicarbonate. The *tert*-butoxide-d_{10} was reacted with carbon dioxide followed by reaction with phosgene to form di-*tert*-butyl tricarbonate-d_9, which was reacted with 1,4-diazabicyclo[2.2.2]octane (Dabco) to produce the desired di-*tert*-butyl dicarbonate-d_9. This product was subsequently reacted with PHOST (M_w=21,000 and PD = 2.1) using a catalytic amount of DMAP to form PBOCST –d_9 (figure II.3). Analysis of this product by thermogravimetric analysis (TGA) showed that the polymer was over 95% protected.

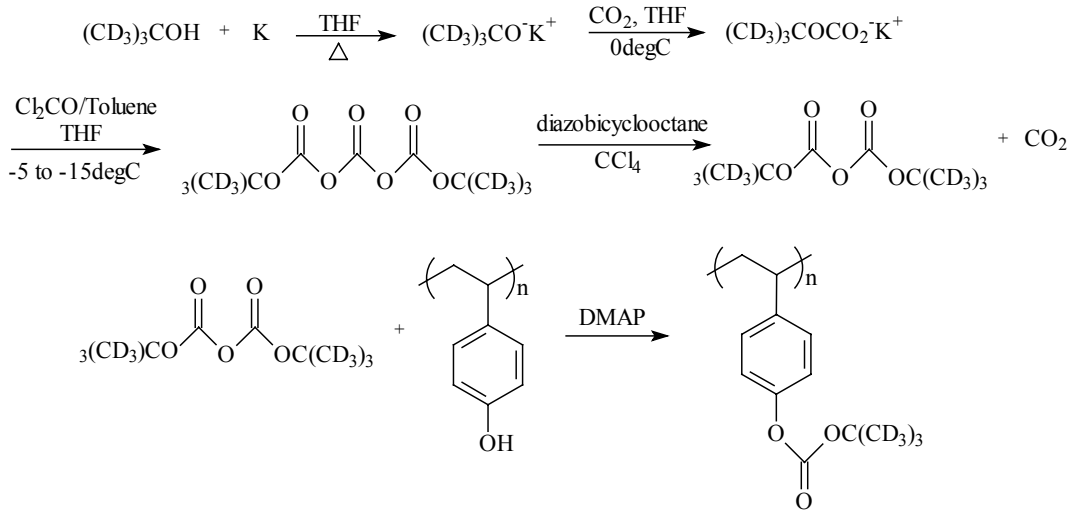

Figure II.3: The synthesis of di-*tert*-butyl dicarbonate-d_9 and PBOCST-d_9.

Once the copolymer was obtained, a reaction kinetics study was performed to confirm that the replacement of the hydrogens on the *tert*-butyl group of PBOCST with deuterium atoms did not effect the reactivity of the polymer deprotection in the presence of acid. Separate films of PBOCST and PBOCSt-d_9 were formulated with photoacid generator and exposed in the UV. The films were then placed on a hotplate that was situated under an IR spectrophotometer. The setup of this tool has been described in the literature.[91,92] As the films were heated, deprotection ensued which could be tracked by IR. As the *t*-boc-carbonate groups deprotected, the absorbance in the carbonyl region (~1700 cm^{-1}) decreased. Such information can be used to determine the extent of reaction and deprotection kinetics.[91,92] A graph of the extent of reaction versus time (figure II.4) of both polymer films shows that there is no significant difference in deprotection kinetics between the two polymer films.

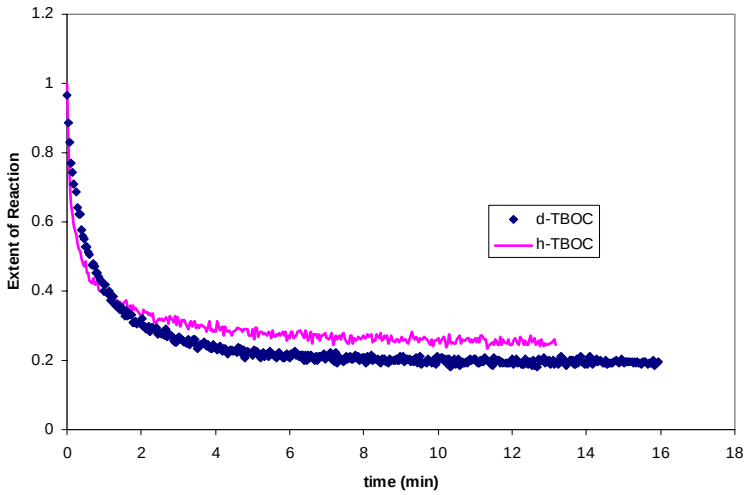

Figure II.4: Comparison of PBOCSt and PBOCSt-d_9 reaction kinetics.

Since there appeared to be no significant difference in reactivity between a *t*-boc protecting group with hydrogen and deuterium atoms on the *tert*-butyl group, we were confident to attempt neutron reflectivity experiments. Preparation of the samples was accomplished in five processing steps. In step 1, the lower layer consisting of the deuterium-labeled polymer was spin-coated from PGMEA solution and baked on a hotplate. In step 2, a resist formulation consisting of PHOST and 5 weight % di(*tert*-butyl phenyl)iodonium perfluorooctanesulfonate (PFOS) was spin-coated from a 1-butanol solution directly onto the lower layer, followed by another post apply bake. In step 3, the sample was exposed in the UV to generate acid in the top layer. A post-exposure bake in step 4 allowed for the propagation of acid from the top layer into the bottom layer. Finally, in step 5, the original PHOST layer and the soluble, deprotected areas were removed by

immersion in 0.26 N TMAH solution. Neutron reflectivity responses were taken at each processing step. Each of the processing steps and the corresponding neutron reflectivity curves are outlined in figure II.5. The curves in figure II.5 are real space profiles corresponding to the best fits of the experimental data. The actual neutron reflectivity curves are not shown.

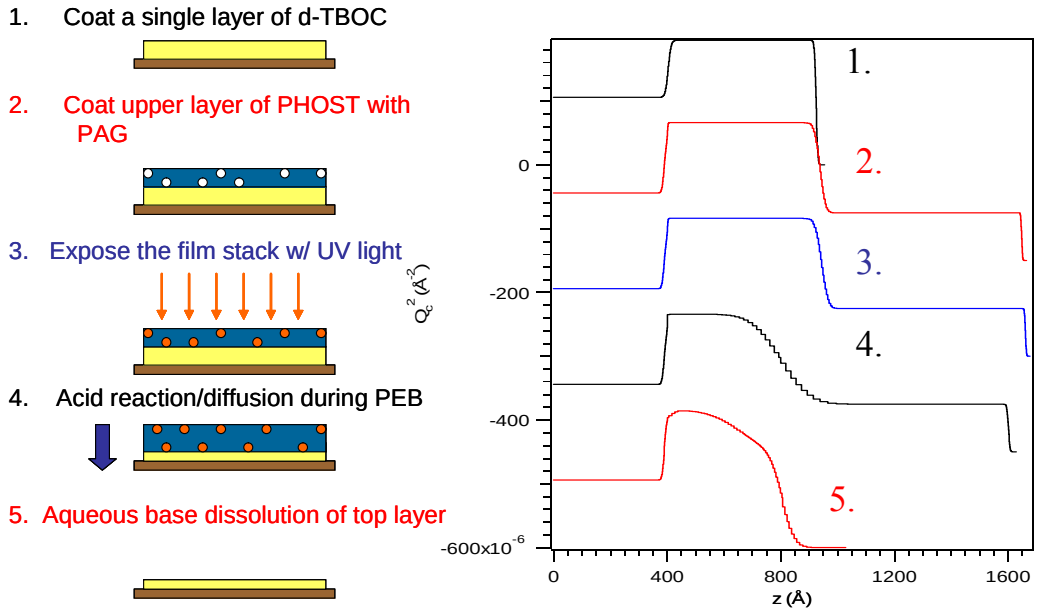

Figure II.5: Sample processing steps (left) with corresponding neutron reflectivity graphs (right). The graphs are vertically offset for clarity.

In step 1 of this process, the initial thickness of the PBOCSt-d_9 layer was ~535 Å. At step 2, the thickness of the PBOCST layer with PFOS was ~720 Å. Neutron reflectivity experiments showed very little intermixing between the two layers. Even after the ultraviolet exposure (step 3), there was no change at the bilayer interface. However, after the post exposure step (step 4), there was a

change in the neutron reflectivity curve due to dramatic changes in the interfacial compositional profile. This corresponds to a reaction front broadening of approximately 160 Å. Control experiments on identical bilayers without PFOS in the PHOST layer confirm that the interfacial width between PBOCSt-d_9 and PBOCST was unaffected by these processing conditions. The observed interfacial broadening is therefore due to propagation of the acid-catalyzed reaction front and not to thermal deprotection. Finally, in step 5, aqueous base was used to remove both the original PHOST acid feeder layer as well as soluble products from the deprotection of PBOCSt-d_9. This led to a further altering of the reaction front profile. The final physical interface between the two layers was 47 Å, which is very close to the initial physical interface of 40 Å

By studying a bilayer of PBOCST and PBOCSt-d_9 with neutron reflectivity, quantitative information about the spatial evolution of the reaction-diffusion process in chemically amplified photoresists was obtained. More details on the above experiment are available in the literature.[93] Preliminary experiments such as those described above will play a vital role in the development of resist technologies for sub-100 nm resist features.

While the above experiments showed that there is good contrast between the bilayers of PBOCST and PBOCSt-d_9, we have therefore synthesized a protected poly(hydroxystyrene) with yet more deuterium. The polymer PBOCSt-d_{11} was prepared though the reaction of di-*tert*-butyl dicarbonate-d_9 with a commercially available poly(hydroxystyrene) that has deuterium substitution in the backbone (figure II.6). In the previous study, the PBOCSt-d_9 loses all

deuterium upon deprotection because the deuterium substitution is on the *tert*-butyl carbonate. The previously protected homopolymer no longer has the sharp contrast difference with the PHOST feeder layer. In the case of PBOCSt-d_{11}, however, the deprotected homopolymer will continue to maintain good contrast with the feeder layer and allow study of any intermixing after deprotection because it still contains deuterium. Neutron reflectivity experiments with this material are currently underway.

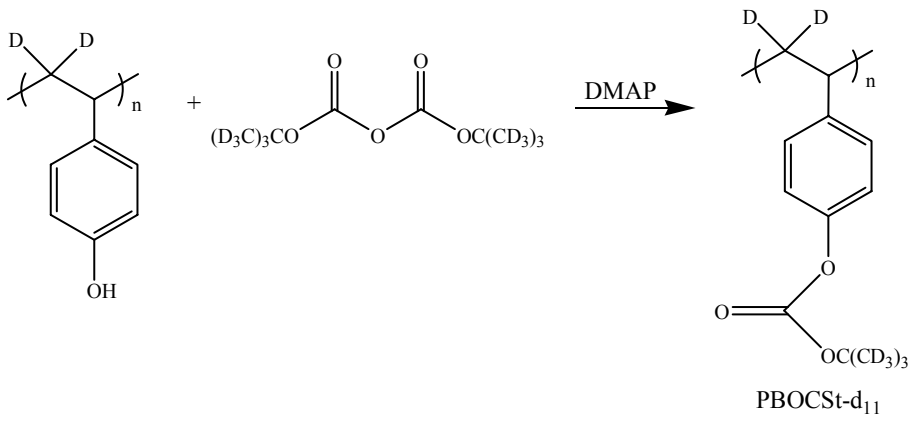

Figure II.6: The synthesis of PBOCST-d_{11}

While a PHOST homopolymer that is totally *t*-boc protected gives good insight into the propagation of a reaction front during chemical amplification, PBOCST is not an actual photoresist. In actuality, a photoresist polymer of this nature would only be about 35% protected, allowing the free phenolic ring to contribute to adhesion and wetability characteristics. In order to prepare a deuterated material that is more analogous to an actual resist polymer, we chose to synthesize a deuterated version of ESCAP, which is a copolymer of hydroxy

styrene and *t*-butyl methacrylate. Again, we aimed to incorporate deuterium into the protecting group moiety (*t*-butyl group). The monomer *t*-butyl methacrylate-d_9 was synthesized by reaction of commercially available 2-methyl-2-propanol-d_{10} with acryloyl chloride in the presence of triethylamine. This monomer was then co-polymerized with acetoxy styrene followed by selective hydrolysis of the acetate with ammonium acetate to provide the desired resist polymer using the reported procedure[94] (figure II.7). Preliminary experiments with this material are underway to investigate if ESCAP-d_9 has enough deuterium content to offer sufficiently high contrast for analysis with an acid feeder layer.

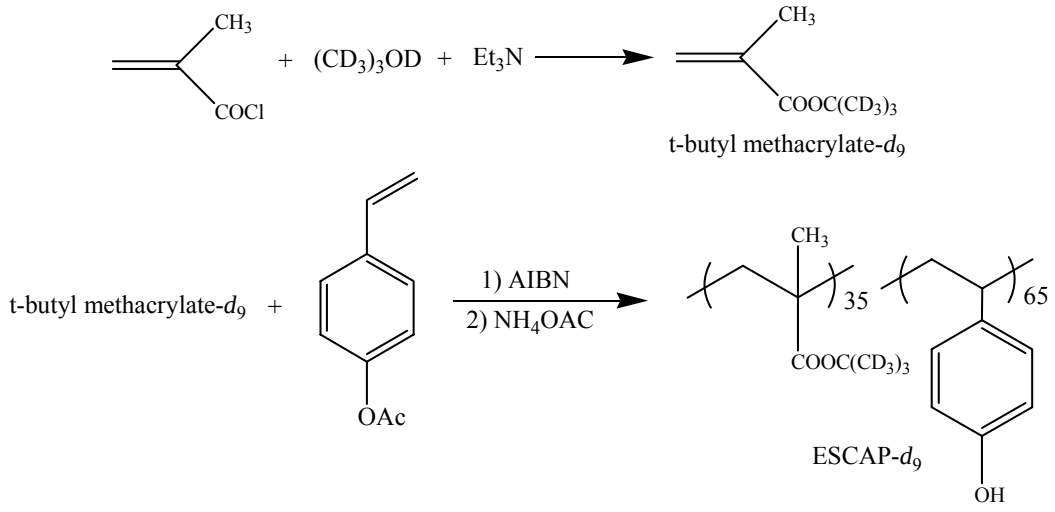

Figure II.7: The synthesis of *t*-butyl methacrylate-d_9 and ESCAP-d_9.

APPENDIX III: THE SYNTHESIS OF POLYMER BOUND PAGS

In the previous section, we discussed how resist requirements will change as the semiconductor industry approaches sub-100 nm device features. For example, PAG diffusivity through the resist film is a concern. The PAG must travel far enough to assure that enough protecting groups are cleaved, but not so far as to limit resolution. Upon exposure, a PAG produces an acidic proton that is bound to its counter anion. It is known that as the size of the counter anion of the generated acid increases, diffusivity decreases.[95,96] However, even PAGs with large counter anions have path lengths that will be unworkable in the sub-50 nm regime. This section discusses efforts to produce polymer-bound photoacid generators. In the limit, if the anion component of the PAG is covalently bound to a polymer backbone, the acidic proton would most likely not diffuse too far away from its counter anion, thereby severely decreasing its mobility. We are eager to study the trade-off between resolution and sensitivity with such materials.

Previous work[96] in our group focused on styrene-bound PAGs. For initial acid diffusion studies, two polymeric bound PAGs were prepared (figure III.1). Both of these materials produce similar acids upon exposure. The anion bound PAG (anPAG) was designed so that the anion component of the acid is covalently bound to the styrene polymer backbone. The cation bound PAG (catPAG) was prepared as a control to compare its results with the first polymer. In this case, the cation component of the PAG is bound to a polymer backbone. Irradiation causes the production of $PhOCF_2CF_2SO_3H$ acid, which is an unbound analogue of the acid produced from the anPAG. The synthesis of these materials has been

described previously.[97] The anionic polymeric PAG was synthesized by copolymerization of the corresponding lithium salt and styrene, followed by metathesis reactions on the resultant copolymer. Synthesis of the lithium salt has been reported in the literature by Feiring et al.[98,99]

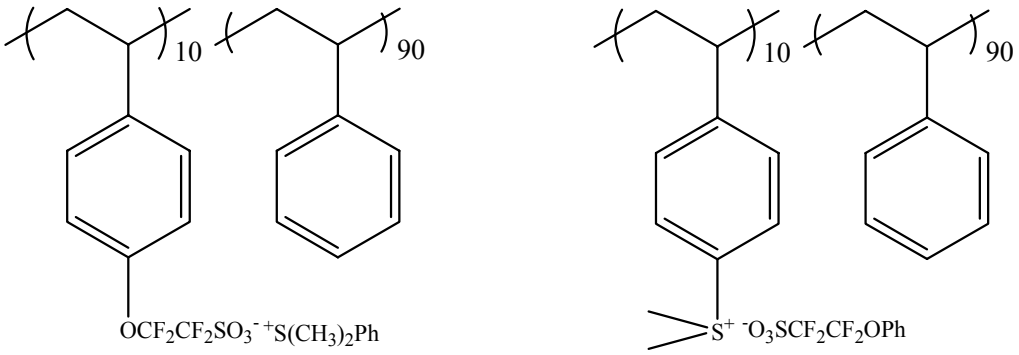

anPAG **catPAG**

Figure III.1: Anion and cation bound PAGs.

These polymers were tested in an IR bilayer experiment very similar to the experiments utilized for neutron reflectivity. The polymer bound PAGs were coated onto a silicon wafer, and a layer of *tert*-butyl carbonate protected poly(hydroxystyrene) (PTBOCST) was spin-coated on top of the first film. In this experiment, the extent of deprotection was monitored during the post exposure bake through the use of IR spectroscopy. Absorbance in the carbonyl region of the IR (~1700 cm^{-1}) decreases as acid cleaves off *tert*-butyl carbonate groups from the polymer. The extent of polymer deprotection can be used to determine the path length of the acid molecule. The mathematical relationship between polymer deprotection as monitored by IR and acid path length has been reported.[95-97]

Figure 2 shows the results of this experiment. As expected, the polymer-bound PAG that has the conjugate base of the photogenerated acid bound to the polymer backbone has a relatively low diffusion length. Alternatively, the cation bound PAG has a much higher diffusion length. This result is expected because the photogeneratded acid is not bound to the polymer backbone.

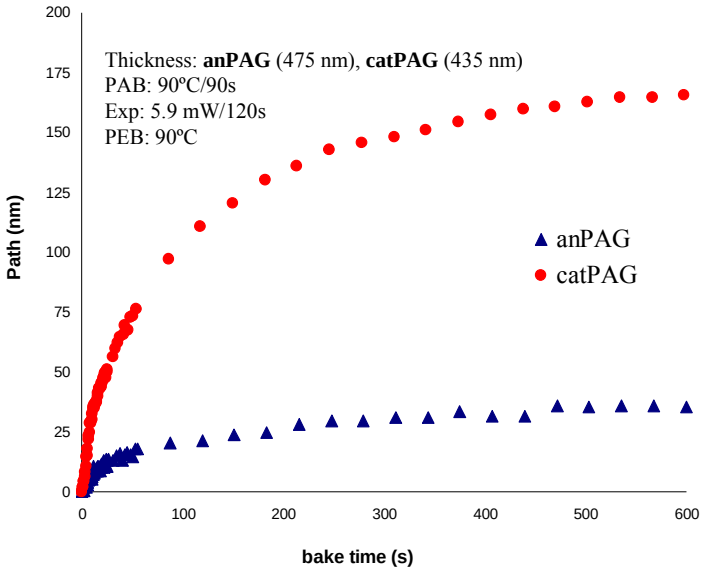

Figure III.2: Path length curves for two polymeric PAGs tested in a bilayer stack experiment.

As stated earlier, one of the main purposes of these efforts was to produce a material that would generate acid upon photolysis that would diffuse relatively low distances thoughout the resist film. Ideally, such a material could be used in an actual resist formulation in order to help in controlling linewidth variations. However, when the anionic bound polymer PAG was mixed with TBOCST and

cast as a film on to a silicon wafer, there was evidence of phase separation after spin-casting. This is indicative of a lack of phase compatibility between the two materials. We envisaged that switching the styrene comonomer to methoxystyrene might increase the miscibility of such a polymer bound PAG and TBOCST. This called for the synthesis of more starting material. As stated earlier, in-depth descriptions of the monomer synthesis have been published.[97-99] Reaction of the potassium salt of 4-bromophenol (**III.1**) with 1,2-dibromotetrafluoroethylene affords the ether (**III.2**). This ether is transformed to the sulfinate salt (**III.3**) in high yield on reaction with sodium dithionite and sodium bicarbonate in aqueous acetonitrile. Oxidation with chlorine gas in water provides the sulfonyl chloride (**III.4**), which was converted to the lithium sulfonate (**III.5**) by reaction with lithium hydroxide in aqueous THF. The styrene (**III.6**) is obtained from the corresponding lithium sulfonate and ethylene under typical Heck reaction conditions in the presence of a palladium catalyst. The lithium salt was polymerized radically with methoxystyrene in a 1 to 9 feed ratio (**III.7**). The polymer was then passed through an acidic ion exchange column and immediately converted to the silver salt by stirring with silver carbonate (**III.9**). The resulting polymer was converted to the final product by addition of thioanisole and iodomethane (**III.10**) (figure III.3). The copolymer composition (9:1) was confirmed by ^{19}F NMR using AgO_2CCF_3 as an internal standard.

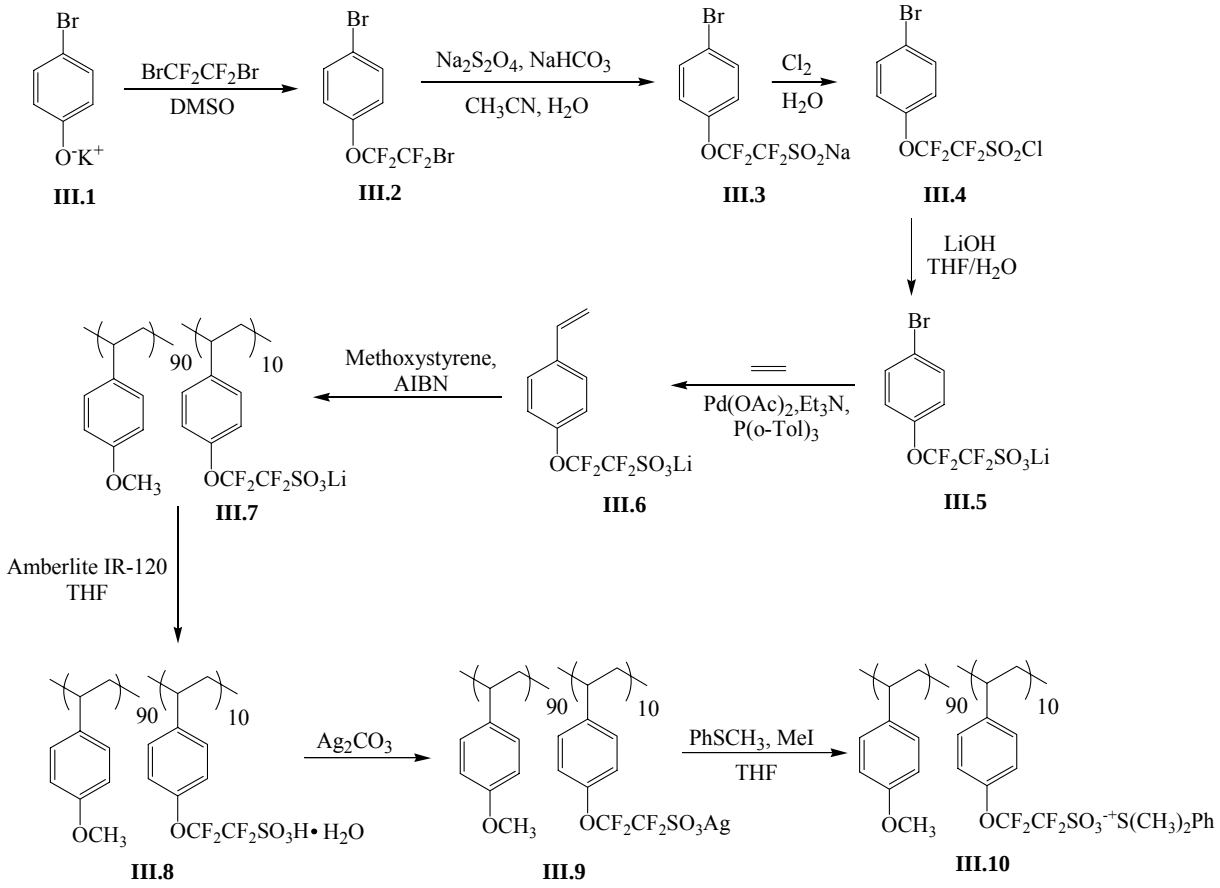

Figure III.3: The synthesis of a methoxy styrene-polymer bound PAG (**III.10**).

Once this copolymer was synthesized, it was subjected it to the bilayer experiment that was used to investigate the styrene-polymer bound PAG. The methoxystyrene polymer bond PAG **III.10** was coated onto a film, and a layer of PBOCST was coated on top of that. The sample was exposed to the UV, and investigations using IR spectroscopy showed that the photo-generated acid displayed a short diffusion length through the TBOCST polymer film when

compared to the cationic bound PAG that was previously synthesized (figure III.4). This new polymer was also blended with PTBOCST (90:10 PTBOCST: **III.10**) and this mixture was spin-coated onto a silcon wafer. A uniform film resulted that displayed no striations. Therefore, producing a polymer bound PAG with a methoxy component did successfully increase miscibility with PBOCST.

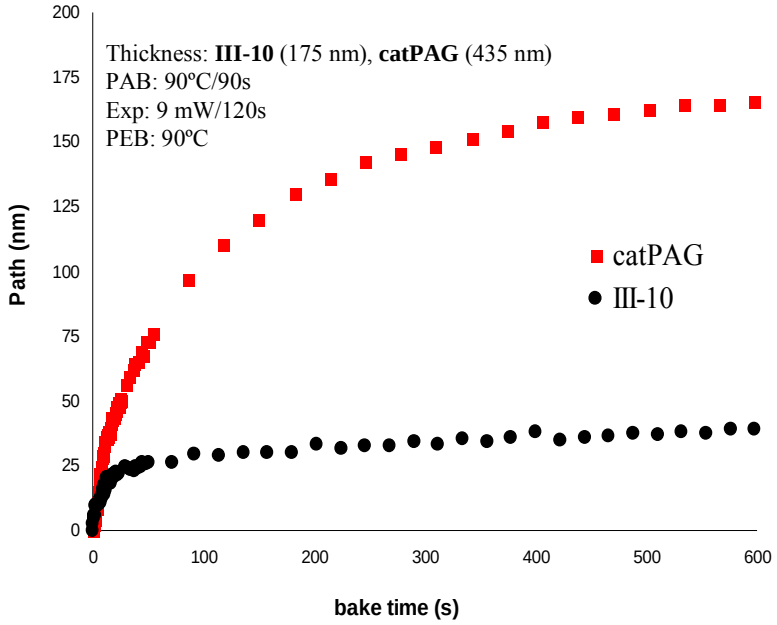

Figure III.4: Path length curve for the methoxy styrene polymeric PAGs tested in a bilayer stack experiment.

It should be mentioned that while both of the anion bound polymer PAGs that were prepared (styrene and methoxystyrene) had low diffusion levels compared to the cation bound PAG, the acids formed from these materials did travel much farther than expected. Results from the bilayer experiments suggest an average diffusion distance of about 30 nm for both materials. Since the counter

anion of the generated acid is attached to a polymer chain, one might expect that the diffusion distance of the acid would be much closer to zero. One possible explanation might be intermixing between the two layers of polymer. But as mentioned before, the styrene bound PAG was extremely immiscible with the TBOCST layer. Also, the sample preparation method is designed to limit opportunities for mixing between layers. Another explanation might be that the polymer bound PAG is actually penetrating into the PBOCST layer due to reaction enhanced diffusion. As areas of the PBOCST are deprotected, the volatile sideproducts carbon dioxide and isobutene are produced. These molecules could possibly create a plasticized film stack that could temporarily allow for interpenetration of the two film layers. While initial investigations into a polymer bound PAG shows promising results, future work involves sorting out these important issues.

EXPERIMENTAL

Imaging

All imaging work was performed on an Exitech 157 nm small field (1.5 x 1.5 mm^2) mini-stepper (0.6 NA) using either a binary mask (σ 0.7) or phase-shift mask (σ 0.3) at International SEMATECH in Austin, TX. Scanning electron micrographs were collected on a JEOL *JWS-7550*, and cross-sectional data were collected on a Hitachi *4500* microscope. Coating, baking, and development of resist films were performed using an FSI *Polaris 2000* track. Thickness measurements were made on a Prometrix interferometer. Unless stated otherwise, a typical resist formulation was prepared by mixing the polymer with 6 wt% (relative to polymer) photoacid generator (triphenylsulfonium nonaflate) and 0.3 wt% tetrabutylammonium hydroxide (TBAH) as the base to control acid diffusion and reduce T-topping. The entire mixture was diluted in PGMEA to produce a viscosity that provides resist thicknesses of approximately 100-200 nm after spinning the resist at 2500 rpm onto a silicon wafer that had been previously coated with ~80 nm BARC (bottom anti-reflective coating, Shipley AR19). The post-apply bakes were between 110°-140°C for 60 sec and the post-exposure bake was 110°-130°C for 90 sec, unless stated otherwise. The exposed resists were developed in the industry-standard 0.26 *N* tetramethylammonium hydroxide (TMAH) developer.

Instruments

Nuclear magnetic resonance (NMR) spectra were obtained using a Varian *Unity Plus 300* spectrometer (^{1}H: 300 MHz, ^{13}C: 75 MHz). Shifts for NMR spectra are reported in ppm relative to the chemical shift of the solvent. Infrared spectra were recorded on a Nicolet *Avatar 360* IR spectrometer, melting points are uncorrected. Mass spectra were measured on a Finnigan *MAT TSQ-700* spectrometer. Molecular weights (M_w) and polydispersity indicies (PDI), measured from THF solutions using a Viscotek GPC equipped with a set of two 5 mm crosslinked polystyrene columns (linear mix and 100 Å, American Polymer Standards) are reported relative to polystyrene standards. Polymers containing acidic functional groups were pretreated with either diazomethane before GPC measurement. Differenctial scanning calorimetry (DSC) measurements and thermal gravimetric analysis (TGA) were performed on a Perkin Elmer *Series-7* thermal analysis system. Gas chromatographs were recorded on a Hewlett Packard *5890 Series II* with an *HP-5* (crosslinked 5% PH ME siloxane) capillary column an flame ionization detector (FID).

Synthesis

2,2-Difluorobicyclo[2.2.1]heptane (2.2)

To a 250 mL three-neck round-bottom flask equipped with stir bar, condenser and nitrongen inlet was added, at 0°C, 45 mL dry DCM**,** 22.53 g (205 mmol) 2-bicyclo[2.2.1]heptanone **(2.1)**, and 50 mL (378 mmol) of diethylaminosulfur trifluoride (DAST), dropwise over 10 minuites (no generation of heat was observed). The reaction mixture was stirred at room temperature for 4

days. After this time the reaction mixture was transferred to a 1 L flask, cooled with an ice bath, and 130 mL of dichloromethane was added, followed by 30 mL of water, 250 mL of 5% sodium hydroxide, and 300 mL of 10% sodium hydroxide, dropwise to kill any remaining DAST. The aqueous layer was extracted with dichloromethane (50 mL x 3). The combined organic fractions were washed with water (100 mL), dried over MgSO4, filtered, and concentrated using Vigreux distillation head. The resulting mass was purified two times with column chromatography using silica gel with n-pentane as the eluent, resulting in 15.45 g (117 mmol, 57%) of the target molecule. Further purification by two sublimations (inside was cooled to ~22 ^{0}C and outside was heated to ~32 ^{0}C) afforded an extremely pure clear sticky solid that was 100% pure by GC. mp 92.5 ^{0}C. bp 117.5^{0}C. ^{1}H NMR (500 MHz, $CDCl_3$, δ): 2.45 (m, H-1, 1H), 2.37 (m, H-4, 1H), 2.03-1.82 (m, H-3, 1H), 1.75-1.64 (m, H-6, 1H), 1.73-1.65 (m, H-7, 1H), 1.68-1.55 (m, H-3, 1H), 1.65-1.56 (m, H-5, 1H), 1.54-1.45 (m, H-6, 1H), 1.40-1.30 (m, H-5, 1H), 1.38-1.30 (m, H-7, 1H). ^{13}C NMR (126 MHz, $CDCl_3$, δ): 131.31 (t, $^1J_{CF}$ = 253.6 Hz, C-2), 44.68 (t, $^2J_{CF}$ = 20.3 Hz, C-1), 42.90 (t, $^2J_{CF}$ = 23.3 Hz, C-3), 37.01 (d, $^3J_{CF}$ = 5.1 Hz, C-7), 35.82 (d, $^3J_{CF}$ = 1.7 Hz, C-4), 27.47 (C-5), 20.87 (t, $^4J_{CF}$ = 6.0 Hz, C-6). ^{19}F NMR (282 MHz, $CDCl_3$, δ): -86.4 (dd, J = 220 Hz, J = 28 Hz), -109.7 (dd, J = 220 Hz, J = 15 Hz). HRMS-CI (m/z): $[M - HF + H]^+$ calcd for $C_7H_{10}F$, 113.0766; found, 113.0757.

2-Fluorobicyclo[2.2.1]heptane (2.4)

To a 250 mL three-neck round-bottom flask equipped with a strirring bar and nitrogen inlet was added 21.04 g (188 mmol) of exo-2-bicyclo[2.2.1]heptanol

(2.3)and 45 mL of dichloromethane. The mixture was cooled to 0 ^{0}C with an ice bath and 35 mL (265 mmol) of diethylaminosulfur trifluoride (DAST) was added dropwise over 40 minutes (exothermic reaction). The ice bath was removed and the mixture was stirred at room temperature for 5 days. After this time, the reaction mixture was transferred to a 1 L flask, cooled with an ice bath, and 130 mL of dichloromethane was added followed by 30 mL of water, 250 mL of 5% sodium hydroxide, and 300 mL of 10% sodium hydroxide, dropwise. The water layer was extracted with dichloromethane (50 mL x 2). The combined organic fractions were washed with water (150 mL), dried over $MgSO_4$, filtered, and concentrated using a Vigreux distillation head. The resulting mass was purified two times with column chromatography using silica gel with n-pentane as the eluent, resulting in 15.45 g (117 mmol, 57%) of the target molecule that was 100% pure by GC. Further purification by two sublimations (inside was cooled to ~22 ^{0}C and outside was heated to ~32 ^{0}C) afforded 2.5g (12%) of a colorless, sticky solid that was 100% pure by GC. mp 88-89 ^{0}C. ^{1}H NMR (500 MHz, $CDCl_3$, δ): 4.58 (dd, $^3J_{HF}$ = 56.0 Hz, J = 5.9 Hz, H-2, 1H), 2.42 (td, J = 6.7 Hz, J = 1.0 Hz, H-1, 1H), 2.30 (s, H-4, 1H), 1.68-1.58 (m, H-3endo, 1H), 1.62-1.54 (m, H-7, 1H), 1.57-1.51 (m, H-3exo, 1H), 1.55-1.45 (m, H-6exo, 1H), 1.45-1.37 (m, H-5exo, 1H), 1.19-1.13 (m, H-7, 1H), 1.05-0.96 (m, H-5endo, 1H), 1.01-0.92 (m, H-6endo, 1H). ^{13}C NMR (126 MHz, $CDCl_3$, δ): 96.16 (d, $^1J_{CF}$ = 181.1 Hz, C-2), 42.01 (d, $^2J_{CF}$ = 20.0 Hz, C-1), 39.95 (d, $^2J_{CF}$ = 19.1 Hz, C-3), 34.88 (C-4), 34.62 (C-7), 27.98 (C-5), 22.38 (d, $^3J_{CF}$ = 10.9 Hz, C-6). ^{19}F NMR (282 MHz, $CDCl_3$, δ): -160.6 (m). CIMS (m/z): $[M - HF + H]^+$ calcd for C_7H_{10}, 95; found, 95.

7,7-Dimethoxy-1,2,3,4-tetrachlorobicyclo[2.2.1.]hept-2-ene (2.7)

To a 200mL Parr pressure vessel equipped with a stirring bar was added 75.00g (0.28 moles) of 5,5-dimethoxy-1,2,3,4-tetrachlorocyclopentadiene **(2.6)** and the reactant was placed under 350 psi ethylene pressure. It was then heated to 180°C for twelve hours after which time it was allowed to cool to room temperature. Vacuum distillation (88°-98°C, .38mmHg) afforded 78.78g (95%) of a slightly yellow liquid that was 98% pure by GC. ^{1}H NMR ($CDCl_3$) δ 1.72-1.77 (m,2H), 2.28-2.33 (m, 2H), 3.51 (s, 3H), 3.57 (s, 3H); ^{13}C NMR ($CDCl_3$) δ 35.39, 51.46, 52.55, 75.14, 110.58, 129.91; IR (neat) 2984.35, 2949.50, 2844.95 cm^{-1}; HRMS (CI) m/z (rel. intensity) 292($M+H^+$,100), 290 (35); HRMS (CI) m/z calculated for $C_9H_{11}O_2Cl_4$ (m+1) 290.950637, found 290.95.1316

7,7-Dimethoxybicyclo[2.2.1]hept-2-ene (2.8)

To a 1000mL three-necked, round-bottom flask equipped with a condenser, mechanical stirrer, and nitrogen inlet was added 750 mL dry, distilled THF, 51.15g (.176 moles) 7,7-dimethoxy-1,2,3,4-tetrachlorobicyclo[2.2.1.]hept-2-ene **(2.7)**, 77.12g (1.04 moles) of t-butyl alcohol and 55g of 5mm cubes of chopped sodium metal. The reaction mixture was heated under reflux with vigorous stirring for 24 hours, over which time it turned from colorless to dark purple. After cooling to room temperature a mass of unreacted sodium was removed, and the reaction mixture was placed on ice and 150mL of methanol was added dropwise to quench any remaining sodium. The resultant mixture was filtered through Celite, concentrated in vacuo, poured over 100mL of ice water and extracted four times

with 150mL portions of diethyl ether. The combined ether extracts were washed three times with 150mL portions of brine, dried over magnesium sulfate, filtered, and the solvent was removed by rotary evaporation. Vacuum distillation (58°-63°C, 17mmHg) left 20.02g (74%) of slightly yellow liquid that was 96.1% pure by GC. ^{1}H NMR ($CDCl_3$) δ .89-.94 (m, 2H), 1.79-1.81 (d, 2H), 2.72-2.75 (d, 4H), 3.12-3.17 (d, 6H), 6.05 (s, 2H); ^{13}C NMR ($CDCl_3$) δ 22.88, 44.07, 49.50, 51.96, 118.65, 133.34 IR (neat) 3064.01, 2979.37, 2944.52, 2825.04, 1729.73 cm^{-1}; HRMS (CI) m/z (rel. intensity) 155($M+H^+$,100), 154 (50); HRMS (CI) m/z calculated for $C_9H_{15}O_2$ (m+1) 155.107205, found 155.107779.

7,7-Dimethoxy-bicyclo [2.2.1] heptane (2.9)

To a 100mL Parr pressure vessel equipped with a stirring bar was added 150mL dry THF, 18.93g (.12 moles) of 7,7-Dimethoxybicyclo[2.2.1]hept-2-ene (2.8) and .95g of Pd-C (10% palladium on activated carbon). The reaction mixture was stirred overnight at room temperature under 200 psi hydrogen pressure. The resultant solution was then filtered to remove the Pd-C and a small amount of diethyl ether was added to the filtrate. The diethyl ether solution was then washed twice with small portions of brine, dried over magnesium sulfate, and the solvent was removed by rotary evaporation resulting in 14.98g (78%) of product that was 93% pure by GC. ^{1}H NMR ($CDCl_3$) δ 1.152-1.176 (d, 4H), 1.689-1.725 (m, 4H), 1.89-1.93 (m, 2H), 3.185 s, 6H); ^{13}C NMR ($CDCl_3$) δ 27.46, 37.26, 50.26, 114.39; IR (chloroform) 2955.33, 2893.88 cm^{-1}; HRMS (CI) m/z (rel. intensity) 125

($M+H^+$,100), 157 (20); HRMS (CI) m/z calculated for $C_9H_{17}O_2$ (m+1) 157.122855, found 157.122134

Bicyclo[2.2.1]hept-2-en-7-one (2.10)

To a 250mL three-necked, round-bottom flask equipped with condenser, stirring bar, and outlet valve was added 30mL of 2M hydrochloric acid, 120 mL of concentrated acetic acid followed by 14.58g (.093g) of 7,7-dimethoxybicyclo[2.2.1]heptane (2.9). The reaction mixture was stirred vigorously for 20 hours at room temperature and then extracted with four 50mL portions of pentane. The combined pentane extracts were washed with 75mL portions of brine (2x), dried over magnesium sulfate, filtered, and the majority of the solvent was removed by distillation leaving 10.27g of a solution that was 37% pentane and 63% product for a yield of 55%. ^{1}H NMR ($CDCl_3$) δ 1.52-1.58 (d, 4H), 1.81-1.85 (m, 2H), 1.88-1.91 (m, 4H); ^{13}C NMR ($CDCl_3$) δ 23.91, 37.61, 217.05; IR (chloroform) 2954.50, 2869.88, 1844.46, 1774.77, 1734.95 cm^{-1}; HRMS (CI) m/z (rel. intensity) 111 ($M+H^+$, 100), 109 (30), HRMS (CI) m/z claculated for $C_7H_{11}O_1$ (m+1) 111.080990, found 111.080703

7,7-Difluoro-Bicyclo[2.2.1]heptane (2.11)

To a 100mL round-bottom flask equipped with stir bar, condenser, and nitrogen inlet was added, at 0°C, 20mL dry DCM, 14.61g (.09 moles) of (Diethylamino) Sulfur Trifloride (DAST), and 5.38g (.05 moles) of Bicyclo[2.2.1]hept-7-one (2.9) in 3.16g of pentane. The reaction mixture was allowed to warm to room temperature and then stir for four days, after which time 30mL 5% NaOH solution was added, dropwise at 0°C to consume any remaining

DAST. The organic layer was then separated, washed with two 30mL portions of water and one 30mL portion of brine. The combined DCM extracts were dried over $MgSO_4$, filtered and concentrated by rotary evaporation resulting in a black tar which was purified by column chromatography using pentane as the eluant. Solvent was carefully removed from the fractions containing pure product by high vacuum. Two sublimations resulted in 1.5g (23%) of a white crystalline solid that was over 99% pure by GC. m.p. 76º-79ºC. ^{1}H NMR ($CDCl_3$) δ 1.34-1.36 (d, 4H), 1.88-1.91 (m, 4H), 1.99-2.00 (m, 2H); ^{13}C NMR δ 26.12, 38.31, 130.37, 133.82, 137.25; ^{19}F NMR ($CDCl_3$) δ -129.98 (s, 2F); IR (chloroform) 3149.93, 2970.70, 2919.49, 2883.64, 2253.77 cm^{-1}; HRMS (CI) m/z (rel. intensity) 113 ($M+H^+$, 100), 132 (15), HRMS (CI) m/z claculated for $C_7H_{10}F_2$ (m+1) 132.075057 found 132.074597.

1,4-Dichloro-7,7-dimethoxybicyclo[2.2.1]heptane (2.12)

To a 1 L Parr Pressure Reactor with a stir bar was added 7,7-dimethoxy-1,2,3,4-tetrachlorobicyclo[2.2.1]hept-2-ene (2.9, 100 g, 0.342 mol), triethylamine (150 mL, 1.08 mol), absolute ethanol (490 mL), and 10 wt% palladium on carbon (5.0 g). Hydrogen gas was added and kept at 200 psi (1.4 MPa) while the mixture was stirred for 16 h at room temperature. The resulting mixture was filtered and the filtered solid was washed with water (500 mL) and diethyl ether (300 mL). The water layer was extracted with diethyl ether (300 mL x 2). The combined organic extracts were dried over potassium carbonate, filtered, and concentrated by rotary evaporation. The resulting solid was recrystallized from n-pentane to yield yellow crystals (119.65 g, 0.531 mol, 84 %). mp 89-92 °C. ^{1}H NMR (300 MHz,

$CDCl_3$, δ): 3.64 (s, CH_3O-, 6 H), 2.38 (m, CH_2, 4H), 1.87 (m, CH_2, 4 H). ^{13}C NMR (75.5 MHz, $CDCl_3$, δ): 103.78 (C-7), 69.11 (CCl), 51.18 (CH_3O-), 36.38 (CH_2). HRMS-CI (m/z): $[M]^+$ calcd for $C_9H_{14}O_2Cl_2$, 224.0371; found, 224.0369.

7,7-Dimethoxybicyclo[2.2.1]heptane (2.8) from 1,4-Dichloro-7,7-dimethoxybicyclo [2.2.1]heptane (2.12)

To a three necked 1 L flask equipped with a stir bar and thermometer was added 1,4-dichloro-7,7-dimethoxybicyclo[2.2.1]heptane (2.12, 36.0 g, 0.160 mol), t-butanol (68.0 g, 0.917 mol), and tetrahydrofuran (250 mL) under nitrogen, followed by the addition of sodium chunks (30.5 g, 1.33 mol). The reaction mixture was stirred and heated to reflux (70 °C) for 22 h. After cooling to room temperature a mass of unreacted sodium was removed, and the reaction mixture was placed on ice and 150mL of methanol was added dropwise to quench any remaining sodium. The resultant mixture was filtered through Celite, concentrated in vacuo, poured over 100mL of ice water and extracted four times with 150mL portions of diethyl ether. The combined ether extracts were washed three times with 150mL portions of brine, dried over magnesium sulfate, filtered, and the solvent was removed by rotary evaporation. Vacuum distillation (67-68 °C at 15 mmHg) yielded 21.15 g (0.136 mol, 85%) of a colorless oil that was over 99% pure by GC. ^1H NMR (300 MHz, $CDCl_3$, δ): 3.23 (s, CH_3O-, 6 H), 1.96 (m, CH, 2 H), 1.75 (m, CH_2, 4H), 1.21 (d, J = 7.2 Hz, CH_2, 4 H). ^{13}C NMR (75.5 MHz, $CDCl_3$, δ): 114.55 (C-7), 50.40 (CH_3O-), 37.36 (CH), 27.56 (CH_2). HRMS-CI (m/z): $[M + H]^+$ calcd for $C_9H_{17}O_2$, 157.1229; found, 157.1228.

7-Bicyclo[2.2.1]heptanol (2.13)

To a 500mL round-bottom flask equipped with stir bar, condenser, and nitrogen inlet was added 300mL dry ethanol, 11.43g (.10 moles) of Bicyclo[2.2.1]hept-7-one (2.10) and 4.71 g (0.125 moles) of $NaBH_4$. The reaction mixture was allowed to stir for 5 hours after which time it was poured into a sep funnel containing 300mL of water. The aqueous layer was extracted three times with 150mL portions of pentane and the combined pentane extracts were dried over $MgSO_4$, filtered, and the solvent was removed by rotary evaporation affording 8.6g (77%) of a white, crystalline solid. ^1H NMR ($CDCl_3$) δ 1.34-1.36 (d, 4H), 1.88-1.91 (m, 4H), 1.99-2.00 (m, 2H); ^{13}C NMR δ 26.12, 38.31, 130.37, 133.82, 137.25; IR (chloroform); HRMS (CI) m/z (rel. intensity) 113 ($M+H^+$, 100), 132 (15), HRMS (CI) m/z claculated for $C_7H_{10}F_2$ (m+1) 132.075057 found 132.074597.

Bicyclo[2.2.1]heptan-7-yl trifluoromethanesulfonate (2.18)

To a 250 mL round-bottom flask containing a stir bar and nitrogen inlet was added bicyclo[2.2.1]heptan-7-ol (2.13, 9.62 g, 85.8 mmol) and pyridine (40 mL). The flask was cooled in an ice bath and trifluoromethanesulfonic anhydride (18 mL, 107 mmol) was added, dropwise. During the addition, the mixture turned yellow, then red. After the addition, white solid was found at the bottom of the flask. The flask was allowed to warm to room temperature and stirred overnight. The resulting dark red reaction mixture was diluted with ether (500 mL) and washed with water (300 mL). The water layer was extracted with ether (100 mL and 50 mL) and these extracts were combined with the first extract. The combined

extracts were washed with 1N HCl (300 mL), water (300 mL), and brine (300 mL), dried over magnesium sulfate, evaporated, and distilled (55 °C at 3 mmHg) affording 17.19 g (70.4 mmol, 82 %) a colorless liquid that was 100% pure by GC. ^{1}H NMR (300 MHz, $CDCl_3$, δ): 4.95 (s, CHOTf, 1 H), 2.36 (m, bridgehead, 2 H), 1.89 (m, CH_2, 2 H), 1.63 (m, CH_2, 2 H), 1.42 (m, CH_2, 2H), 1.30 (m, CH_2, 2H). ^{13}C NMR (75.5 MHz, $CDCl_3$, δ): 118.50 (q, $^{1}J_{CF}$ = 319 Hz, CF_3), 94.68 (CHOTf), 39.40 (CH), 26.44 (CH_2), 25.31 (CH_2). ^{19}F NMR (282 MHz, $CDCl_3$, δ): -75.83 (s, CF_3, 3 F). EIMS m/z (% relative intensity, ion): 289 (2, M^+), 111 (6, $C_7H_{11}O^+$), 95 (100, $C_7H_{11}^+$). HRMS-CI (m/z): $[M + H]^+$ calcd for $C_8H_{12}F_3SO_3$, 245.0459; found, 245.0471.

7-Fluorobicyclo[2.2.1]heptane (2.19)

To a 300 mL Parr pressure reactor was added bicyclo[2.2.1]hept-7-yl trifluoromethanesulfonate (2.18, 17.0 g, 69.6 mmol), sulfolane (180 g), and cesium fluoride (15.8 g, 104 mmol). The cesium fluoride was dried at 140 °C for 24 h under vacuum prior to use and weighed in a dry box. The mixture was stirred at 120 °C for 16 h. The resulting brown solution was poured in 1.9 L of water and extracted with pentane (500 mL x 3). The extracts were combined, dried over magnesium sulfate, filtered, evaporated using fractional distillation head. The resulting yellow solution was heated to 50 °C under reduced pressure (12 mmHg) and transferred to 2-propanol/ dry ice cooled trap. The trapped solution was purified twice with column chromatography on silica gel using pentane as an eluent. Removal of solvent of the pure fractions using a fractional distillation head gave 0.83 g of colorless solution. The solution was purified by sublimation

(outside 30°C, cold finger 0 °C, pressure 80 mmHg) to give 0.234 g of white crystals that were 100% pure by GC. mp 105 °C. ^{1}H NMR (500 MHz, $CDCl_3$, δ): 4.77 (d, $^{2}J_{HF}$ = 58.0 Hz, CHF, 1 H), 2.13 (m, bridgehead, 2 H), 1.86 (m, syn-exo, 2H), 1.54 (m, anti-exo, 2 H), 1.32 (m, syn-endo, 2 H), 1.19 (m, anti-endo, 2H). ^{13}C NMR (126 MHz, $CDCl_3$, δ): 99.51 (d, $^{1}J_{CF}$ = 192 Hz, CHF), 38.49 (d, J_{CF} = 15.9 Hz, bridgehead), 26.62 (d, J_{CF} = 2.3 Hz, syn), 25.27 (d, J_{CF} = 8.6 Hz, anti). ^{19}F NMR (282 MHz, $CDCl_3$, δ): -202.92 (dt, J_{HF} = 58.0 and 6.0 Hz, 1 F). HRMS-CI (m/z): $[M + H]^+$ calcd for $C_7H_{12}F$, 115.0923; found, 115.0919.

2,2,2-Trifluoroethyl 3,3,3-trifluoropropionate (2.22)

To a 50 mL round-bottom flask equipped with a stir bar and nitrogen inlet was added DMAP (0.53 g, 4.3 mmol), DCC (13.5 g, 65 mmol), and 2,2,2-trilfuoroethanol (6.8 g, 68 mmol) at room temperature. The mixture was cooled to 0ºC, then 3,3,3-trifluoroproioic acid (6.6 g, 52 mmol) was added, dropwise. Generation of heat and a white precipitate were observed during this addition. After the addition, the mixture was warmed to room temperature, and distillation over phosphorous pentoxide (108º-110ºC) gave the pure product (3.9 g). . ^{1}H NMR (300 MHz, $CDCl_3$, δ): 4.54 (q, $^{3}J_{HF}$ = 8.2 Hz, -OC*H*$_2$CF$_3$, 2H), 3.29 (q, $^{3}J_{HF}$ = 9.7 Hz, -COC*H*$_2$CF$_3$, 2H). ^{19}F NMR (282 MHz, $CDCl_3$, δ): -64.07 (t, *J* = 9.9 Hz, -COCH$_2$C*F*$_3$, 3F), -74.38 (t, *J* = 8.2 Hz, -OCH$_2$C*F*$_3$, 3F).

Trifluoroacetone cyanohydrin (3.2)

To a 500mL round-bottom flask equipped with a stirring bar was added 190mL water, 65.6g sodium cyanide, and 25mL trifluoroacetone (3.1), dropwise at 0ºC. The reaction mixture was allowed to warm to room temperature, and after five hours the reaction was poured into 700mL 6N H_2SO_4. This was allowed to warm to room temperature and after 2 hours was extracted with three 500mL portions of diethyl ether. The combined ether extracts were washed with 500mL saturated sodium bicarbonate followed by 500mL saturated sodium chloride, dried over $MgSO_4$, filtered, and concentrated by rotary evaporation. Vacuum distillation (53-56ºC, 35mmHg) yielded 33.02g (85%) of a colorless liquid. ^{1}H NMR ($CDCl_3$) δ 1.717 (s, 3H), 5.104 (s, 1H); ^{13}C NMR ($CDCl_3$) δ 21.058, 68.884; IR (neat) 3400, 1706 cm^{-1}; HRMS (CI) m/z (rel. intensity) 113 ($M+H^+$, 100), 140 (50), HRMS (CI) m/z claculated for $C_4H_5NOF_3$(m+1) 140.032324, found 140.032618

Methyl α-hydroxy-α-(trifluoromethyl) propionate (3.3)

To a 500mL three-neck round-bottom flask equipped with stir bar and condenser was added 60 mL concentrated H_2SO_4. The flask was cooled to 0ºC and 90g (.647 moles) trifluoroacetone cyanohydrin (3.2) dissolved in 54mL methanol was added, followed by 11.7g (.647 moles) water, dropwise. This was warmed to room temperature, and the reaction mixture was heated at 100-110ºC for 5 hours and then to 80ºC for 15 hours. After this time, the reaction mixture was cooled to room temperature, poured into a sepratory funnel containing 300mL of water, and then extracted three times with 250mL portions of ether. The combined ether fractions were washed once with 150mL water followed by

150mL brine, dried over $MgSO_4$, and filtered. Distillation at atmospheric pressure (100-130ºC) yielded 59.47g (53.4% by ^1H NMR) of a colorless liquid that forms a complex with ether. ^1H NMR ($CDCl_3$) δ 1.515 (s, 3H), 3.824 (s, 3H), 3.927 (s, 1H); ^{13}C NMR ($CDCl_3$) δ 18.814, 53.994, 74.885; IR (neat) 3492, 3013, 2964, 1741 cm^{-1}; HRMS (CI) m/z (rel. intensity) 173 ($M+H^+$, 100), 158 (30), HRMS (CI) m/z claculated for $C_5H_8O_3F_3$ (m+1) 173.042554, found 173.043268

Methyl α-acetoxy-α-(trifluoromethyl) propionate (3.4)

To a 500mL three-neck round-bottom flask equipped with stir bar, condenser and nitrogen inlet was added 86.6g (.503 moles) of methyl α-hydroxy-α-(trifluoromethyl) propionate (3.3), 150mL dry acetic anhydride, and 7.5g (.091 moles) sodium acetate. This was stirred at 110ºC for 8 hours, after which time it was cooled to room temperature and then poured into a 2000mL beaker containing 700g of ice. This was stirred for 1 hour at room temperature, after which time it was poured into a seperatory funnel and extracted three times with 200mL portions of ether. The combined ether fractions were washed 4 times with 200mL portions of saturated sodium bicarbonate and once with 200mL brine, dried over $MgSO_4$, filtered, and concentrated by rotary evaporation. Vacuum distillation (80-84°C, 60mm Hg) yielded 105.4g (98%) of a colorless liquid. ^1H NMR ($CDCl_3$) δ 1.732 (s, 3H), 2.079 (s, 3H), 3.743 (s, 3H); ^{13}C NMR ($CDCl_3$) δ 16.422, 20.529, 53.345, 79.276, 122.595, 165.486, 168.603; IR (neat) 3502, 3015, 2962, 1829, 1772, 1717 cm^{-1}; HRMS (CI) m/z (rel. intensity) 215 ($M+H^+$, 100), 183 (20), HRMS (CI) m/z claculated for $C_{i7}H_{10}O_4F_3$ (m+1) 215.053119, found 215.052772

Methyl 2-trifluoromethylacrylate (3.5)

A quartz pyrolysis column was utilized. The dimensions for the column were 42cm high (heated length) with a 4cm OD. The filler for the column consisted of 20 feet of 5 mm OD, 3 mm ID quartz tubing and 44 feet of 3 mm OD, 1mm ID quartz tubing cut into length that varied from 0.5cm to 1cm. The column was wrapped with 240V heating tape and the temperature was monitored with a thermocouple placed in between the heating tape and the outside wall of the column.

Into the aforementioned pyrolysis column was dripped 67g methyl alpha-acetoxy-alpha-(trifluoromethyl) propionate (3.4) at 500ºC. Dry nitrogen was allowed to flow through the column at ~1 bubble per second. The liquid in the collection flask was then rinsed twice with 200mL portions of water, 100mL brine, and dried over sodium sulfate. Distillation from the drying agent at atmospheric pressure (102-108ºC) yielded 31.73g (66%) of a colorless liquid. ^{1}H NMR ($CDCl_3$) δ 3.833 (s, 3H), 6.44-6.46 (d, 1H), 6.71-6.73, (d, 1H); ^{13}C NMR ($CDCl_3$) 52.573, 119.437, 123.049, 132.801, 161.750; IR (chloroform) 3136, 3014, 2962 cm^{-1}; HRMS (CI) m/z (rel. intensity) 155 ($M+H^+$, 100), 127 (40), HRMS (CI) m/z calculated for $C_5H_6O_2F_3$ (m+1) 155.031842 found 155.03198

Poly[Methyl 2-trifluoromethylacrylate] (3.6)

To a 100ml round-bottom flask equipped with a stir bar was added 7.4g (.045moles) of methyl 2-trifluoromethylacrylate, .043g (.9 mmoles) of potassium acetate, and .24g (.9 mmoles) of 18-crown-6. After 15 minutes, the reaction mixture had turned into a thick, colorless mass. After 24 hours, the reaction

mixture was dissolved in THF, precipitated in methanol, filtered, and dried overnight in a vacuum oven at 50ºC, affording 2.93g of a white polymer. ^{1}H NMR ($CDCl_3$) δ 2.488 (s br, 2H), 3.66 (s, 3H); ^{13}C NMR (CD_2Cl_2) δ 42.14, 52.74, 54.75, 123.56, 165.94 .

2-Trifluoromethylacrylic Acid (3.7)

To a 1L Parr Hydrogen apparatus equipped with a stirring bar was added 500mL dry THF, 139g (.794 moles) 2-bromo-3,3,3-trifluoropropene, 20g (1.11 moles) water, 109g (1.08 moles) triethylamine, and 5.5g (.00785 moles) dichlorobis[triphenylphosphine]-palladium. The reaction mixture was heated at 80ºC for 2 hours with stirring under 35 atm of carbon monoxide. The pressure vessel was then cooled to 0ºC and depressurized. Three-hundred mL of 2N hydrochloric acid was added to the reaction mixture and the mixture was extracted 4 times with 300mL portions of ether, dried over sodium sulfate, filtered, and concentrated by rotary evaporation. Vacuum distillation (66-72ºC, 25mmHg), followed by recrystalization from pentane afforded 40.38g (33%) of a white solid (m.p. 50-51ºC). ^{1}H NMR ($CDCl_3$) δ 6.571 (s, 1H) 6.848 (s, 1H) 10.756 (b, 1H); IR (neat) 3110, 725 cm^{-1}; HRMS (CI) m/z (rel. intensity) 141 ($M+H^+$, 100), 159 (30), HRMS (CI) m/z claculated for $C_4H_4O_2F_3$ (m+1) 141.016339, found 141.016254

***tert*-Butyl 2-trifluoromethylacrylate (3.8)**

To a 200ml Parr pressure vessel equipped with a stirring bar was added approximately 25mL (.438 moles) isobutylene that was condensed through a cold finger containing a mixture of dry ice and acetone, 22.57 grams (.146 moles) 2-trifluoromethylacrylic acid, 2mL concentrated sulfuric acid and 50mL dry diethyl ether at -78°C. The reaction mixture was allowed to warm to room temperature and stir overnight, after which time it was neutralized with 5% NaOH and extracted three times with 50mL portions of diethyl ether. The combined ether extracts were dried over magnesium sulfate, filtered, and the solvent was removed by rotary evaporation. Vacuum distillation (50-55°C, 45mmHg) gave 20.14 (70%) of a colorless liquid that was 97% pure by GC. ^{1}H NMR ($CDCl_3$) δ 1.49 (s, 9H), 6.30 (s, 1H), 6.57 (s, 1H); ^{13}C NMR δ 29.76, 82.95, 116.03, 119.64, 123.24, 126.85, 131.57, 133.15, 160.36; ^{19}F NMR ($CDCl_3$) δ –66.01 (s, 2F); IR (neat) 2975.82, 2929.73, 1736.56 cm^{-1}

Methyl α-hydroxy-α-(trifluoromethyl) propionoic acid (3.9)

To a 250mL three-neck round-bottom flask equipped with stir bar and condenser was added 80mL concentrated H_2SO_4. The flask was cooled to 0ºC and 40mL water followed by 100g (.719 moles) trifluoroacetone cyanohydrin was added, dropwise. This was allowed to warm to room temperature, and the reaction mixture was heated at 100-110ºC for 5 hours and then 80ºC for 15 hours. The reaction mixture was then cooled to room temperature, poured into a seperatory funnel containing 300mL of water, and then extracted three times with 250mL portions of ether. The combined ether fractions were washed once with 150mL

brine, dried over $MgSO_4$, and filtered. Concentration by rotary evaporaton yielded 133g of a colorless oil that was 35% diethyl ether by ^1H NMR (70% yield). ^1H NMR ($CDCl_3$) δ 1.578 (s, 3H); ^{13}C NMR ($CDCl_3$) δ 20.055, 74.239; IR (neat) 3421, 3055, 1747 cm^{-1}; HRMS (CI) m/z (rel. intensity) 159 ($M+H^+$, 100), 113 (50), HRMS (CI) m/z claculated for $C_4H_6O_3F_3$ (m+1) 159.026904, found 159.026054

Methyl α-acetoxy-α-(trifluoromethyl)propionoic acid (3.10)

To a 250mL three-neck round-bottom flask equipped with stir bar, condenser and nitrogen inlet was added 34.22g (.216 moles) of methyl α-hydroxy-α-(trifluoromethyl) propionoic acid (3.9), 75mL dry acetic anhydride, and 3.07g (.0374 moles) sodium acetate. This was stirred at 110ºC for 8 hours, after which time it was cooled to room temperature and then poured into a 1000mL beaker containing 400g of ice. This was stirred for 1 hour at room temperature, after which time it was poured into a seperatory funnel and extracted three times with 150mL portions of ether. The combined ether fractions were washed 3 times with 100mL portions of saturated sodium bicarbonate and once with a 100mL portion of brine, dried over $MgSO_4$, filtered, and concentrated by rotary evaporation. Vacuum distillation (30-40ºC, 3mmHg) yielded 13.22g (30%) of a colorless liquid. ^1H NMR ($CDCl_3$) δ 1.808 (d, 3H), 2.155 (s, 3H); ^{13}C NMR ($CDCl_3$) δ 16.472, 20.616, 79.765, 123.121; IR (neat) 3006, 1734 cm^{-1}; HRMS (CI) m/z (rel. intensity) 201 ($M+H^+$, 100), 183 (40), HRMS (CI) m/z claculated for $C_6H_8O_4F_3$ (m+1) 201.037469, found 201.037009

Methyl α-acetoxy-α-(trifluoromethyl)benzylester (3.11)

To a 500mL three-neck round-bottom flask equipped with stir bar, condenser, and nitrogen inlet was added 200mL dry benzene, 19.22 g (.0961g) methyl α-acetoxy-α-(trifluoromethyl) propionoic acid (3.10) and 15.22g (.1 moles) of 1,8 diazabicyclo[5.4.0]undec-7-ene, dropwise at room temperature. After fifteen minutes, 17.10g (.1 moles) of benzyl bromide was added, dropwise, and the reaction mixture was then refluxed overnight, cooled to room temperature and poured into a seperatory funnel where it was washed twice with 100mL portions of water and once with a 100mL portion of brine. The organic layer was dried over $MgSO_4$, filtered, and concentrated by rotary evaporation. Vacuum distillation (89-92ºC, .9mmHg) yielded 23.32g of a colorless liquid (84%). ^1H NMR ($CDCl_3$) δ 1.820 (s, 3H), 2.105 (s, 3H), 5.166-5.269 (q, 2H), 7.342 (b, 5H); IR (neat) 3250, 1496 cm^{-1}; HRMS (CI) m/z (rel. intensity) 181 ($M+H^+$, 100), 291 (60), HRMS (CI) m/z claculated for $C_{13}H_{14}O_4F_3$ (m+1) 291.084419, found 291.084180

Benzyl 2-trifluoromethylacrylate (3.12)

Into a pyrolysis column (see 2-trifluoromethylacrylate) was dripped 48.5g (.167 moles) methyl α-acetoxy-α-(trifluoromethyl) benzyl ester (3.11) at 485ºC. Dry nitrogen was allowed to flow through the column at ~1 bubble per second. The liquid in the collection flask was then rinsed with twice with 200mL portions of water and once with a 100mL portion of brine, and dried over sodium sulfate. Distillation from the drying agent (102-108ºC, 1mmHg) yielded 7.33g (19%) of a colorless liquid that was 95% pure by GC. ^1H NMR ($CDCl_3$) δ 5.288 (s, 2H),

6.437 (s, 1H), 6.737 (s, 1H), 7.376 (b, 5H); ^{13}C NMR ($CDCl_3$) δ 67.350, 128.067, 128.482, 128.621, 133.034, 134.942; IR (neat) 3419, 3125, 1725, 1600 cm^{-1}; HRMS (CI) m/z (rel. intensity) 181 ($M+H^+$, 100), 231 (20), HRMS (CI) m/z claculated for $C_{11}H_9O_2F_3$ (m+1) 230.055464, found 230.054417

Poly[methyl 2-trifluoromethylacrylate-co-*tert*-butyl-2-trifluoromethylacrylate -co-benzyl 2-trifluoromethylacrylate] (3.13)

To a dry, round-bottom flask containing a stir bar was added 2.4g (.0156 moles) methyl 2-trifluoromethylacrylate (3.5), 6.3g (.032 moles) *tert*-butyl 2-trifluoromethyl acrylate (3.8), 2.24g (.0096 moles) benzyl 2-trifluoromethylacrylate (3.12), .12g (.00046 moles) 18-crown-6, and .022g (.00046 moles) potassium acetate. After 72 hours, the solid reaction mixture is dissolved in THF, precipitated into hexanes, and filtered. The polymer was dried in a vacuum oven at 50°C, affording 4.42g of a white polymer that was 4.33:3.47:2.20 methyl : t-butyl : benzyl by ^{1}H NMR. M_w=5,250; M_n=3,360; ^{1}H NMR ($CDCl_3$) δ 1.425 (br, 2H), 3.645 (br, 9H), 5.036 (br, 2H) 7.312 (br, 5H); IR (KBr) 3011.66, 2955.33, 1767.28, 1757.04 cm^{-1}

Poly[2-trifluoromethylacrylic acid-co-*tert*-butyl-2-trifluoromethylacrylate-co-methyl 2-trifluoromethyacrylate] (3.14)

To a Parr pressure vessel equipped with a stir bar was added 4g poly poly[methyl 2-trifluoromethylacrylate-co-*tert*-butyl-2-trifluoromethylacrylate-co-benzyl 2-trifluoro methacrylate] (3.13, 4.33:3.47:2.20 methyl : t-butyl : benzyl by ^{1}H NMR), .4g palladium (10 wt. % on activated carbon) and 60mL ethyl acetate and the reactor was pressurized to 100psi with H_2, then heated to 50°C for 48

hours, after which time it was cooled to room temperature, filtered first through paper and then through a .45um syringe filter. The solvent was removed entirely by rotary evaporation, the polymer dissolved in THF, isolated by precipitation into hexanes, filtered, and dried in a 50°C vacuum oven affording 2.7g of a white polymer that was 4.13:3.47:2.39 methyl : t-butyl : acid by ^{1}H NMR. ^{1}H NMR ($CDCl_3$) δ 3.726 (br, 3H), 1.434 (br, 9H); IR (KBr) 3467.72, 2984.37, 1749.88, 1515.93 cm^{-1}; M_w=5,130; M_n=3,120

2-Trifluoromethylacryloyl chloride (3.15)

To a 25ml round-bottom flask equipped with a stir bar and nitrogen inlet was added 10g (.071 moles) 2-trifluoromethyacrylic acid and 21.65g (0.10 moles) phthalloyl dichloride. The reaction mixture was heated up to 90°C and stirred for 24 hours, after which time a distillation apparatus was attached to the reaction flask and 5.7 (50%) of a colorless liquid was distilled off (93-98°C). ^{1}H NMR ($CDCl_3$) δ 6.87 (s, 1H), 7.06 (s, 1H); ^{13}C NMR ($CDCl_3$) δ 118.37, 122.01, 135.07, 135.49, 139.36, 161.97; ^{19}F NMR ($CDCl_3$) δ -66.99 (s, 2F); HRMS (CI) m/z (rel. intensity) 111 ($M+H^+$, 100), 109 (30), HRMS (CI) m/z claculated for $C_7H_{11}O_1$ (m+1) 111.080990, found 111.080703

Benzyl 2-trifluoromethylacrylate (3.12) from 2-Trifluoromethylacryloyl chloride

To a 100mL, three neck, round-bottom flask equipped with a stir bar and nitrogen inlet was added 30mL dry DCM, 1g (0.0063 moles) 2-trifluoromethylacryloyl chloride **(3.15)**, .62 g (0.0057 moles) benzyl alcohol, and .60g (0.0059 moles) triethylamine, dropwise at 0°C. The reaction mixture was

allowed to warm to room temperature and stir for twenty-four hours after which time it was washed with water (20mL) and 1N HCl (20mL). The organic layer was dried over $MgSO_4$, filtered and the solvent was removed by rotary evaporation. Purification by column chromatography (5% Ethyl acetate in n-hexanes) gave .96g (74%) of a slightly yellow liquid that was 53% pure by GC. ^{1}H NMR ($CDCl_3$) δ 5.288 (s, 2H), 6.437 (s, 1H), 6.737 (s, 1H), 7.376 (b, 5H); ^{13}C NMR ($CDCl_3$) δ 67.350, 128.067, 128.482, 128.621, 133.034, 134.942; IR (neat) 3419, 3125, 1725, 1600 cm^{-1}; HRMS (CI) m/z (rel. intensity) 181 ($M+H^+$, 100), 231 (20), HRMS (CI) m/z claculated for $C_{11}H_9O_2F_3$ (m+1) 230.055464, found 230.054417

Adamatyl 2-trifluoromethylacrylate (3.17)

To a 100mL, three neck, round-bottom flask equipped with a stir bar and nitrogen inlet was added 30mL dry DCM, 2g (0.0126 moles) 2-trifluoromethylacryloyl chloride **(3.15)**, 1.74g (0.0115 moles) 1-adamantol, and 1.16g (0.0115 moles) triethylamine, dropwise at 0°C. The reaction mixture was allowed to warm to room temperature and stir for twenty-four hours after which time it was washed with water (20mL) and 1N HCl (20mL). The organic layer was dried over $MgSO_4$, filtered and the solvent was removed by rotary evaporation. Purification by column chromatography (5% Ethyl acetate in n-hexanes) gave 2.7g (86%) of a colorless liquid. ^{1}H NMR ($CDCl_3$) δ 1.648 (s, 7H), 2.143 (s, 9H), 6.290 (s, 1H), 6.56 (s, 1H); ^{13}C NMR ($CDCl_3$) δ 30.834, 36.005,

41.132, 83.023, 131.563, 159.981, IR (neat) 2980, 1823, 1782 cm^{-1}; HRMS (CI) m/z (rel. intensity) 135 ($M+H^+$, 100), 273 (20), HRMS (CI) m/z claculated for $C_{14}H_{16}O_2F_3$ (m+1) 273.109412, found 273.110240

Norbonyl 2-trifluoromethylacrylate (3.16)

To a 100mL, three neck, round-bottom flask equipped with a stir bar and nitrogen inlet was added 30mL dry DCM, 2g (0.0126 moles) 2-trifluoromethylacryloyl chloride **(3.15)**, 1.29g (0.0115 moles) *exo*-norborneol, and 1.16g (0.0115 moles) triethylamine, dropwise at 0°C. The reaction mixture was allowed to warm to room temperature and stir for twenty-four hours, after which time it was washed with water (20mL) and 1N HCl (20mL). The organic layer was dried over $MgSO_4$, filtered and the solvent was removed by rotary evaporation. Purification by column chromatography (5% Ethyl acetate in n-hexanes) gave 2.33g (86%) of a colorless liquid. ^{1}H NMR ($CDCl_3$) δ .833-1.089 (t, 2H), 1.089-1.243 (m, 5H), 1.406-1.516 (m, 5H), 1.714-1.791 (m, 1H), 2.297-2.363 (d, 1H), 4.738-4.762 (d, 2H), 6.353 (s, 1H), 6.649 (s, 1H); ^{13}C NMR ($CDCl_3$) δ 14.084, 22.641, 24.025, 28.052, 35.233, 39.304, 41.423, 79.221, 119.554, 123.166, 132.284, 160.891; ^{19}F NMR ($CDCl_3$) δ -65.959; HRMS (CI) m/z (rel. intensity) 391 ($M+H^+$, 100), 235 (30), HRMS (CI) m/z claculated for $C_{11}H_{14}O_2F_3$ (m+1) 235.095549, found 235.094590

Acetic acid 5-1,1,1-trifluoromethyl bicyclo[2.2.1]hepten-5-ol-2-yl ester (3.19)

Dicyclopentadiene was cracked at 180°C and collected by distillation. To a 1L Parr pressure vessel equipped with a stirring bar was added 140.00g (0.908 moles) 2-(trifluoromethyl) vinyl acetate **(3.18)**, 70.25g (1.063 moles) cyclopentadiene and 0.1g hydroquinone. The reaction mixture was stirred for twenty-four hours at 175°C then cooled to room temperature, and the resulting solution was separated from remaining dicyclopentadiene by silica gel chromatography using hexanes as the eluant. The product was flushed out with 1:1 hexanes: ethyl acetate. The resulting liquid was concentrated by rotary evaporation and vacuum distilled (83°-90°C, 25 mmHg), affording 62.51g (31%) of a colorless liquid that was 95% pure by GC. ^{1}H-NMR ($CDCl_3$) δ 1.80-1.95 (m, 1H aliphatic), 2.18-2.37 (m, 1H, aliphatic), 2.85-3.0 (s, 1H, bridgehead), 3.50-3.60 (s, 0.7H, bridgehead), 3.79-3.83 (s, 0.3H, bridgehead), 5.89-6.00 (m, 1H, alkene), 6.23-6.40 (m, 1H, alkene); ^{13}C-NMR ($CDCl_3$) δ 22.0, 22.3 (methyl), 37.0, 38.1 (bridgehead), 41.0, 41.9 (bridgehead), 48.2, 50.1 (bridge), 66.0 (aliphatic), 86.4, 88.7 (aliphatic), 123.8, 127.0 (trifluoromethyl), 131.2, 133.8 (alkene), 140.0, 141.7 (alkene); 169.1 (carbonyl); ^{19}F NMR ($CDCl_3$) δ -68.916, 73.620; IR (neat) 3079.61, 2990.29, 2955.34, 2885.44, 1763.11, 1452.43 cm^{-1}; HRMS (CI) m/z (rel. intensity) 161 ($M+H^+$, 100), 221 (30), HRMS (CI) m/z calculated for $C_{10}H_{12}O_2F_3$ (m+1) 221.078940, found 221.078882

2-Trifluoromethyl-bicyclo[2.2.1]hept-5-en-2-ol (3.20)

To a 500mL round bottom flask equipped with a stir bar was added 200mL methanol, 200mL 1M NaOH, and 20g (0.09 moles) Acetic acid 2-trifluoromethyl-bicyclo [2.2.1] hept-5-en-2-yl ester **(3.19)**. The reaction mixture was allowed to stir at room temperature for twenty-four hours, after which time it was poured into a sep funnel containing 300mL of 1N HCl and extracted three times with ether (200mL). The organic layer was dried over $MgSO_4$, filtered and the solvent was removed by rotary evaporation. Vacuum distillation (84-85°C, 4.6cm Hg) gave 12.9g (80%) of a colorless liquid that was 98% pure by GC. ^{1}H NMR ($CDCl_3$) δ 1.159-1.206 (d, 1H), 1.576-1.759 (m, 5H), 1.982-2.011 (d, 1H), 2.068 (s, 1H), 2.160-2.216 (d, 1H), 6.001 (s, 1H), 6.184 (s, 1H), 6.253 (s, 1H), 6.500 (s, 1H); ^{13}C NMR ($CDCl_3$) δ 39.122, 41.489, 42.275, 48.590, 49.092, 49.121, 50.833 132.364, 133.136, 139.698, 141.198; ^{19}F NMR ($CDCl_3$) δ -77.632, -75.927 IR (neat) 3590, 3462, 2986, 2253, 1342 cm^{-1} HRMS (CI) m/z (rel. intensity)161 ($M+H^+$, 100), 179 (40), HRMS (CI) m/z calculated for $C_8H_{10}O_1F_3$ (m+1) 179.068375, found 179.067513

2-Trifluoromethyl-bicyclo[2.2.1]heptan-2-ol (3.21)

To a 200mL Parr pressure vessel equipped with a stir bar was added 100mL ethyl acetate, 6.45g (0.036 moles) 2-trifluoromethyl-bicyclo[2.2.1]hept-5-en-2-ol **(3.20)** and 0.31g palladium on activated carbon (10 wt. %). The reaction mixture was stirred for twenty-four hours at room temperature under 100psi

hydrogen pressure, after which time the vessel was depressurized, the resulting solution was filtered to remove the catalyst, and the solvent was concentrated by rotary evaporation. Vacuum distillation (74-82°C, 40mmHg) gave 5.17g (79%) of a colorless liquid that was 99% pure by GC. ^{1}H NMR ($CDCl_3$) δ 1.081-1.764 (m, 6H), 1.852-2.138 (m, 2H), 2.278-2.405 (m, 2H); ^{13}C NMR ($CDCl_3$) δ 22.277, 26.829, 27.258, 36.231, 37.600, 39.005, 41.059, 41.970, 42.836, 45.735, 80.001, 124.688, 128.446; ^{19}F NMR ($CDCl_3$) δ -75.941, -80.836; IR (neat) 3395, 2965, 2878, 1726.32, 1623 cm^{-1}; HRMS (CI) m/z (rel. intensity) 163 ($M+H^+$, 100), 180 (10), HRMS (CI) m/z calculated for $C_8H_{11}O_1F_3$ (m+1) 180.076200, found 180.075574

2-(Trifluoromethyl)-Norborn-2-yl 2-Trifluoromethylacrylate (3.22)

To a 250mL, three neck, round-bottom flask equipped with a stir bar and nitrogen inlet was added 150mL dry DCM, 7.0g (0.044 moles) 2-trifluoromethylacryloyl chloride, 7.20g (0.040 moles) 2-trifluoromethyl-bicylco[2.2.1]heptan-2-ol **(3.21)**, and 4.04g (0.040 moles) triethylamine, dropwise at 0°C. The reaction mixture was allowed to warm to room temperature and stir for twenty-four hours, after which time it was washed with water (50mL), 1N HCl (50mL), and brine (50mL). The organic layer was dried over $MgSO_4$, filtered and the solvent was removed by rotary evaporation. Vacuum distillation (74-83°C, 20mm Hg) gave 7.06g (58%) of a colorless liquid that was 95% pure by GC. ^{1}H NMR ($CDCl_3$) δ 1.191-1.610 (m, 7H), 1.910-2.213 (d, 1H), 2.118-2.213 (m, 2H),

3.124-3.166 (d, 1H), 6.410-6.439 (d, 1H), 6.679-6.715 (d, 1H); ^{13}C NMR ($CDCl_3$) δ 22.219, 23.806, 26.464, 26.821, 27.273, 34.920, 36.070, 36.274, 37.352, 37.913, 39.756, 42.632, 43.557, 89.111, 89.883, 119.350, 122.947, 123.144, 126.917, 133.588, 158.886; ^{19}F NMR ($CDCl_3$) δ -74.681, -69.227, -66.051, -65.909; IR (neat) 2965, 2877, 2254, 1751 cm^{-1} HRMS (CI) m/z (rel. intensity) 303 ($M+H^+$, 100), 283 (20), HRMS (CI) m/z calculated for $C_{12}H_{13}O_2F_6$ (m+1) 303.081974, found 303.080945

Poly[methyl 2-trifluoromethylacrylate-co-t-butyl-2-trifluoromethylacrylate acrylate-co-benzyl 2-trifluoromethylacrylate-co-norbornyl 2-trifluoromethylacrylate]

To a 25mL dry, round bottom flask containing a stir bar was added 1g (.0065 moles) methyl 2-trifluoromethylacrylate, 1g (.005 moles) *t*-butyl 2-trifluoromethylacrylate, 1g (.004 moles) benzyl 2-trifluoromethylacrylate, .75g norbornyl 2-trifluoromethylacrylate, .048g (.00018 moles) 18-crown-6, and .009g (.00018 moles) potassium acetate. After 12 days, the solid reaction mixture was dissolved in THF, precipitated into hexanes, and filtered. The polymer was dried in a vacuum oven at 50°C, affording .57g of a white polymer that was 4.98:1.58:1.65:1.77 methyl : t-butyl : benzyl : norbornyl by ^1H NMR and TGA. M_w=2,190; M_n=1,110; ^1H NMR ($CDCl_3$) δ 1.438 (bs, 9H), 2.271 (bm, 7H), 3.70 (bs, 3H), 5.093 (bs, 2H), 7.423 (bs, 7H); IR (KBr) 2955.33, 2878.52, 1751.92 cm^{-1}

Poly[methyl 2-trifluoromethylacrylate-co-*t*-butyl 2-trifluoromethylacrylate-co-2-trifluoromethylacrylic acrylic acid-co-norbornyl 2-trifluoromethylacrylate] (3.23)

To a 200mL Parr pressure vessel equipped with a stir bar was added 25mL ethyl acetate, .25 g Poly[methyl 2-trifluoromethylacrylate-co-t-butyl-2-trifluoromethylacrylate acrylate-co-benzyl 2-trifluoromethylacrylate-co-norbornyl 2-trifluoromethylacrylate] and 0.025g palladium on activated carbon (10 wt. %). The reaction mixture was placed under 100psi hydrogen pressure and stirred at 50°C for seventy-two hours, after which time it was cooled to room temperature and depressurized. The resulting reaction mixture was filtered to remove the catalyst, and the solvent removed by rotary evaporation. The resulting white polymer was dissolved in THF, precipitated into hexanes, filtered, and dried for twenty-four hours in a 50°C vacuum oven, affording .15g of a white polymer. ^{1}H NMR ($CDCl_3$) δ 1.438 (bs, 9H), 2.271 (bm, 7H), 3.70 (bs, 3H); IR (KBr) 3492.10, 2964.46, 2879.84, 1744.91 cm^{-1}

Poly[t-butyl-2-trifluoromethylacrylate-co-benzyl 2-trifluoromethylacrylate-co-1-trifluoromethyl-norbornyl 2-trifluoromethylacrylate]

To a 25mL dry, round bottom flask containing a stir bar was added .325g (.0015 moles) *t*-butyl 2-trifluoromethylacrylate, 0.345g (.0015 moles) benzyl 2-trifluoromethylacrylate, 1g 1-trifluoromethyl-norbornyl 2-trifluoro- methacrylate, .048g (.00018 moles) 18-crown-6, and .019g (.00018 moles) potassium cyanide. The reaction mixture was placed under 100 psi hydrogen pressure and stirred for

twenty-four hours at room temperature, after which time the resulting solid mass was dissolved in THF, precipitated into a cold 1:1 methanol:water solution, re-dissolved in THF, re-precipitated into the 1:1 solution, and filtered. The polymer was dried in a vacuum oven at 50°C, affording .78g of a white polymer. M_w=1,110; M_n=2,190; ^{1}H NMR ($CDCl_3$) δ 1.430 (bs, 9H), 2.105-3.210 (bm, 7H), 5.092 (bs, 2H), 7.423 (bs, 5H); IR (KBr) 2984.37, 2879.84, 1759.84 cm^{-1} The copolymer composition was approximately 20:55:35 (benzyl : norborny l: *tert*-butyl) by ^{1}H NMR and TGA analysis.

Poly[Methyl 2-trifluoromethylacrylate-co-*tert*-butyl-2-trifluoromethyacrylate co-2-trifluoromethylacrylic acid co-norbornyl 2-trifluoromethylacrylate] (3.24)

To a 200mL Parr pressure vessel equipped with a stir bar was added 25mL ethyl acetate, .25 g Poly[t-butyl-2-trifluoromethylacrylate-co-benzyl 2-trifluoromethylacrylate-co-1-trifluoromethyl-norbornyl 2-trifluoromethylacrylate]and 0.025g palladium on activated carbon (10 wt. %). The reaction mixture was placed under 100 psi hydrogen pressure and stirred at 50°C for seventy-two hours, after which time it was cooled to room temperature and depressurized. The resulting reaction mixture was filtered to remove the catalyst, and the solvent removed by rotary evaporation. The resulting white polymer was dissolved in THF, precipitated into hexanes, filtered, and dried for twenty-four hours in a 50°C vacuum oven, affording .15g of a white polymer. ^{1}H NMR

($CDCl_3$) δ 1.438 (bs, 9H), 2.271 (bm, 7H), 3.70 (bs, 3H); IR (KBr) 3492.10, 2964.46, 2879.84, 1744.91 cm^{-1}.

***Tert*-Butyl 3-(bicyclo[2.2.1]hept-5-ene-2-yl)-1,1,1-trifluoro-2-(trifluoromethyl) -2-propyl carbonate (3.30)**

To a dry, 250mL, three neck, round-bottom flask equipped with a stir bar and nitrogen inlet was added 100mL dry THF, 12.00g (0.044 moles) bicyclo[2.2.1]hept-5-ene-2-(1,1,1-trifluoro-2-trifluomethylpropane-2-ol, 3.29), 10.08g (0.0462 moles) di-*tert*-butyl dicarbonate and 0.056g (0.000462 moles) 2-(dimethylamino)pyridine at room temperature. The reaction mixture was stirred for twenty-four hours, after which time it was washed with 0.05N HCl (50mL) and water (50mL). The organic layer was dried over $MgSO_4$, filtered and the solvent was removed by rotary evaporation. Vacuum distillation (52°-63°C, 0.026 mmHg) over sodium bicarbonate afforded 14.55g (88%) of a colorless liquid that was 96% pure by GC. ^{1}H NMR ($CDCl_3$) δ 0.64 (m), 1.23-1.45 (m), 1.50 (d, 9H), 1.52 (d, 9H), 1.56 (s), 1.92-2.06 (m), 2.25 (bs), 2.43 (m), 2.48 (m), 2.63 (bs), 2.79 (bs), 2.85 (bs), 5.98 (m), 6.07 (m), 6.21, (m); ^{13}C NMR ($CDCl_3$) δ 27.440, 31.744, 32.152, 32.298, 32.728, 34.410, 34.869, 41.824, 42.683, 45.400, 46.922, 47.606, 49.573, 82.455, 82.841, 83.227, 83.613, 83.999, 84.574, 116.189, 119.998, 123.836, 127.674, 131.876, 136.209, 137.047, 149.071; ^{19}F NMR ($CDCl_3$) δ -72.828, -72.793, 72.757, -72.658, -72.630, -72.594, -72.446, -72.418, -72.389; IR (neat) 3060.19, 2978.64, 2869.90, 1774.76 cm^{-1}; HRMS (CI) m/z (rel. intensity) 319 ($M+H^+$, 100), 375 (30), HRMS (CI) m/z calculated for $C_{16}H_{21}O_3F_6$ (m+1) 375.139489, found 375.138333

1,4-Bis(2-hydroxyhexafluoroisopropyl)cyclohexane (3.32)

To a 250mL Parr pressure vessel equipped with a stirring bar was added 90mL 2-propanol, 26.31g (.064moles) 1,4-bis(2-hydroxyhexafluoro-isopropyl)benzene (3.31) and 3.58g of Rh-C (rhodium 5% on activated carbon). The reaction mixture was stirred for twenty-four hours at 150°C under 600psi hydrogen pressure. After this time, the vessel was cooled to room temperature and the pressure released. The reaction mixture was filtered to remove the catalyst and concentrated by rotary evaporation. Vacuum distillation (77°-80°C, 1 mmHg) afforded 22.27g (83%) of a colorless liquid that was 99% pure by GC. ^{1}H NMR ($CDCl_3$) δ 1.680-1.762 (m, 2H), 1.927-2.026 (m, 2H), 2.137-2.163 (m, 1), 2.906 (s 1H); ^{13}C NMR ($CDCl_3$) δ 23.449, 26.610, 36.289, 41.569, 77.655, 77.787, 77.796, 78.151, 78.347, 78.711, 79.076, 79.156, 79.447, 117.609, 121.498, 125.329, 129.160; ^{19}F NMR ($CDCl_3$) δ -74.123, 73.705; IR (neat) 3595.97, 3479.47, 2978.52, 2893.52, 1471.80 cm^{-1}; HRMS (CI) m/z (rel. intensity) 417 ($M+H^+$, 100), 379 (60), HRMS (CI) m/z calculated for $C_{12}H_{13}O_2F_{12}$ (m+1) 417.072394, found 417.071444

1,4-Bis(2-hydroxyhexalfuoroisopropyl)cyclohexane 2-trifluoromethylacrylate (3.33)

To a dry, 500mL, three neck, round-bottom flask equipped with a stir bar and nitrogen inlet was added 250mL dry DCM, 4.00g (0.025 moles) 2-trifluoromethylacryloyl chloride, 10.40g (0.025 moles) 1,4-bis(2-hydroxyhexalfuoroisopropyl)cyclohexane **(3.32)**, and 2.53g (0.025 moles)

triethylamine, dropwise at 0°C. The reaction mixture was allowed to warm to room temperature and stir for twenty-four hours, after which time it was washed with water (150mL) and 1N HCl (150mL). The organic layer was dried over $MgSO_4$, filtered and the solvent was removed by rotary evaporation. Purification by column chromatography (1:1 hexanes:DCM) gave 6.62g (49%) of white crystals that were 100% pure by GC. ^{1}H NMR ($CDCl_3$) δ 0.839-0.986 (t, 4H), 1.249 (s, 4H), 1.843-1.968 (m, 2), 2.025-2.046 (m, 2H), 3.031 (s, 1H), 4.10 (s, 1H), 6.572 (s, 1H), 6.795 (s, 1H); ^{13}C NMR ($CDCl_3$) δ 14.088, 21.830, 22.659, 24.035, 31.604, 33.833, 34.946, 120.021, 123.866, 125.323, 135.355, 157.242; ^{19}F NMR ($CDCl_3$) δ -74.285, -68.477, -68.364, -68.307, -66.326, -66.298; IR (DCM) 3553.26, 3052.31, 2990.17, 2889.21, 1774.70 cm^{-1}; HRMS (CI) m/z (rel. intensity) 539 ($M+H^+$, 100), 519 (30), HRMS (CI) m/z calculated for $C_{16}H_{14}O_3F_{15}$ (m+1) 539.070343, found 539.069410

Poly[*tert*-butyl 2-trifluoromethyacrylate- co-2-trifluoromethyl-bicyclo(2.2.1) hept-5-en-2-ol-ol] (3.34)

To a 25mL round-bottom flask equipped with a stir bar, condenser and nitrogen inlet was added 8.85g (0.045 moles) *tert*-butyl 2-trifluoromethyl acrylate, 8.04g (0.045 moles) 2-trifluormethylbicyclo[2.2.1]hept-5-en-2-ol and 0.74g (0.0045 moles) 2-2' azobisisobutyronitrile. The flask was immersed in a Dewar containing liquid nitrogen, and after three cycles of freeze-thaw treatment under N_2, the flask was placed in an oil bath at 80°C for 48 hours. After this time, the

reaction mixture was cooled to room temperature, and the resulting yellow mass was dissolved in THF. Precipitation into hexanes afforded 3.01g of a white polymer. TGA analysis showed a 66.6:33.3 (acrylate:norbornane) incorporation ratio. M_w=4,910; M_n=2,230; ^{1}H NMR ($CDCl_3$) δ 1.452 (bs), 1.788 (bs); ^{19}F NMR ($CDCl_3$) δ -80.872, -79.910, -76.740, -73.910, -72.814, -69.297, -66.368, -58.734; IR (KBr) 3436, 2986, 2939, 1728.10, 1452.38, 1378.6 cm^{-1}

Poly[2-(Trifluoromethyl)-Norborn-2-yl-2-trifluoromethylacrylate-co-t*ert*-Butyl 3-(bicyclo[2.2.1]hept-5-ene-2-yl)-1,1,1-trifluoro-2-(trifluoromethyl)-2-propyl carbonate (3.35)

To a 25mL round-bottom flask equipped with a stir bar, condenser and nitrogen inlet was added 1.21g (0.004 moles) 2-(trifluoromethyl)-norborn-2-yl-2-trifluoromethylacrylate, 1.5g (0.004 moles) t*ert*-butyl 3-(bicyclo[2.2.1]hept-5-ene-2-yl)-1,1,1-trifluoro-2-(trifluoromethyl)-2-propyl carbonate and 0.0656g (0.0004 moles) 2-2'-azobisisobutyronitrile. The flask was immersed in a Dewar tube containing liquid nitrogen, and after three cycles of freeze-thaw treatment under N_2, the flask was placed in an oil bath at 80°C for 48 hours. After this time, the reaction mixture was cooled to room temperature, and the resulting yellow mass was dissolved in THF. Precipitation into hexanes afforded .60 g of a white polymer. TGA analysis showed a 65:35 (acrylate:norbornane) incorporation ratio. M_w=9,860; M_n=7,230; ^{1}H NMR ($CDCl_3$) δ 1.452 (bs), 1.788 (bs); ^{19}F NMR

($CDCl_3$) δ -72.708 (bs), -68.895 (bs), -62.902 (bs); IR (KBr) 2982.52, 2893.20, 1770.87, 1487.38, cm^{-1}

Poly[1,4-bis(2-hydroxyhexalfuoroisopropyl)cyclohexane 2-trifluoromethylacrylate co-*tert*-butyl 3-(bicyclo[2.2.1]hept-5-ene-2-yl)-1,1,1-trifluoro-2-(trifluoromethyl)-2-propyl carbonate (3.36)

To a 25mL round-bottom flask equipped with a stir bar, condenser and nitrogen inlet was added 1.39g (0.0026 moles) 1,4-bis(2-hydroxyhexalfuoroisopropyl)cyclohexane 2-trifluoromethylacrylate, 0.967g (0.0026 moles) t*ert*-butyl 3-(bicyclo[2.2.1]hept-5-ene-2-yl)-1,1,1-trifluoro-2-(trifluoromethyl)-2-propyl carbonate and 0.042g (0.00026 moles) 2-2'-azobisisobutyronitrile. The flask was immersed in a Dewar tube containing liquid nitrogen, and after three cycles of freeze-thaw treatment under N_2, the flask was placed in an oil bath at 80°C for 48 hours. After this time, the reaction mixture was cooled to room temperature, and the resulting yellow mass was dissolved in THF. Precipitation into hexanes afforded .63 g of a white polymer. TGA analysis showed a 85:15 (acrylate:norbornane) incorporation ratio. M_w=7,110; M_n=4,200; ^1H NMR ($CDCl_3$) δ 1.452 (bs), 1.788 (bs); ^{19}F NMR ($CDCl_3$) δ -72.708 (bs), -68.895 (bs), -62.902 (bs); IR (KBr) 3448.41, 2978.52, 2885.32, 1774.70 cm^{-1}

1-(2-hydroxyhexafluoroisopropyl)cyclohexane-4-*tert*-butyl carbonate

To a dry, 5000mL, three neck, round-bottom flask equipped with a stir bar and nitrogen inlet was added 250mL dry THF, 10.00g (0.024 moles) 1,4-Bis(2-

hydroxyhexafluoroisopropyl)cyclohexane, 5.24g (0.024 moles) di-*tert*-butyl dicarbonate and 0.29g (0.0024 moles) 2-(dimethylamino)pyridine at room temperature. The reaction mixture was stirred for twenty-four hours, after which time it was washed with 0.05N HCl (50mL) and water (50mL). The organic layer was dried over $MgSO_4$, filtered and the solvent was removed by rotary evaporation. Column chromatography (1:1 hexanes:DCM) afforded 2.59g (55%) of white crystals that were 100% pure by GC. ^{1}H NMR ($CDCl_3$) δ 1.475 (s, 9H), 1.613-1.724 (m, 2H), 1.846-2.026 (m, 3H), 2.133-2.259 (m, 1H), 3.098, (s, 1H); ^{14}C ($CDCl_3$) δ 22.036, 23.835, 27.411, 34.417, 34.672, 37.949, 41.744, 84.880, 85.040, 149.173; ^{19}F NMR ($CDCl_3$) δ -73.668 (s, 2F), -68.305 (s, 6F); HRMS (CI) m/z (rel. intensity) 517 ($M+H^+$, 100), 493 (500), HRMS (CI) m/z calculated for $C_{17}H_{21}O_4F_{12}$ (m+1) 517.124823, found 517.123779

1-(2-hydroxyhexafluoroisopropyl)cyclohexane-4-*tert*-butyl carbonate 2-trifluoromethylacrylate

To a dry, 1000mL, three neck, round-bottom flask equipped with a stir bar and nitrogen inlet was added 500mL dry DCM, 2.09g (0.0132 moles) 2-trifluoromethylacryloyl chloride, 6.80g (0.0132 moles) 1-(2-hydroxyhexafluoroisopropyl)cyclohexane-4-*tert*-butyl carbonate, and 1.33g (0.0132 moles) triethylamine, dropwise at 0°C. The reaction mixture was allowed to warm to room temperature and stir for twenty-four hours, after which time it was washed with water (150mL) that was made slightly acidic with a few drops of

concentrated HCl. The organic layer was dried over $MgSO_4$, filtered and the solvent was removed by rotary evaporation. Purification by column chromatography (1:1 hexanes:DCM) gave 5.74g (68%) of white crystals that were 100% pure by GC. ^{1}H NMR ($CDCl_3$) δ 0.838-0.954 (m, 1H), 1.237-1.306 (bs, 1H), 1.480 (s, 9H), 1.590-1.691 (bs, 3 H), 1.822-1.935 (bs, 4H), 3.034-3.233 (bs, 2H), 6.569 (s, 1H), 6.78 (s, 1H); ^{13}C NMR ($CDCl_3$) δ 14.091, 21.126, 21.534, 26.741, 27.418, 31.592, 32.385, 33.106, 37.964, 84.909, 135.539, 148.925, 157.126; ^{19}F NMR ($CDCl_3$) δ -68.443 (s, 4F), -68.288 (s, 2F), -68.192 (s, 6F), -68.324 (s, 3F) HRMS (CI) m/z (rel. intensity) 639 ($M+H^+$, 100), 583 (100), HRMS (CI) m/z calculated for $C_{21}H_{22}O_5F_{15}$ (m+1) 639.122773, found 639.122613

Poly[1-(2-hydroxyhexafluoroisopropyl)cyclohexane-4-*tert*-butyl carbonate 2-trifluoromethylacrylate]

To a 25mL round-bottom flask equipped with star bar was added 5.63g (0.0088 moles) 1-(2-hydroxyhexafluoroisopropyl)cyclohexane-4-*tert*-butyl carbonate 2-trifluoromethylacrylate, 1.3g THF, 0.018g (.00037 moles) potassium acetate, and 0.100 g (0.000378 moles) 18-crown-6. The reaction was stirred for 72 hours under nitrogen at room temperature, after which time ~5mL THF added, and the solution was precipitated into methanol. The resulting polymer was filtered and dried on a high vacuum line, resulting in 1.17g (21 %) of a white polymer. ^{1}H NMR (acetone-d_6) δ 1.536 (bs), 1.841-1.951 (broad peaks), 2.935-3.643 (broad peaks); ^{19}F NMR ($CDCl_3$) δ-68.857 - -68.773 (broad peaks); IR (KBr) 1471.84,

1774.76, 2900.97, 3001.94 cm^{-1}; M_w=2490, PDI=1.751

Poly[1,4-Bis(2-hydroxyhexalfuoroisopropyl) cyclohexane 2-trifluoromethylacrylate] (3.38)

To a 50mL round-bottom flask equipped with stir bar was added 8mL DCM, 0.78g poly[1-(2-hydroxyhexafluoroisopropyl)cyclohexane-4-*tert*-butyl carbonate 2-trifluoromethylacrylate] and 4mL trifluoroacetic acid. The reaction was stirred at room temperature overnight, after which time the solvent and acid was removed by rotary evaporation, and the resulting sticky mass was dried on a high vacuum line for 24 hours. This mass was dissolved in DCM, precipitated into hexanes (2X), filtered, and dried overnight on a high vacuum line affording 0.26g white polymer. ^{1}H NMR (acetone-d_6) δ 1.835 (bs), 2.089 (bs), 2.966 (bs); ^{19}F NMR ($CDCl_3$) δ-68.975 - -69.031 (broad peaks); M_w=2125, PDI=1.873

2-(Trifluoromethy)bicyclo[2.2.1]hept-5-ene-2-carboxylic acid *tert*-butyl ester (3.39)

To a 100 ml three-neck round-bottom flask equipped with a stir bar, addition funnel, and reflux condenser was added 11.7g (59.8 mmol) *tert*-butyl 2-trifluoromethylacrylate in THF (50 mL). Freshly cracked cyclopentadiene (11.9g, 89.7 mmol) was added dropwise, and the resulting solution was stirred at room temperature overnight. Vacuum distillation (75º-77ºC, 10mmHg) afforded 13.5g (84%) of a colorless material that was 99% pure by GC. ^{1}H NMR ($CDCl_3$) δ 1.18-1.72 (m, 1H), 1.85-2.02 (m, 1H), 2.54-2.59 (m, 1H), 2.01-2.08 (m, 1H), 2.91 (bs,

1H), 3.283.37 (m, 1H), 2.91 (BS, 1H), 3.28-3.37 (m, 1H), 6.01-6.03 (m, 1H), 6.25-6.28 (m, 1H); ^{19}F NMR ($CDCl_3$) δ –64.07, -67.2; IR (neat) 3071.82, 2979.73, 2887.65, 1731.64 cm^{-1}; HRMS (CI) m/z (rel. intensity) 141 ($M+H^+$, 100), 159 (30), HRMS (CI) m/z claculated for $C_{13}H_{17}O_2F_3$ (m+1) 263.126, found 263.126

Poly[1,4-bis(2-hydroxyhexafluoroisopropyl)cyclohexane 2-trifluoromethylacrylate co-2-trifluoromethyl-bicyclo[2.2.1] hept-5-ene-2-carboxylic acid-*tert*-butyl ester] (3.40)

To a 25mL round-bottom flask equipped with a stir bar, condenser and nitrogen inlet was added 4.20g (0.0078 moles) 1,4-bis(2-hydroxyhexafluoroisopropyl)cyclohexane 2-trifluoromethylacrylate, 2.92g (0.0078 moles) trifluoromethyl-bicyclo[2.2.1] hept-5-ene-2-carboxylic acid-*tert*-butyl ester and 0.140g (0.0009 moles) 2-2'-azobisisobutyronitrile. The flask was immersed in a dewar containing liquid nitrogen, and after three cycles of freeze-thaw treatment under N_2, the flask was placed in an oil bath at 80°C for 48 hours. After this time, the reaction mixture was cooled to room temperature, and the resulting yellow mass was dissolved in THF. Precipitation into hexanes afforded .214 g of a white polymer. TGA analysis showed a 60:40 (acrylate:norbornane) incorporation ratio. M_w=5,440; M_n=3,430; ^1H NMR ($CDCl_3$) δ 1.426 (bs), 1.567 (bs), 1.840 (bs), 2.005 (bs), 2.213 (bs), 3.021 (bs) ; IR (KBr) 3502.91, 2986.41, 1778.64, 1724.27, 1227.18 cm^{-1}

2-Trifluoromethyl-bicyclo[2.2.1]hept-5-ene-2carboxylic acid (3.41)

To a dry 250mL three neck round-bottom flask equipped with a stir bar and nitrogen inlet was added, dropwise at room temperature, 200mL dry THF, 34.49g (0.2463 moles) 2-trifluolomethyl acrylic acid and 16.28g (0.243 moles) cyclopentadiene. The reaction mixture was allowed to stir for twenty-four hours at room temperature, after which time the THF was removed by rotary evaporation resulting in a white solid that was dissolved with 200mL diethyl ether. The organic layer was extracted three times with 200mL portions of 1M NaOH, the combined aqueous layers were neutralized with 10% HCl, and extracted three times with 500mL portions of diethyl ether. The combined organics were dried over $MgSO_4$, filtered, and rotovapped resulting in 20.00g (40%) of a white solid that was 97% pure by GC. ^{1}H NMR ($CDCl_3$) endo/exo δ 1.366-1.498 (d, 1H), 1.454-1.498 (d, 1H), 1.734-1.872 (m 1H), 2.019 (s, 2H), 2.618-2.672 (m, 1H), 2.606 (s, 2H), 3.747-3.802 (m, 1H), 6.034-6.042 (m, 1H), 6.289-6.347 (m, 1H), 10.6384 (s, 1H); ^{13}C NMR ($CDCl_3$) δ 14.933, 32.033, 32.247, 41.782, 42.523, 47.533, 47.626, 48.399, 49.637, 65.911, 132.189, 134.764, 139.973, 140.475174.232, 175.446; ^{19}F ($CDCl_3$) δ -67.211, -64.728; IR (neat) 2978.64, 2248.54, 1712.62, 1168.93; HRMS (CI) m/z (rel. intensity) 207 ($M+H^+$, 100), 187 (60), HRMS (CI) m/z claculated for $C_9H_{10}O_2F_3$ (m+1) 207.063289, found 207.062515

2-Trifluoromethyl-bicyclo[2.2.1]hept-5-ene-2carboxylic acid ethoxy methyl ester (3.42)

To a dry 250mL three neck round-bottom flask equipped with a stir bar, condenser and nitrogen inlet was added, dropwise at 0ºC, 200mL dry THF, 7.00 g (.034 moles) 2-trifluoromethyl-bicyclo[2.2.1]hept-5-ene-2carboxylic acid and 2.61g (0.04 moles) butyl lithium (2.7M in heptane). After stirring for thirty minutes, 3.84g (0.04 moles) of chloromethyl ethyl ether was added, dropwise. The reaction mixture was allowed to warm to room temperature and stir for another twenty-four hours, after which time it was poured into a seperatory funnel containing 100mL of water. This solution was extracted three times with 300mL portions of diethyl ether, and the combined organic layers were washed with 200mL brine, dried over $MgSO_4$, filtered and concentrated by rotary evaporation. Vacuum distillation (8mmHg, 75-82ºC) afforded 6.81g (76%) of a colorless liquid that was 98% pure by GC. ^{1}H NMR ($CDCl_3$) endo/exo δ 1.182-1.234 (t, 3H), 1.291-1.320 (d, 1H), 1.725-1.756 (d, 1H), 2.028-2.058 (m, 1H), 2.606-2.662 (m, 1H), 2.956 (s, 2H), 3.372 (s, 1H), 3.451 (s, 1H), 3.623-3.725 (q, 2H), 5.226-5.390 (m, 2H), 6.011-6.040 (m, 1H), 6.270-6.313 (m, 1H); ^{13}C NMR ($CDCl_3$) δ 14.921,32.077, 32.320, 41.786, 42.486, 47.517, 48.237, 49.383, 66.174, 90.270, 90.598, 132.073, 134.432, 140.018, 140.434; ^{19}F ($CDCl_3$) δ -67.013, -64.480; IR (neat) 3067.96, 2978.64, 1739.81, 1475.73; HRMS (CI) m/z (rel. intensity) 265 ($M+H^+$, 100), 189 (60), HRMS (CI) m/z claculated for $C_{12}H_{16}O_3F_3$ (m+1) 265.105154, found 265.105839

Poly[1,4-bis(2-hydroxyhexafluoroisopropyl)cyclohexane 2-trifluoromethylacrylate co-2-trifluoromethyl-bicyclo[2.2.1] hept-5-ene-2-carboxylic acid ethoxy methyl ester] (3.43)

To a 25mL round-bottom flask equipped with a stir bar, condenser and nitrogen inlet was added 3.78 g (.007 moles) 1,4-bis(2-hydroxyhexafluoroisopropyl)cyclohexane 2-trifluoromethylacrylate, 1.85g (0.007 moles) trifluoromethyl-bicyclo[2.2.1] hept-5-ene-2-carboxylic acid ethoxy methyl ester and 0.16g (0.0007 moles) V601. The flask was immersed in a dewar containing liquid nitrogen, and after three cycles of freeze-thaw treatment under N_2, the flask was placed in an oil bath at 80°C for 48 hours. After this time, the reaction mixture was cooled to room temperature, and the resulting yellow mass was dissolved in THF. Precipitation into hexanes afforded 1.23 g of a white polymer. ^{19}F analysis showed a 60:40 (acrylate:norbornane) incorporation ratio. M_w=4,060; M_n=2,790; ^1H NMR ($CDCl_3$) δ 1.188 (bs), 1.662 (bs), 3.657 (bs), 5.344 (bs); ^{19}F NMR ($CDCl_3$) δ -74.25, -68.321; IR (KBr) 3417.34, 2997.94, 1766.93 cm^{-1}

Radical Copolymerizations of 2-trifluoromethylacrylic acid and Norbornene *tert*-Butyl Ester for Reactivity Ratio Studies (Figure 4.3)

To a 25mL round-bottom flask equipped with a stir bar, condenser and nitrogen inlet was added varying ratios of 2-trifluoromethylacrylate (TMAA) and norbornene *tert*-butyl ester (NBtBE) with 4 mole % AIBN. The flask was

immersed in a dewar containing liquid nitrogen, and after three cycles of freeze-thaw treatment under N_2, the flask was placed in an oil bath at 70°C for varying amounts of time to assure a conversion lower than 13%. After this time, the reaction mixture was cooled to room temperature, precipitated in to hexanes, filtered, the resulting polymer was dissolved in acetone, precipitated into chloroform, filtered, redissolved in acetone, precipitated into hexanes, filtered, and the resulting polymer was dried in vacuo at 50ºC for 24 hours. Polymer composition was analyzed with ^{13}C NMR in acetone-d_6 using an inverse gated ^{1}H decoupled mode with $Cr(acac)_3$ as a relaxation agent. Experimental data is shown below.

TFMAA (moles)	NBtBE (moles)	Reaction Time	Yield	^{13}C NMR comp. (acrylate/NB)	M_w	PDI
0.0312	0.0311	2h	12.0	57.38/42.62	1848	1.02
0.0721	0.0080	2h	5.2	72.45/27.55	1675	1.01
0.0573	0.0143	2h	5.4	65.48/34.52	1805	1.01
0.0500	0.0214	2h	11.4	60.68/39.32	1828	1.02
0.0394	0.0287	2h	11.6	58.26/41.74	1843	1.02
0.0163	0.0381	2h	3.2	57.54/42.46	1726	1.01
0.0090	0.0316	4h	6.8	55.62/44.38	1668	1.01
0.0042	0.0381	5h	5.9	51.88/48.12	1623	1.01
0.0532	0.0030	3h	5.3	81.48/18.52	2116	1.05
0.0024	0.0435	7.5h	3.9	45.96/54.04	2501	1.07

Butyl-1-Magnesium Chloride (4.1)

To a dry, 100ml three necked round-bottom flask equipped with a stir bar and nitrogen inlet was added 27.5 mL of a 2M solution of butyl magnesium bromide was slowly added 15g (0.055 moles) of mercuric chloride. The reaction

was stirred overnight at room temperature, after which time it was filtered, and the resulting solid was stirred with 150 mL ether, and then filtered. The combined organic filtrates were dried over magnesium sulfate, filtered, and the solvent was removed by rotary evaporation. The resulting white powder was recrystalized from ethanol, resulting in 10.2 g (66%) of white crystals. ^{1}H NMR ($CDCl_3$) δ 0.908-0.945 (t, 3H), 1.344-1.435 (q, 2H), 1.667-1.740 (q, 2H), 2.060-2.096 (t, 2H); ^{13}C NMR (acetone-d_6) δ 13.800, 28.402, 31.262, 31.598

1,1,1-Trifluorobutyl-4-Magnesiumchloride (4.2)

To a dry, 100ml three necked round-bottom flask equipped with a stir bar and nitrogen inlet was added 30mL dry ether, 0.63 g (0.026 moles) magnesium chips followed by 5.0g (0.026 moles) of 4-bromo-1,1,1-trifluoro-butane, dropwise at room temperature. The reaction mixture was heated to reflux for 3 hours, after which time it was cooled to room temperature and vacuum transferred through a cannula to a dry, 100mL 3 necked round-bottomed flask equipped with a stir bar and nitrogen inlet, leaving behind any unreacted magnesium. To this flask was slowly added 7.06g (0.026 moles) mercuric chloride at room temperature. The reaction was stirred overnight at room temperature, after which time it was filtered, and the resulting solid was stirred with 150 mL ether, and then filtered. The combined organic filtrates were dried over magnesium sulfate, filtered, and the solvent was removed by rotary evaporation. The resulting white powder was recrystalized from ethanol, resulting in 5.1 g (55%) of white crystals. ^{1}H NMR (acetone-d_6) δ 1.708 (s, 1H), 2.203-2.223 (m, 3H), 2.287-2.317(m, 2H); ^{13}C NMR

(acetone-d_6) δ 22.134, 31.800, 37.073, 37.350, 37.619, 37.895; ^{19}F NMR (acetone-d_6) δ -65.00 (s, 3F)

2-Methyl-heptanoic acid *tert*-butyl ester (4.3)

To a 100ml three necked round-bottom flask equipped with a stir bar and nitrogen inlet was added 50 mL dichloromethane, 2.51 g (0.0177 moles) *tert*-butyl methacrylate, 2.5 g (0.0085 moles) butyl mercuric chloride, followed by 0.67 g (.0177 moles) sodium borohydride dissloed in 5 mL of water, dropwise at room temperature. The reaction was stirred for 3 hours, after which time it was filtered, dried over magnesium sulfate, filtered, and solvent removed by rotary evaporation. Vacuum distillation (1 mm Hg, 48-53ºC) afforded 0.43g (24%) of a colorless liquid that was 95% pure by GC. ^{1}H NMR ($CDCl_3$) δ 0.813-0.872 (m, 3H), 0.985-1.047 (d, 3H), 1.220-1.311 (m, 8H), 1.390 (s, 9H), 1.524-1.559 (m, 1H); ^{13}C NMR ($CDCl_3$) δ 13.948, 17.104, 22.479, 26.814, 28.014, 28.334, 31.709, 33.833, 40.401, 43.994

2-Trifluoromethyl-heptanoic acid *tert*-butyl ester (4.4)

To a 100ml three necked round-bottom flask equipped with a stir bar and nitrogen inlet was added 50 mL dichloromethane, 2.99 g (0.0153 moles) *tert*-butyl 2-trifluoromethylacrylate, 2.24 g (0.00764 moles) butyl mercuric chloride, followed by 0.578 g (.0153 moles) sodium borohydride dissloved in 5 mL of water, dropwise at room temperature. The reaction was stirred for 3 hours, after which time it was filtered, dried over magnesium sulfate, filtered, and solvent removed by rotary evaporation. Vacuum distillation (0.75 mm Hg, 45-48ºC) afforded 1.10 g (57%) of a colorless liquid that was 97% pure by GC. ^{1}H NMR

($CDCl_3$) δ 0.810-.887 (m, 3H), 1.250-1.378 (m, 6H), 1.465 (s, 9H), 1.722-1.757 (m, 1H), 1.836-1.898 (m, 1H), 2.857-2.915 (m, 1H); ^{13}C NMR ($CDCl_3$) δ 13.844, 22.261, 26.012, 26.057, 27.801, 31.233, 50.920, 51.183, 51.456, 51.719, 82.430; ^{19}F NMR ($CDCl_3$) δ -69.680

7,7,7-Trifluoro-2-methyl-heptanoic acid *tert*-butyl ester (4.5)

To a 100ml three necked round-bottom flask equipped with a stir bar and nitrogen inlet was added 50 mL dichloromethane, 2.26 g (0.0159 moles) *tert*-butyl methacrylate, 2.0 g (0.0071 moles) trifluorobutyl mercuric chloride, followed by 0.436 g (.01152 moles) sodium borohydride dissolved in 5 mL of water, dropwise at room temperature. The reaction was stirred for 3 hours, after which time it was filtered, dried over magnesium sulfate, filtered, and solvent removed by rotary evaporation. Vacuum distillation (1.00 mm Hg, 45-53ºC) afforded 0.40g (27%) of a colorless liquid that was 94% pure by GC. ^1H NMR ($CDCl_3$) δ 1.067-1.085 (d, 3H), 1.328-1.361 (m, 3H), 1.412 (s, 9H), 1.511-1.552 (m, 3H), 2.003-2.070 (m, 2H), 2.291-2.310 (m, 1H); ^{13}C NMR ($CDCl_3$) δ 17.192, 21.803, 26.312, 28.022, 33.149, 33.331, 33.331, 33.426, 33.709, 40.183, 79.946; ^{19}F NMR ($CDCl_3$) δ -67.611

7,7,7-Trifluoro-2-trifluoromethyl-heptanoic acid *tert*-butyl ester (4.6)

To a 100ml three necked round-bottom flask equipped with a stir bar and nitrogen inlet was added 50 mL dichloromethane, 2.78 g (0.014 moles) *tert*-butyl 2-trifluoromethylacrylate, 2.0 g (0.0071 moles) trifluorobutyl mercuric chloride, followed by 0.530 g (.014 moles) sodium borohydride dissolved in 5 mL of water, dropwise at room temperature. The reaction was stirred for 3 hours, after which

time it was filtered, dried over magnesium sulfate, filtered, and solvent removed by rotary evaporation. Vacuum distillation (0.90 mm Hg, 70-74ºC) afforded 0.65g (30%) of a colorless liquid that was 97% pure by GC. ^{1}H NMR ($CDCl_3$) δ 1.436 (s, 9H), 1.535-1.593 (q, 2H), 1.700-1.718 (m, 1H), 1.813-1.878 (m, 1H), 2.010-2.080 (m, 2H), 2.911-2.958 (m, 1H); ^{13}C NMR ($CDCl_3$) δ 21.599, 253745, 27.680, 32.902, 33.477, 33.760, 50.649, 50.918, 51.187, 82.826, 122.920, 123.440, 125.644, 126.218, 128.386, 131.135, 166.396; ^{19}F NMR ($CDCl_3$) δ -69.383, -67.334

Competative Reaction Studies Using the Mercury Method

To a mixture of the appropriate alkyl mercuric chloride and at least a ten fold excess of *tert*-butyl 2-trifluoromethylacrylate and *tert*-butyl methacrylate in 10mL of degassed dichloromethane was added 10mg (0.3 mmol) of sodium borohydride in 1mL of degassed water at 20ºC. The reaction was stirred for 3 hours, after which time it was filtered, dried over magnesium sulfate, and the solvent was removed by rotary evaporation. The ratio of the products (CH_3/ CH_3 vs. CH_3/CF_3 or CF_3/CH_3 vs. CF_3/CF_3) were determined by gas chromatography. Experimental data from this study is shown in chapter 4.

(1-Bicyclo[2.2.1]hept-5-en-2-ylmethyl-2,2,2-trifluoro-1-trifluoromethyl-ethoxy)-acetic acid methyl ester (I.1)

To a 500mL three neck round-bottom flask equipped with a stir bar, condenser, and nitrogen inlet was added, dropwise at 0ºC, 250mL dry THF, 5.00g bicyclo[2.2.1]hept-5-ene-2-(1,1,1-trifluoro-2-trifluoromethylpropane-2-ol), and .76g (.019 moles) NaH (60% dispersion in mineral oil). After stirring at this

temperature for thirty minutes, 4.18g (.019 moles) of methylbromo acetate was added, dropwise. The reaction mixture was refluxed for 48 hours, after which time it was cooled to room temperature, and 100mL water was added to react any remaining NaH. This solution was poured into a seperatory funnel and extracted three times with 300mL portions of diethyl ether. The combined organic layers were washed once with 150mL brine, dried over $MgSO_4$, filtered, and concentrated by rotary evaporation. Vacuum distillation (.126mmHg, 56-61ºC) afforded 4.96g (79%) of a colorless liquid that was 97% pure by GC. ^{1}H NMR ($CDCl_3$) endo/exo δ 0.596-0.658 (m, 1H), 1.211-1.292 (d, 1H), 1.345-1.466 (d, 1H), 1.605-1.717 (m, 1H), 1.800-1.945 (m, 1H), 2.027-2.064 (d, 2H), 2.320 (s, 1H), 2.748 (s, 1H), 2.911 (s, 1H), 3.787 (s, 3H), 4.357 (s, 2H), 5.927-6.079 (m, 1H), 6.149-6.190 (m, 1H); ^{13}C NMR ($CDCl_3$) δ 32.072, 33.878, 34.257, 34.425, 42.487, 46.762, 49.529, 52.144, 63.927, 132.357, 136.319, 132.357, 138.030, 138.132; ^{19}F ($CDCl_3$) δ -72.198, -71.738, -71.625, -70.564; IR (neat) 2955.34, 2869.90, 1778.64, 1436.89; HRMS (CI) m/z (rel. intensity) 347 ($M+H^+$, 20), 257 (100), HRMS (CI) m/z claculated for $C_{14}H_{17}O_3F_6$ (m+1) 347.108189, found 347.107562

2-(1-Bicyclo[2.2.1]hept-5-en-2ylmethyl-2,2,2-trifluoro-1-trifluoromethyl-ethoxy)-ethanol (NBHFPA, I.2)

To a 1000mL round-bottom flask equipped with a stir bar, nitrogen inlet and condenser was added, dropwise at 0ºC, 500mL dry THF, 3.64g (.096 moles) $LiAlH_4$ and 16.60g (0.048 moles) (1-bicyclo[2.2.1]hept-5-en-2-ylmethyl-2,2,2-trifluoro-1-trifluoromethyl-ethoxy)-acetic acid methyl ester. This solution was

allowed to warm to room temperature after which time it was refluxed for 48 hours, then cooled to 0ºC and 150mL of methanol was added, dropwise, to kill any remaining $LiAlH_4$. This solution was poured into a seperatory funnel containing 200mL water and the aqueous layer was extracted three times with 500mL portions of diethyl ether. The combined organic layers were washed once with 300mL of brine, dried over $MgSO_4$, filtered, and concentrated by rotary evaportation. Vacuum distillation (1mmHg, 60-69ºC) afforded 13.93g (91%) of a colorless liquid that was 98% pure by GC. ^1H NMR ($CDCl_3$) endo/exo δ 0.596-0.692 (m, 1H), 1.249-1.334 (d. 1H), 1.361-1.464 (m, 1H), 1.607-1.684 (m, 1H), 1.771-2.009 (m, 3H), 2.54 (s, 1H), 3.775-2.877 (d, 2H), 5.929-5.958 (m, 1H), 6.022-6.083 (m, 1H), 6.174-6.204 (m, 1H) ; ^{13}C NMR ($CDCl_3$) δ 32.004, 33.923, 34.509, 35.120, 42.612, 47.104, 48.330, 49.540, 61.722, 67.849, 131.940, 138.403; ^{19}F ($CDCl_3$) δ --72.170, 71.420; IR (neat) 3382.52, 2970.87, 2873.79, 1203.88; HRMS (CI) m/z (rel. intensity) 319 ($M+H^+$, 100), 275 (60), HRMS (CI) m/z claculated for $C_{13}H_{17}O_2F_6$ (m+1) 319.113274, found 319.112346

Poly(2-Trifluoromethylacrylic acid co-NBHFPA) (I.3)

To a 25mL round-bottom flask equipped with a stir bar, condenser and nitrogen inlet was added 0.9g (.0064 moles) 2-trifluoromethylacrylic acid, 2.04g (0.0064 moles) HFANBPA and 0.14g (0.00063 moles) V601. The flask was immersed in a dewar containing liquid nitrogen, and after three cycles of freeze-thaw treatment under N_2, the flask was placed in an oil bath at 80°C for 48 hours. After this time, the reaction mixture was cooled to room temperature, and the

resulting yellow mass was dissolved in THF. Precipitation into hexanes afforded 1.69 g of a white polymer. ^{19}F analysis showed a 60:40 (acrylate:norbornane) incorporation ratio. M_w=4,520; M_n= 2,860; ^{19}F NMR ($CDCl_3$) δ -66.53 (bs, 3F), -74.32 (bs, 6F) ; IR (KBr) 3420.63, 2972.76 cm^{-1}

Poly[methoxystyrene-co-lithium 2-(4-ethenylpheonoxy) tetrafluoroethane sulfonate] (III.7)

To a 50 mL round-bottom flask equipped with a magnetic stir bar and reflux condenser was added 1.50 g (0.0049 moles) lithium 2-(4-ethenylphenoxy)tetrafluoroethane-sulfonate, 5.88 g (0.0438 moles) methoxy styrene, and .08 g (0.00049 moles) AIBN in 15 mL THF. The flask was immersed in a dewar containing liquid nitrogen, and after three cycles of freeze-thaw treatment under N_2, the flask was placed in an oil bath at 80°C for 24 hours. The polymer was twice precipitated into hexanes, filtered, washed with water (to remove unreacted lithium salt monomer), and dried in vacuo to give 2.66 g of a white powder. ^1H NMR (DMSO-d_6) δ 0.799-1.703 (broad peaks), 3.622 (s, -OC$\underline{H}_3$), 6.590 (bs); ^{19}F NMR ($CDCl_3$) δ -117.186 (s, 2F), -81.563 (s, 2F)

Poly[methoxystyrene-co-2-(4-ethenylphenoxy)tetrafluoroethanesulfonic acid hydrate] (III.8) and **poly[methoxystyrene-co-silver 2-(4-ethenylphenoxy)tetrafluoro-ethane sulfonate] (III.9)**

Poly[methoxystyrene-co-lithium 2-(4-ethenylpheonoxy) tetrafluoroethane sulfonate] (1.9g) was dissolved in 5 mL THF and slowly passed through Amberlite

IR-120 (plus) ion exchange resin (previously washed several times with dilute HCl, water, and THF) using THF as the eluent. The THF fractions were concentrated to about 20 mL, and excess silver carbonate (~2.0 g) was added. The resulting misture was stirred overnight in the dark and the filtered thorough a bed of celite, which was washed with THF. The filtrate was concentrated to about 5 mL, precipitated into hexanes, and dried in vacuo to yield 1.15 g of a white powder. ^{1}H NMR (DMSO-d_6) δ 1.386-1.710 (broad peaks), 3.640 (s, -OC$\underline{H}_3$), 6.584 (bs); ^{19}F NMR ($CDCl_3$) δ -117.846 (s, 2F), -82.225 (s, 2F)

Poly[methoxystyrene-co-dimethylphenylsulfonium 2-(4-ethenylphenoxy)tetra-fluoroethanesulfonate] (III.10)

Thioanisole (.165 g, 0.00133 moles) was added to 1.1 g poly[methoxystyrene-co-silver 2-(4-ethenylphenoxy)tetrafluoro-ethane sulfonate] dissolved in 20mL freshly distilled THF. The solution was cooled to 0ºC with an ice water bath. Iodomethane (.612 g, 0.00431 moles) was added dropwise, and silver iodide precipitated immediately. The resulting mixture was stirred in the dark at room temperature for 20 hours, filtered through a bed of celite, and then filtered through a 0.45 μm filter. The filtrate was concentrated to half its initial volume, precipitated into hexanes, and dried in vacuo to yield 0.98 g of a white powder. ^{1}H NMR (acetone-d_6) δ 1.530 (bs), 1.869 (bs), 2.785 (bs, -SC$\underline{H}_3$), 3.740 (s, -OC$\underline{H}_3$), 6.636 (bs); ^{19}F NMR ($CDCl_3$) δ -117.745 (s, 2F), -82.695 (s, 2F)

BIBLIOGRAPHY

(1) Moore, G. *Proc. SPIE-Int. Soc. Opt. Eng.* **1994**, *2438*, 2-17.
(2) from http://www.intel.com/research/silicon/mooreslaw.htm.
(3) McAdams, C. L. *Polymers and Photoactive Compounds for Non-Chemically Amplified Deep-UV Photoresists*; University of Texas at Austin: Austin, 2000.
(4) Honda, K.; Beauchemin, B. T., Jr.; ; Harditch, R. J.; Blahney, A. J.; Kawabe, Y.; Kokubu, T. *Proc. Soc. Photo-Opt. Instrum. Eng.* **1990**, *1262*, 493.
(5) Willson, C. G.; Miller, R. D.; McKean, D.; Clecak, N. J.; Tompkins, T.; Hofer, D.; Michl, J.; Downing, J. *Polym. Eng. Sci* **1983**, *23*, 1004.
(6) Shirai, M.; Tsunooka, M. *Bull. Chem. Soc. Japan* **1998**, *71*, 2483.
(7) Crivello, J. V.; Lam, J. H. W. *Polym. Sci. Polym. Chem. Ed.* **1980**, *18*, 2677.
(8) Crivello, J. V.; Lam, J. H. W. *Macromolecules* **1977**, *10*, 1307.
(9) Wallraff, G. M.; Hinsberg, W. D. *Chem. Rev.* **1999**, *99*, 1801.
(10) Gokan, H.; Esho, S.; Ohnishi, Y. *J. Electrochem. Soc.* **1983**, *130*, 143.
(11) Okoroanyanwu, U.; Byers, J.; Shimokawa, T.; Willson, C. G. *Chem. Mat.* **1998**, *10*, 3328.
(12) Klopp, J. M.; Pasini, D.; Byers, J. D.; Willson, C. G.; Frechet, J. M. J. *Chem. Mater.* **2001**, *13*, 4147.
(13) Allen, R. D.; Wan, I.-Y.; Wallraff, G. M.; DiPietro, R. A.; Hofer, D. C.; Kunz, R. R. *ACS Symposium Series 614*, 1995.
(14) Ito, J.; Breyta, G.; Sooriyakumaran, R.; Hofer, D. C. *J. Phtopolym. Sci. Technol.* **1995**, *8*, 505.
(15) MacDonald, S. A.; Hinsberg, W. D.; Wendt, H. R.; Cleak, N. J.; Willson, C. G. *J. Am. Chem. Soc.* **1993**, *5*, 348.
(16) Oikawa, A.; Hatakenaka, Y.; Ikeda, Y.; Miyata, S.; Santoh, N.; Abe, N. *J. Phtopolym. Sci. Technol.* **1995**, *8*, 519.
(17) Pryzbilla, K. J.; Kinoshita, Y.; Kudo, T.; Masuda, S.; Okazaki, H.; Padmanaban, M.; Pawloski, G.; Roeschert, H.; Spiess, W.; Suehiro, N. *Proc. SPIE-Int. Soc. Opt. Eng.* **1993**, *1925*, 76.
(18) Kunz, R. R.; Bloomstein, T. M.; Hardy, D. E.; Goodman, R. B.; Downs, D. K.; Curtin, J. E. *Proc. SPIE-Int. Soc. Opt. Eng.* **1999**, *3678*, 13.
(19) Brodsky, C.; Byers, J.; Conley, W.; Hung, R.; Yamada, S.; Patterson, K.; Somervell, M.; Trinque, B.; Tran, H. V.; Cho, S.; Chiba, T.; Lin, S.-H.; Jamieson, A.; Johnson, H.; Vander Heyden, T.; Willson, C. G. *J. Vac. Sci. Technol., B* **2000**, *18*, 3396.

(20) Patterson, K.; Yamachika, M.; Hung, R. J.; Brodsky, C. J.; Yamada, S.; Somervell, M. H.; Osborn, B.; Hall, D.; Dukovic, G.; Byers, J.; Conley, W.; Willson, C. G. *Proc. SPIE-Int. Soc. Opt. Eng.* **2000**, *3999*, 365.
(21) Paquette, L. A., Ed. *Encyclopedia of Reagents for Organic Synthesis*: New York, 1995; Vol. 3.
(22) Baumgarten, H. E., Ed. *Organic Synthesis*; John Wiley and Sons: New York, 1973; Vol. 5.
(23) Carey, F. A.; Sundberg, R. J. *Advanced Organic Chemistry: Part B*, 3rd ed.; Plenum Press: New York, 1990.
(24) Gassman, P. G.; Pape, P. G. *J. Org. Chem* **1964**, *29*, 160.
(25) Lightner, D. A.; Gawronski, J. K.; Bouman, T. D. *J. Am. Chem. Soc.* **1980**, *102*, 1983.
(26) Scherer, J., K. V. *Tet. Lett.* **1966**, *7*, 5685.
(27) Boswell, G. A.; Ripka, W. C.; Scribner, R. M.; Tullock, C. W. In *Organic Reactions*; Wiley & Sons: New York, 1974; Vol. 21, pp 1-124.
(28) Bergmann, E. D.; Cohen, A. M. *Tetrahedron* **1966**, *22*, 3545.
(29) Bergmann, E. D.; Cohen, A. M. *Israel J. Chem* **1970**, *8*, 925.
(30) Sharts, C. M.; Sheppard, W. A. In *Organic Reactions*; Wiley & Sons: New York, 1974; Vol. 21, p 125.
(31) Olah, G. A.; Nojima, M.; Kerekes, I. *Synthesis* **1973**, 786.
(32) Schleyer, P. R.; Watts, W. E.; Fort, R. C., Jr.; Comisarow, M. B.; Olah, G. A. *J. Am. Chem. Soc.* **1964**, *86*, 5679.
(33) Grandler, J. R.; Jencks, W. P. *J. Am. Chem. Soc.* **1982**, *104*, 1937.
(34) Ito, H.; Reichmanis, E.; Nalamasu, O.; Ueno, T., Eds. *Micro- and Nanopatterning Polymers*; American Chemical Society: Washington, D.C., 1998.
(35) Matsuzawa, N. N.; Shigeyasu, M.; Yano, E.; Shinji, O.; Akihiko, I.; Dixon, D. *Proc. SPIE-Int. Soc. Opt. Eng.* **2000**, *3999*, 375.
(36) Varetti, E. L.; Aymonino, P. J. *J. Mol. Struct* **1971**, *7*, 155.
(37) Thomson, L. F.; Willson, C. G.; Bowden, M. J. *Introduction to Microlithography*, 2nd ed.; American Chemical Society: Washington, DC, 1994.
(38) Willson, C. G.; Ito, H.; Miller, D. C.; Tessier, T. G. *Polym. Eng. Sci.* **1983**, *23*, 1000.
(39) Pittman, C. U., Jr.; Chen, C.-Y.; Udea, M.; Helbert, J. N.; Kwiatkowski, J. H. *J. Polym. Sci., Polym. Chem. Ed.* **1980**, *18*, 3413.
(40) Lai, J. H.; Helbert, J. N.; Cook, C. F., Jr.; Pittman, C. U., Jr. *J. Vac. Sci. Technol.* **1979**, *16*, 1992.
(41) Helbert, J. N.; Chen, C.-Y.; Pittman, C. U., Jr.; Hagnauer, G. L. *Macromolecules* **1978**, *11*, 1104.
(42) Ito, H.; Miller, D. C.; Willson, C. G. *Macromolecules* **1982**, *15*, 915.

(43) Odian, G. *Principles of Polymerization*, 3rd ed.; John Wiley & Sons, Inc.: New York, 1991.
(44) Iwatsuki, S.; Kondo, A.; Harashina, H. *Macromolecules* **1984**, *17*, 2473.
(45) Hogen-Esch, T. E.; Smid, J., Eds. *Recent Advances in Anionic Polymerization*: New York, 1987.
(46) Buxton, M. W.; Stacey, M.; Tatlow, J. C. *J. Chem. Soc.* **1954**, 366.
(47) Brodsky, C.; Byers, J.; Conley, W.; Hung, R.; Yamada, S.; Patterson, K.; Somervell, M.; Trinque, B.; Tran, H. V.; Cho, S.; Chiba, T.; Lin, S.-H.; Jamieson, A.; Johnson, H.; Vander Heyden, T.; Willson, C. G. *J. Vac. Sci. Technol., B* **2000**, *18*, 3396.
(48) Allen, R. D. W., I-Y.; Wallraff, G. M.; DiPietro, R. A.; Hofer, D. C.; Kunz, R. R. *ACS Symposium Series 614*, 1995.
(49) Fuchikami, T.; Yamanouchi, A.; Ojima, I. *Synthesis* **1984**, 766.
(50) Ito, H.; Wallraff, G. M.; Brock, P. J.; Fender, N.; Truong, H. D.; Breyta, G.; Miller, D. C.; Sherwood, M. H.; Allen, R. D. *Proc. SPIE-Int. Soc. Opt. Eng.* **2001**, *4345*, 273.
(51) Maruno, T.; Nakamura, K.; Murata, N. *Macromolecules* **1996**, *29*, 2006.
(52) Tran, H. V.; Hung, R. J.; Chiba, T.; Yamada, S.; Mrozek, T.; Hsieh, Y.-T.; Chambers, C. R.; Osborn, B. P.; Trinque, B. C.; Pinnow, M. J.; MacDonald, S. A.; Willson, C. G.; Sanders, D. P.; Connor, E. F.; Grubbs, R. H.; Conley, W. *Macromolecules* **2002**, *35*, 6539.
(53) Ito, H.; Truong, H. D.; Okazaki, M.; Miller, D. C.; Fender, N.; Brock, P. J.; Wallraff, G. M.; Larson, C. E.; Allen, R. D. *J. Photopoly. Sci. and Tech.* **2002**, *15*, 591-602.
(54) Patterson, K.; Yamachika, M.; Hung, R. J.; Brodsky, C. J.; Yamada, S.; Somervell, M. H.; Osborn, B.; Hall, D.; Dukovic, G.; Byers, J.; Conley, W.; Willson, C. G. *Proc. SPIE-Int. Soc. Opt. Eng.* **2000**, *3999*, 365.
(55) Odian, G. *Principles of Polymerization*, 3rd ed.; John Wiley & Sons, Inc.: New York, 1991.
(56) Ito, H.; Miller, D. C.; Willson, C. G. *Macromolecules* **1982**, *15*, 915.
(57) Ito, H.; Truong, H. D.; Okazaki, M.; Miller, D. C.; Fender, N.; Brock, P. J.; Wallraff, G. M.; Larson, C. E.; Allen, R. D. *J. Photopolym. Sci. Technol.* **2002**, *15*, 591.
(58) Ito, H.; Truong, H. D.; Okazaki, M.; Miller, D. C.; Fender, N.; Breyta, G.; Brock, P. J.; Wallraff, G. M.; Larson, C. E.; Allen, R. D. *Proc. SPIE-Int. Soc. Opt. Eng.* **2002**, *4690*, 18.
(59) Fordyce, R. G.; Ham, G. E. *J. Am. Chem. Soc* **1951**, *73*, 1186.
(60) Gaylord, N. G.; Deshpande, A. B.; Mandal, B. M.; Martan, M. *J. Macromol. Sci.-Chem.* **1977**, *A11*, 1053.
(61) Tran, H. V.; Hung, R. J.; Chiba, T.; Yamada, S.; Mrozek, T.; Hsieh, Y.-T.; Chambers, C. R.; Osborn, B. P.; Trinque, B. C.; Pinnow, M. J.;

MacDonald, S. A.; Willson, C. G.; Sanders, D. P.; Connor, E. F.; Grubbs, R. H.; Conley, W. *Macromolecules* **2002**, *35*, 6539.
(62) Kelen, T.; Tudos, F. *J. Macromol. Sci.-Chem.* **1975**, *A9*, 1.
(63) Ito, H.; Wallraff, G. M.; Brock, P. J.; Fender, N.; Truong, H. D.; Breyta, G.; Miller, D. C.; Sherwood, M. H.; Allen, R. D. *Proc. SPIE-Int. Soc. Opt. Eng.* **2001**, *4345*, 273.
(64) Giese, B.; Kretzschmar, G.; Meixner, J. *Chem. Ber.* **1980**, *113*, 2787.
(65) Giese, B.; Meister, J. *Angew. Chem. Int. Ed. Engl.* **1977**, *16*, 178.
(66) Ito, H.; Giese, B.; Engelbrecht, R. *Macromolecules* **1984**, *17*, 2204.
(67) Jones, S. A.; Prementine, G. S.; Tirrell, D. A. *Polym. Prepr.* **1985**, *26*, 63.
(68) Jones, S. A.; Prementine, G. S.; Tirrell, D. A. *J. Am. Chem. Soc* **1985**, *107*, 5275.
(69) Ito, H.; Miller, D.; Sveum, N.; Sherwood, M. *Macromolecules* **2000**, *38*, 3521.
(70) Udea, M.; Motokazu, M.; Ito, H. *J. Polym. Sci. A* **1988**, *26*, 2395.
(71) Giese, B. *Angew. Chem. Int. Ed. Engl.* **1983**, *22*, 753.
(72) Giese, B.; Engelbrecht, R. *Polm. Bul.* **1984**, *12*, 55.
(73) Coote, M. L.; Davis, T. P.; Radom, L. *J. Mol. Struct. (THEOCHEM)* **1999**, *461-462*, 91.
(74) Best, M. E.; Kasai, P. H. *Macromolecules* **1989**, *22*, 2622.
(75) Hudson, A.; Root, K. J. *Advances in Magnetic Resonance*; Academic Press: New York, 1990; Vol. 5.
(76) Cywar, D. A.; Tirrell, D. A. *J. Am. Chem. Soc* **1989**, *111*, 7544.
(77) Tanaka, H.; Sasi, K.; Sato, T.; Ota, T. *J. Am. Chem. Soc* **1988**, *21*, 3536.
(78) Coote, M. L.; Davis, T. P.; Radom, L. *Macromolecules* **1999**, *32*, 5270.
(79) Coote, M. L.; Davis, T. P.; Radom, L. *Macromolecules* **1999**, *32*, 2935.
(80) Coote, M. L.; Davis, T. P. *Macromolecules* **1999**, *32*, 3626.
(81) Brunner, T. A.; Fonseca, C. *Proc. SPIE-Int. Soc. Opt. Eng.* **2001**, *4345*, 30.
(82) Tran, H. V.; Hung, R. J.; Chiba, T.; Yamada, S.; Mrozek, T.; Hsieh, Y.-T.; Chambers, C. R.; Osborn, B. P.; Trinque, B. C.; Pinnow, M. J.; MacDonald, S. A.; Willson, C. G.; Sanders, D. P.; Connor, E. F.; Grubbs, R. H.; Conley, W. *Macromolecules* **2002**, *35*, 6539.
(83) Conley, W.; Brunsvold, W.; Ferguson, R.; Gelrome, J.; Holmes, S.; Martino, R.; Petryniak, M.; Rabidoux, P.; Sooriyakumaran, R.; Sturtevant, J. *Proc. SPIE-Int. Soc. Opt. Eng.* **1993**, *1925*, 120.
(84) Conley, W.; Gelorme, J. *J. Vac. Sci. Technol. B* **1992**, *10*, 2570.
(85) Kunz, R. R.; Bloomstein, T. M.; Hardy, D. E.; Goodman, R. B.; Downs, D. K.; Curtin, J. E. *Proc. SPIE-Int. Soc. Opt. Eng.* **1999**, *3678*, 13.
(86) Grandler, J. R.; Jencks, W. P. *J. Am. Chem. Soc.* **1982**, *104*, 1937.
(87) Ito, H.; Wallraff, G. M.; Brock, P. J.; Fender, N.; Truong, H. D.; Breyta, G.; Miller, D. C.; Sherwood, M. H.; Allen, R. D. *Proc. SPIE-Int. Soc. Opt. Eng.* **2001**, *4345*, 273.

(88) Schmid, G. M.; Smith, M. D.; Mack, C. A.; Singh, V. K.; Burns, S. D.; Willson, C. G. *Proc. SPIE-Int. Soc. Opt. Eng.* **2001**, *4345*, 1037.
(89) Higgins, J. S.; Benoit, H. C. *Polymers and Neutron Scattering*; Oxford University Press: New York, 1994.
(90) Pope, B. M.; Yamamoto, Y.; Tarbell, D. S. *Organic Synthesis*, 1988; Vol. Col. Vol. 6.
(91) Stewart, M. D.; Tran, H. V.; Schmid, G. M.; Stachowiak, T. B.; Becker, D. J.; Willson, C. G. *J. Vac. Sci. Technol. B* **2002**, *20*, 2946.
(92) Postnikov, S. V.; Stewart, M. D.; Tran, H. V.; Nierode, M. A.; Medeiros, D. R.; Cao, T.; Beyers, J.; Webber, S. E.; Willson, C. G. *J. Vac. Sci. Technol. B* **1999**, *17*, 3335.
(93) Lin, E. K.; Soles, C. L.; Goldfarb, D. L.; Trinque, B. C.; Burns, S. D.; Jones, R. L.; Lenhart, J. L.; Angelopoulos, M.; Willson, C. G.; Satija, S. K.; Wu, W. *Science* **2002**, *297*, 372.
(94) Barclay, G. G.; Cronin, M. F.; Dellaguardia, R. A.; Thackeray, J. W.; Ito, H.; Breyta, G.: US Patent # 5,861,231, 1996.
(95) Postnikov, S. V.; Stewart, M. D.; Tran, H. V.; Nierode, M. A.; Medeiros, D. R.; Cao, T.; Beyers, J.; Webber, S. E.; Willson, C. G. *J. Vac. Sci. Technol. B* **1999**, *17*, 3335.
(96) Stewart, M. D.; Tran, H. V.; Schmid, G. M.; Stachowiak, T. B.; Becker, D. J.; Willson, C. G. *J. Vac. Sci. Technol. B* **2002**, *20*, 2946.
(97) Tran, H. V. *Ph.D. Dissertation*; University of Texas at Austin: Austin, 2002.
(98) Feiring, A. E.; Choi, S. K.; Doyle, M.; Wonchoba, E. R. *Macromolecules* **2000**, *33*, 9262.
(99) Feiring, A. E.; Wonchoba, E. R. *J. Fluorine Chem.* **2000**, *105*, 129.

Vita

Brian C. Trinque was born in Providence, Rhode Island on March 20, 1977, the son of Donald and Maureen Trinque. After graduating from Cranston West High School, Cranston, RI, in 1995, he entered the University of Rhode Island, and graduated in May of 1999 with Bachelor of Arts degrees in English and Biology. In June of 1999 he entered a Ph.D. program in Organic Chemistry at the University of Texas at Austin under the tutelage of Professor C. Grant Willson. From May-August, 2002, he did research at the IBM Almaden Research Center in San Jose, California under the guidance of Dr. Hiroshi Ito. On August 31, 2002, he married Anne Kathryn Subourne.

Permanent address: 43 Church Hill Drive, Cranston, RI, 02920

This dissertation was typed by the author.